STUDY OF MACROCYCLIC COMPLEXES IN NONAQUEOUS SOLVENTS

By

Gholamhossein Rounaghi

A DISSERTATION

Submitted to
Michigan State University
in partial fulfillment of the requirements
for the degree of

DOCTOR OF PHILOSOPHY

Department of Chemistry

1980

ABSTRACT

STUDY OF MACROCYCLIC COMPLEXES
IN NONAQUEOUS SOLVENTS

By

Gholamhossien Rounaghi

The complexation of the Na^+, Cs^+, Tl^+, Li^+, and Ag^+ ion by the macrocyclic ligands 1,10-dithia-18-Crown-6 (DT18C6) and 1,4,7-trithia-12-Crown-4 (TT12C4) were studied by the multinuclear magnetic resonance technique in several nonaqueous solvents and their stabilities are compared with the complexes formed by the analogues polyethers 18-Crown-6 and 12-Crown-4. In all cases the substitution of the sulfur atoms for the oxygen atoms results in a substantial decrease in the stability of the complexes. In addition, the formation constants of the complexes varies significantly with the solvent. In general, the stabilities of the complexes vary inversely with the cationic solvating abilities of solvents as expressed by the Gutmann donicity scale.

Comparison of the data obtained from ^{205}Tl, ^{23}Na, and ^{133}Cs NMR studies in various solvents shows that the stability of the appropriate complexes decreases in the order $(DT18C6 \cdot Tl)^+ > (DT18C6 \cdot Na)^+ > (DT18C6 \cdot Cs)^+$ regardless

of the solvent in which the complexation takes place.

The formation constants for the complexation of the Cs^+ ion with large macrocyclic crown ethers, dibenzo-27-Crown-9 (DB27C9), and dibenzo-24-Crown-8 (DB24C8) were studied at different temperatures in various organic solvents using the Cesium-133 NMR technique. Enthalpies (ΔH_c°) and entropies (ΔS_c°) of the complex formation were calculated from the Van't Hoff relationship, and it was found that both quantities are quite sensitive to the solvent. In all cases the complexes were enthalpy stabilized but entropy destabilized ($\Delta S_c^\circ < 0$). The origins of the enthalpies and entropies of complexation are discussed in terms of structural features (flexibility) of the ligands and of the solvation effect, and both parameters show interesting and consistent changes as a function of the ligand cavity size and number of binding sites in the polyether rings.

The thermodynamics of the complexation of the Cs^+ ion by the macrocyclic polyethers, DB27C9, and DB24C8 was studied in dimethylformamide-acetonitrile binary systems. Experimental values of ΔG_c°, ΔH_c°, and ΔS_c° again indicate that these quantities are quite sensitive to the solvent composition. In addition, in all cases the complexes are enthalpy stabilized but entropy destabilized.

Complex formation by the cesium ion with cryptand-222 (C222) was investigated in acetone-dimenthylsulfoxide,

acetonitrile-dimethylsulfoxide, propylene carbonate-dimethylsulfoxide, and propylene carbonate-dimethylformamide binary mixtures. The formation constant, K_f, of the $(C222 \cdot Cs)^+$ complex in these systems increases with increasing amounts of acetone, acetonitrile, and propylene carbonate in the respective binary mixtures, indicating a poorer solvating ability of these solvents for the Cs^+ ion and the ligand. In all cases the limiting chemical shifts of the cesium-cryptate are dependent on the solvent compositions, indicating that the Cs^+ ion is only partially insulated (by the ligand) from the solvent.

Cesium-133 NMR measurements were performed on competitive solvation of the Cs^+ ion in dimethylsulfoxide-water, acetonitrile-water, and methanol-water binary solvents. The geometric equilibrium constant, $K^{1/n}$, and the free energy of preferential solvation were obtained using the Convington equation. The order of solvating ability of these solvants was found to be dimethylsulfoxide > water ~ methanol > acetonitrile.

The complexing ability of the macrocyclic ligand, cyclo-(tetraethylene-glycol-2,6-pyridine dicarboxate) with the Na^+ and Cs^+ ion was studied in various nonaqueous solvents. This ligand forms a very stable complex with the Na^+ ion in acetone, acetonitrile, and propylene carbonate solutions. In the case of the Cs^+ ion the data clearly show the formation of both 1:1 (metal ion:ligand) and 1:2

(sandwich) complexes in propylene carbonate and dimethylformamide solutions.

The results obtained from the chemical shift measurement of the ^{205}Tl resonance on complexing of Tl^+ ion by benzo-15-Crown-5 in nonaqueous solvents demonstrate the weaker complexing ability of this ligand than that of 18-Crown-6 for thallium ion.

The complexation reaction between the Tl^+ ion and C222 was studied in acetone, acetonitrile, and dimethylsulfoxide solutions using ^{205}Tl NMR technique. Cryptand-222 forms a very stable complex with Tl^+ ion in these solvents. The rate of exchange between the free Tl^+ ion and the complexed-Tl^+ ion is fast on the NMR time scale; therefore, two ^{205}Tl signals are observed as long as the mole ratio of the C222/Tl^+ is between zero and unity.

ACKNOWLEDGMENTS

The author wishes to thank Professor Alexander I. Popov for his guidance, counseling and encouragement throughout this study.

He also wishes to thank Professor Michael J. Weaver for his helpful suggestions as second reader.

The financial aids of the people of Iran, as administered by the Ministry of Science and Higher Education is acknowledged. Gratitude is also extended to the Department of Chemistry, Michigan State University and the National Science Foundation for financial aid.

I would like to thank all the members of the laboratory of Dr. A.I. Popov for their friendship and discussion, and Mr. Wayne Burkhardt for his effort in keeping the NMR spectrometer in operating condition.

Finally, deep appreciation is extended to my mother, my wife, and my sisters for their patience, consideration, and encouragement throughout this study.

To them and to our son, Ali, I dedicate this thesis.

TABLE OF CONTENTS

LIST OF TABLES

LIST OF FIGURES

LIST OF ABBREVIATIONS

I. LIGANDS

18C6	18-Crown-6
DT18C6	1,10-dithia-18-Crown-6
TT12C4	1,4,7-trithia-12-Crown-4
DB21C7	Dibenzo-21-Crown-7
DB24C8	Dibenzo-24-Crown-8
DB27C9	Dibenzo-27-Crown-8
B15C5	Monobenzo-15-Crown-5
C222	Cryptand-222

II. SOLVENTS

NM	Nitromethane
AN	Acetonitrile
PC	Propylene carbonate
AC	Acetone
MeOH	Methanol
DMF	Dimethylformamide
DMSO	Dimethylsulfoxide
PY	Pyridine
TMG	Tetramethylguanidine
THF	Tetrahydrofuran

CHAPTER I

HISTORICAL REVIEW

A. Introduction

Although alkali metal cations play important role both in chemistry and in biology, the complexes of alkali metal ions were not considered by chemists for many years, and most chemists assumed that such complexes are not stable. In recent years, however, the coordination chemistry of alkali metal ions has mainly developed by the synthesis of crowns by Pedersen (1) and cryptands by Lehn and co-workers (2).

Macrocyclic polyethers (crowns) and macrobicyclic polyethers (cryptands) have been shown to form very stable complexes with the alkali and alkaline earth metal cations. These complexes can be used as models for investigation of ion transport through membranes in biological systems (3). Under ordinary conditions, the movement of electrolytes across the membranes would be extremely small because of low solubility of electrolytes in the organic layer. However, by proper choice of cyclic polyether complexing agent one may be able to achieve the selective cation complexation, and rapid and reversible reaction of the cation with the cyclic polyether followed by diffusion of the soluble cation-cyclic polyether through the membrane.

A large number of physicochemical techniques have been used to study the thermodynamic and kinetic aspects

of macrocyclic complexation (4). Of the various methods used for such studies, alkali metal NMR has been shown to be a very sensitive and powerful technique, since the chemical shifts of alkali nuclei are very sensitive to the immediate environment of an alkali ion in solution.

B. Macrocyclic Crown Ethers and Their Properties

a. Cation Selectivity and Complex Stability

Naturally occurring macrocycles were shown to be capable of actively transporting metal ions across membranes, beginning with valinomycin in 1964 (5). Macrocyclic polyethers, which are similar to the antibiotic ligands, both in structure and in their ability to form stable complexes with alkali cations were first reported in 1967 by Pedersen (1).

After the first publication by Pedersen, the chemistry of crown ethers has developed rapidly, and in many areas of chemistry and biology these compounds have started to play important roles. They have been successfully used for complexation, where they show a high degree of cation selectivity (6).

The crown ethers are uncharged molecules in which donor oxygens are arranged in a ring, usually each separated from the other by two methylen groups, $-CH_2-CH_2-$. The rings are of different sizes, containing from 4 to 20 oxygen atoms. Many of those (macrocyclic polyethers) containing five to ten oxygen atoms form stable complexes

with alkali and alkaline earth cations as well as some of the transition metal ions. Pedersen (7) found that the most favorable linkage for complexation process is $-O-CH_2-CH_2-O-$ followed by $-O-(CH_2)_3-O-$ and becomes ineffective beyond $-O-(CH_2)_4-O-$.

The structural formula of several synthetic crown ethers are shown in Figure 1. Since the names of these compounds are too cumbersome for use, the abbreviated names suggested by Pedersen are usually used for their identification. For example the name of compound (I) is 18-Crown-6 (or 18C6), in which the first number refers to the total number of atoms in the polyether ring, while the second number stands for the number of oxygen or other donor atoms. When sulfur atoms are substituted for the oxygen atoms a "thia" prefix is used. Therefore compound (II) is called 1,10-Dithia-18-Crown-6 (or DT18C6).

The most important property of the macrocyclic polyethers is their tendency to form very stable complexes with alkali ions with the stabilities that are comparable to those of transition metal complexes. The metal ion-crown ether complexes are normally considered to be formed by an electrostatic attraction between the cation and the dipolar end of the -C-O dipoles. It has been shown that the cation selectivity and complex stability of macrocyclic ligands depend on several important parameters. The more obvious ones being:

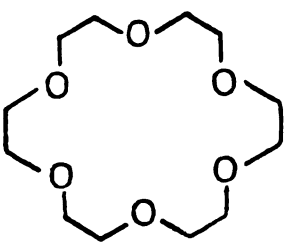

18-CROWN-6
(18C6)
(I)

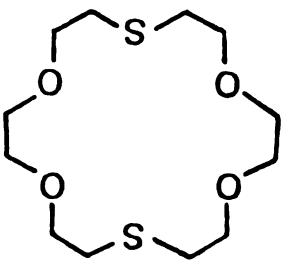

1,10-DITHIA-18-CROWN-6
(DT18C6)
(II)

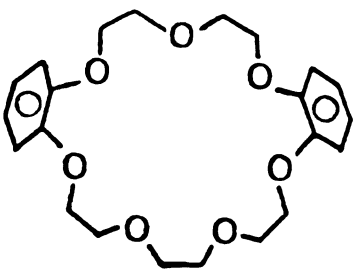

DIBENZO-21-CROWN-7
(DB21C7)
(III)

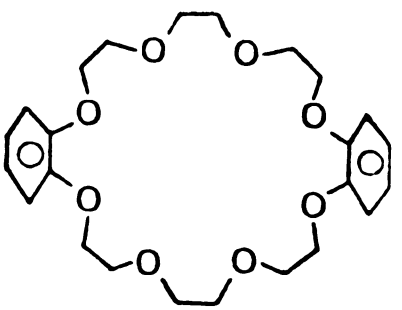

DIBENZO-24-CROWN-8
(DB24C8)
(IV)

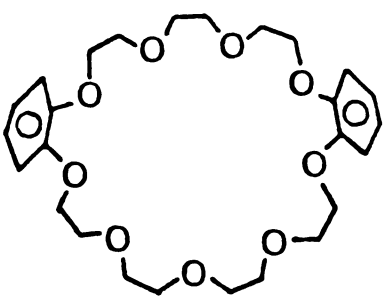

DIBENZO-27-CROWN-9
(DB27C9)
(V)

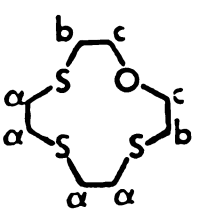

1,4,7-TRITHIA-12-CROWN-4
(TT12C4)
(VI)

Figure 1. Structure of Some Synthetic Macrocyclic Ligands.

1. The relative sizes of cation and the macrocyclic cavity:

The stability of the polyether complexes depends primarily upon how well the cation fits into the polyether ring. The prefered cation being that which has the best fit into the cavity. The size selectivity is determined by several types of primary effects such as: electrostatic and van der Waals attraction and repulsion between metal and ligand, ligand conformational changes, desolvation of the metal ion and the ligand, solvation of the metal ion-ligand complex, and the nature and number of binding sites.

The ionic diameters and the sizes of cavities of some of the crown ethers are listed in Table 1, and the relationship between the log of stability constant and

Table 1. Diameter in A° of macrocyclic crown ethers and some univalent cation (in crystals)

Cation	Cation diameter[a]	Crown ethers	Crown ether diameter
Li^+	1.20	All 15-Crown-5[b]	1.7 - 2.2
Na^+	1.90	All 18-Crown-6[b]	2.6 - 3.2
K^+	2.66	All 21-Crown-7[b]	3.4 - 4.3
Rb^+	2.96	Larger than 21-Crown-7[a]	over 4
Cs^+	3.34		
Ag^+	2.52		
Tl^+	2.80		

[a] Reference 1 [b] Reference 8

cation radius for interaction of macrocyclic crown ethers, 15C4, 18C6, and 21C7 with some of the univalent cations in methanol is shown in Figure 2.

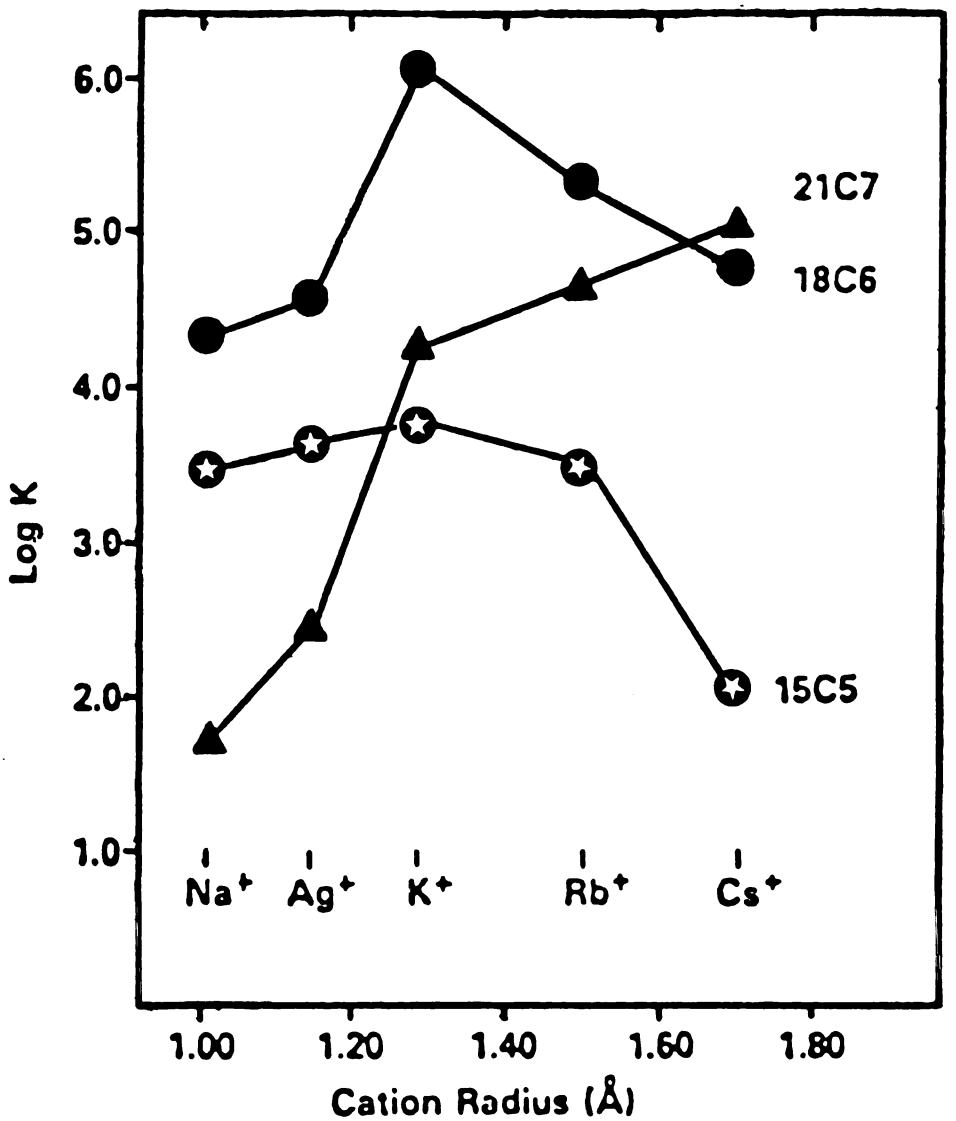

Figure 2. Variation of Log K vs. Cation Radius for Interaction of 15C5, 18C6, and 21C7 with Univalent Cation in Methanol at 25°C (9).

Although the fitness of the ligand ring cavity size and the cation size is an important factor in determining the stability of macrocyclic complexes, however, in some cases the size correspondence is not the predominant factor in determining selectivity,and other factors such as cation solvation energies, the solvation energy of the ligand and of the complex, and the formation of complexes of stiochiometry other than 1:1 may govern the selectivity of macrocyclic complexes. For example it has been shown (9) that in methanolic solutions K^+ is bound more strongly by 15-Crown-5 than Na^+ even though Na^+ ion has a better fit for the ligand cavity than K^+ ion.

It should be noted that the fit of the alkali cations in the ligand cavity can not explain the selectivities of large crown ethers (24-Crown-8 and larger) because their cavities are all larger than the largest alkali cation, Cs^+ (see Table 1). However, large stability constants still can be found, even when the cavity is much bigger than the metal cation. For example, the log of stability constants for complexes of K^+ ion with 18-Crown-6, 21-Crown-7, 24-Crown-8, 30-Crown-10, and 60-Crown-20 in methanol have been reported by Frensdorff (10) to be 5.0, 4.3, 3.5, 4.6, and 3.9 respectively. Apparently, the relatively large number of oxygen ethers and probably the flexibility of the ligand compensates for a decrease in stability when the size of the cavity is much larger than that of the cation.

2. Solvation power of the medium

The complexation process between the ligand and the metal cation is represented by the following general equation:

$$(\text{metal}^{n+})S_x + (\text{polyether})S_y \rightleftharpoons (\text{polyether - metal})^{n+}S_z + (x + y - z)S$$

in which S is the solvent molecule, x, y, and z are the solvation number of metal cation, ligand, and complex respectively. To what extent the complexation takes place obviously depends greatly upon the strength of the solvation of all species involved. In complexed species, the macrocyclic polyether replaces solvent molecules in the solvation sphere of the cation, therefore, the cation must lose the solvent molecules from its coordination sphere before it can accept a ligand. It should be stressed, however, that not only the metal ion, but also the ligand is solvated. The formation of a complex in solution is therefore, not only a competition for the metal ion between the ligand and the solvent molecules, but also a competition for the ligand between metal ion and the solvent molecules. Hence, the formation of the complex for a particular ion may be minimized, or even prevented, if the metal cation and the ligand are strongly solvated by the solvent. In addition, selectivity for certain cations over others may be altered according to the nature of the solvent.

The solvation of the ligand and metal ion can be influenced by the donor ability and dielectric constant of the solvents as well as the stereochemistry and size of the solvent molecules.

Popov and co-workers have studied extensively the complexation of alkali cations by macrocyclic ligands in a wide variety of nonaqueous solvents using alkali metal NMR technique (11-17). Their studies revealed that the stability of cation-macrocyclic complexes depends not only on the relative size of the ion and macrocyclic cavity but to a large extent on the nature of the solvent in which complexation takes place, i.e., on the solvent-ion, solvent-ligand, and ion-ion interactions.

Arnett and Moriarity (18) who studied complexation of alkali cations with dicyclohexo-18-Crown-6 in various solvents reported that the stabilities of the complexes of large cations are less affected by solvent than those of smaller ones.

3. Type(s) of binding sites in the ring

Various modifications have been made to the basic crown ether structure to enhance the selectivity of these ligands and the stability of complexes formed. Among these modifications are the substitution of ligand donor atoms such as sulfur and nitrogen for one or several of the polyether oxygens in the polyether ring.

Substitution of nitrogen or sulfur for oxygen reduces affinity for alkali ions but greatly increases the complexing power of these ligands for silver ion, because the covalent bonding plays a role in the silver ion complexes of polyethers containing nitrogen or sulfur (10). In general, for a ligand with a donor atom such as O, N, or S, the stability constant for alkali metal cations follows the trend, O > NR > NH > S. An opposite stability trend may be expected when the cation-ligand bond has appreciable covalent character as in the case of $Ag^+...N$ or $Ag^+...S$ interactions. Replacement of all of the oxygen donor sites in a macrocyclic ligand with sulfur causes the ligand completely loses its complexing ability for the alkali and alkaline earth cations (19).

4. Number of donor atoms

The number of binding sites certainly play a role in the complexing properties of macrocyclic polyethers. The polyether must have the sufficient number of the donor atoms in order to get the large complexation energy which is required for the desolvation step of the cation and ligand. Although little quantitative work has been done to investigate the effect of varying the number of donor atoms in the polyether ring, however, the relationship between the number of oxygen atoms in the crown ligand and the complex stability can be pointed out.

Cram et al. (20) reported that 18-Crown-5 is a much poorer complexing agent for t-butly amonium ion than 18-Crown-6. Studies of complexation reactions of C222 and $C22C_8$ (Figure 3) with Na^+ and K^+ in methanolic solutions by Lehn and co-workers showed that the C222 complexes of Na^+ and K^+ ions are much more stable than the complexes formed between $C22C_8$ with these ions (21). Both ligands have about the same cavity size but $C22C_8$ has two fewer oxygen sites. A corresponding decrease in the stability by a factor of 10^4-10^5 is observed.

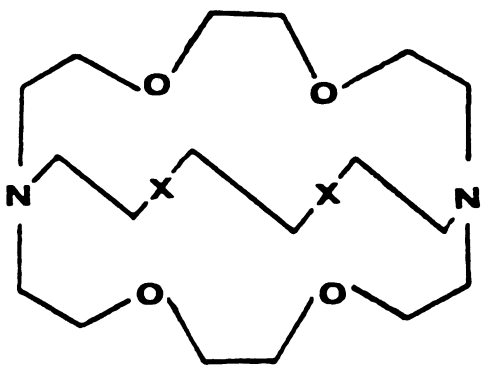

X = 0 C222

X = CH_2 $C22C_8$

Figure 3. Structure of Cryptand-222 and Cryptand-$22C_8$.

5. The electric charge of the cation

In general, with a similar cation radius, a bivalent ion has a higher stability constant than a monovalent ion. For example, it has been shown (6) that complexes of bivalent cations with dicyclohexyl-18-Crown-

6 are more stable in aqueous solution than those of univalent cations. However, comparing monovalent and bivalent cations having small but similar radii, the monovalent cation forms the more stable complex (i.e. $Na^{+} > Ca^{2+}$) with dicyclohexyl-18-Crown-6 (6), because the divalent ion is much more solvated than the monovalent ion.

b. Structure and Stiochiometry of Alkali Cation-Crown Ether Complexes

Because of strong interaction between alkali metal cations and the cyclic polyether complexing agents it is often possible to prepare crystalline salts that contain the complexed cation. The crystal structures of a number of such salts have been determined (22-28). The crystalline structure of macrocyclic polyether complexes can provide useful information about the structure of the cationic complex, and its interaction with the anion and with solvent of crystallization as well as the stiochiometry of the complex.

Evidently the stiochiometry of these complexes depends on the relative sizes of the cation and the macrocyclic cavity, the flexibility of the crown ether molecule, and the nature of the anion and of the medium (29). However the stiochiometry of the resulting metal-crown complexes is determined basically by the fit of metal cation in the cavity of the ligand. For those having the best fit, 1:1 (metal ion:ligand) complexes are considered to

be formed in solution as well as in the solid state. For a given size of metal cation, as the cavity size of the crown ether increases 1:1 complexes are formed, but the ligand increasingly tends to fold around the cation. Such folding of the ligand has been observed for dibenzo-24-Crown-8 in complexation with the Na^+ ion (30). A similar behavior (twisted conformation) of the polyether chain in the solid potassium iodide complex of dibenzo-30-Crown-10 has been demonstrated by Bush and Truter (31). Live and Chan (32) carried out PMR and ^{13}C NMR studies for the complexation of K^+ with dibenzo-30-Crown-10 in different solvents. The conclude that the structure of $(K \cdot DB30C10)^+$ in solution is similar to that in the crystalline state in which the K^+ ion is coordinated with all of the oxygen atoms of the ligand so as to form a "wrap around" complex. Figure 4 shows the crystalline structure of potassium iodide-dibenzo-30-Crown-10.

A 2:1 (metal ion:ligand) complex (or bimetalic complex) may be formed when the size of the cation is much smaller than the cavity size of the ligand. As illustrated in Figure 5, in such a compound, two cations are complexed in the unfold cavity of the ligand. The bimetalic products has been found by X-ray analysis of the complexes $(KNCS)_2$ (DB24C8) (33) and (Na-0-nitrophenolate)$_2$ (DB24C8) (34) and as expected for the complex of sodium with DB30C10 (30).

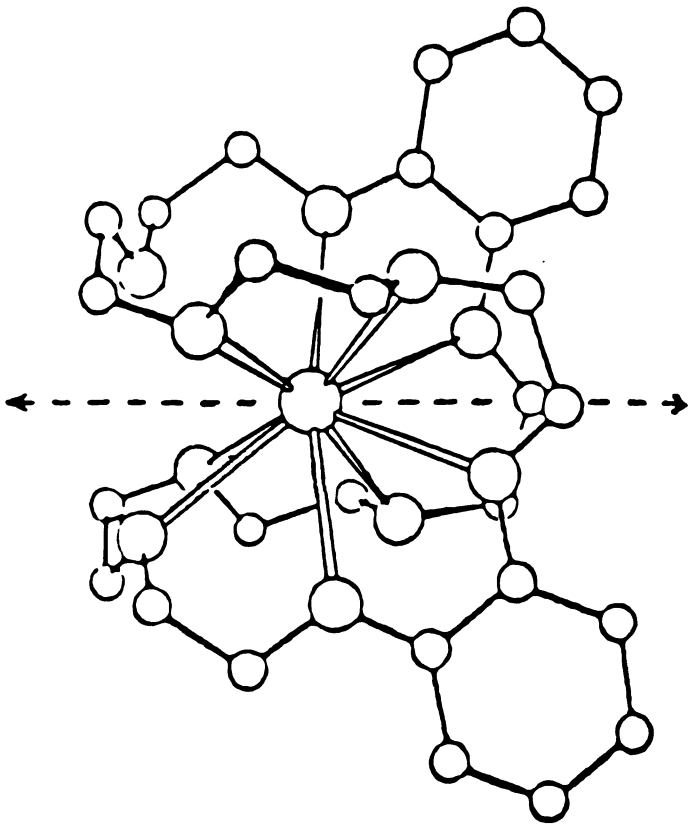

Figure 4. Crystalline Structure of (KI·DB30C10).

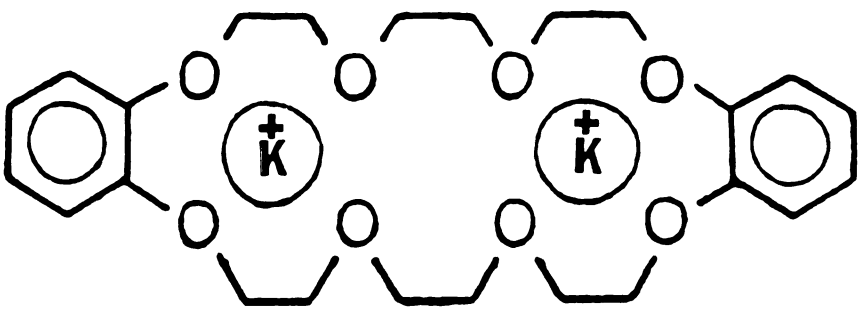

Figure 5. Structure of DB24C8·$(K^+)_2$.

A recent ^{23}Na and ^{13}C NMR study (35) of complexation between DB30C10 and the sodium ion in nitromethane and acetonitrile solutions showed that three kinds of sodium DB30C10 complexes with the respective stiochiometry of $Na\cdot(DB30C10)$, $Na_2\cdot(DB30C10)$, and $Na_3\cdot(DB30C10)_2$ are present in solutions.

When the size of metal cation exceeds the cavity of crown ether, sandwich complexes, in which the cation is located between two molecules of crown ether, can form in solution, Figure 6. The formation of such complexes can

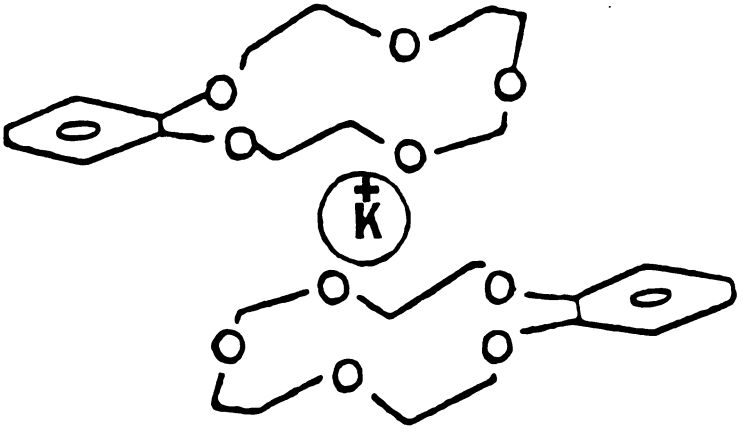

Figure 6. Sandwich Structure of $(B15C5)_2\cdot K^+$ Complex.

be easily detected by the alkali metal NMR techniques especially when the 1:1 complex is strong. The formation of sandwich complexes of Cs^+ with 18-Crown-6 and K^+ with 15-Crown-5 in different solvents has been reported by Mei (36) and Shih (37). The formation of cation-crown ether complexes with stiochiometry other than 1:1 has also been reported by Pedersen and Frensdorf (1, 8, 10, 29).

C. Sulfur-Oxygen Mixed Donor Macrocyclic Ligands

Donor atoms such as sulfur and nitrogen have been used to replace oxygen in crown ether rings in order to vary the cation binding properties of these ligands (10, 38-40). Substitution of sulfur for oxygen atoms in crown compounds markedly affects their complexing properties. Alkali and alkaline earth metal cations give no evidence of complexation when all of the oxygen donors are replaced by sulfur atoms (19). However, complexation is expected with the ligands containing both sulfur and oxygen as the binding sites.

Several methods have been used to prepare sulfur-oxygen mixed donor ligands (41-45). In general, a dimercaptan or sodium sulfide is reacted with an oligo-etheylene glycol dichloride in a medium of an appropriate base.

Macrocyclic polyether sulfides containing two to four sulfur atoms and two to four oxygen atoms have been found to form 1:1 complexes with alkali, alkaline earth, and silver ions (10, 41). Ultraviolet spectra of some of the sulfur crowns in solutions of methanol has been studied (41) and it has been found that these spectra are little affected by the addition of the salts of alkali and alkaline earth elements, suggesting that the interaction between these ligands and the alkali and alkaline earth cations is not strong in methanol. Complexation of

1,10-dithia-18-Crown-6 with potassium and silver ions has been studied in methanolic solutions by Frensdorff (10) using potentiometric technique. It was found that the silver ion has a greater affinity for the ligand than potassium ion. In this case, Frensdorff postulated that the bonding between 1,10-dithia-18-Crown-6 and silver ion is not purely electrostatic. Silver ion can form both ionic bonds with oxygen atoms and covalent bonds with sulfur atoms, but the potassium ion may only form ionic bonds.

Izatt (6) compared the thermodynamic stabilities of the K^+, Tl^+ and Ag^+ complexes formed by 15-Crown-5 and its sulfur analog (Table 2). A marked enhancement of the

Table 2. Log K_f values for reaction of 15C5 and thia-15C5 with some univalent cations in water (6)

Metal cation	15C5	thia-15C5
K^+	0.74	(a)
Tl^+	1.23	0.80
Ag^+	0.94	5.2

[a]No measurable reaction.

stability of the Ag^+ complex relative to that of either K^+ or Tl^+ complexes is observed as sulfur is replaced for oxygen.

In general, macrocyclic polyethers containing sulfur atoms are poorer complexing agents for alkali cations than their oxygen analogs, but they are good complexing agents for silver ion. In complexing ability, Pedersen (41) attributed the differences between the macrocyclic polyethers and their sulfur analogs to the differences in the sizes and electronegativities of oxygen and sulfur atoms. Oxygen is a smaller atom than sulfur and the C-O-C bond angle is greater than the C-S-C bond angle; therefore, in the sulfur substituted ligand, the symmetrical distribution of the negative charge around the "hole" of the polyethers is disturbed due to the large size of the sulfur atom. In addition, the electronegativity of the oxygen atom is higher than that of the sulfur atom which makes the C-S bonds less ionic than the C-O bonds.

Crystalline structures of some of the cyclic polyethers containing sulfur atoms and their complexes have been determined by several researchers. Dally and coworkers (46) determined the crystal structure of 1,4,7-trithia-12-Crown-4 (Figure 7). As shown in this figure

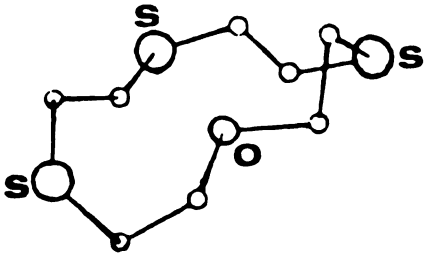

Figure 7. Crystalline Structure of 1,4,7-trithia-12-Crown-4.

the oxygen atom is directed toward the center or the ring but the sulfur atoms are directed away from the polyether ring. X-ray analyses for 1,10-dithia-18-Crown-6 and 1,4-dithia-15-Crown-5 also showed that the large sulfur atoms are directed away from the ring (46). This may be attributed to the differences in bond length of the C-O and C-S bonds and in the van der Waals radii for oxygen and sulfur atoms.

It has been shown that the mercury atom in the $HgCl_2$ complex with 1,4-dithia-18-Crown-6 and the paladium atom in the $PdCl_2$ complex with 1,10-dithia-18-Crown-6 bind only with two sulfur atoms and lying outside the cavity (47, 48). Therefore, binding of sulfur containing crowns to Hg^{2+} and Pd^{2+} may not be of inclusion type which may account for no "macrocyclic effect" (see page 30) for these thia-substituted ligands (47).

D. Complexing of Metal Cations by Macropolycyclic Ligands-Cryptands

Soon after Pedersen's publication on the synthesis of the first crown ethers in 1967, Lehn and co-workers reported the synthesis of macrobicyclic ligands, or cryptands (2, 49). These compounds also form complexes (cryptate) with the same cations as the cyclic polyethers. In cryptates, the complexed cation is enclosed inside in a three dimensional cavity, whose size, shape, and the nature of binding sites determine the stability and the selectivity of the complexes. The size of the cavity can be varied by changing

the length of the ether bridges. The three bridges of a bicyclic ligand shield the cation from the medium if the cation fits or is smaller than the diameter of the cavity.

The cryptand compound shown in Figure 8 is called cryptand-222 (K = m = n = 2) or C222 where the "C" refers to cryptand and "222" stands for the number of oxygen atoms in the chains. The cryptand-222, which contains six oxygen atoms in the bridges and two nitrogens at the bridge heads, is a bicyclic ligand, therefore it is called a [2]-cryptand. Ligands containing three and four macrocycle are called [3] and [4]-cryptands respectively (50).

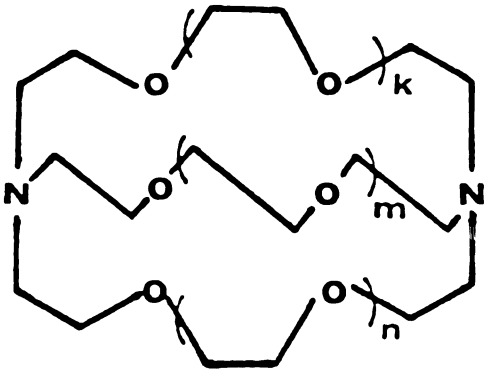

K = m = 0, n = 1	C211 (1.6 A°)
K = m = 1, n = 0	C221 (2.2 A°)
K = m = n = 1	C222 (2.8 A°)

Figure 8. Structure of Cryptands (with internal diameter).

Complexation constants of cryptands have been determined mainly in water and methanol solutions. Lehn and co-workers (2, 51, 52) have studied the formation constants of alkali metal cryptates in aqueous and methanolic solutions

using potentiometric technique. Stability constants of complexes of a different cryptands with cesium ion in a number of solvents are reported by Hsu (53). In general, cryptands form much stronger complexes with the alkali ions than the crown ethers.

Complexation studies of C222, C221, and C211 with the lithium ion were performed in water and several non-aqueous solvents by Cahen et al. (14) using ^{7}Li NMR technique. Their results revealed that the chemical shift of the lithium ion complexed by C211 is solvent and anion independent. Cryptand-211 has a cavity size nearly equal to that of the unsolvated lithium ion. It is expected, therefore, that the lithium ion is completely isolated by the ligand. On the other hand, with C222 and C221, whose radii are much larger than that of the lithium ion, the resonance frequency of the complexed lithium ion does depend somewhat on the solvent, suggesting that in these cases the lithium ion is not completely shielded by the ligand, and the loose structure of the Li^{+}-C222 and Li^{+}-C221 complexes permits the solvent molecules to approach to the metal ion so as to affect its resonance frequency.

Popov and co-workers (14, 54-56) studied the complexation reaction between cryptands and alkali cations in several solvents using alkali metal NMR techniques. As with the crown ethers, they found that the stability constants of appropriate complexes are greater in the dipolar protophobic than in the protophilic solvents.

It has been suggested that the mechanism of complexation is complicated because of conformational equilibrium in the ligand (52, 57). As shown in Figure 9 both the free macrobicyclic ligands and their complexes may exist in three forms, exo-exo (or out-out), endo-endo (or in-in), and exo-endo (or out-in), differing by the orientation of the nitrogen bridgheads toward the inside or outside of the intramolecular cavity (58-60).

Macrobicyclic ligands in their in-in conformation contain an internal cavity of about spherical shape (61). Therefore, they should be suitable for the spherical ions such as alkali and alkaline-earth cations. The exo-exo

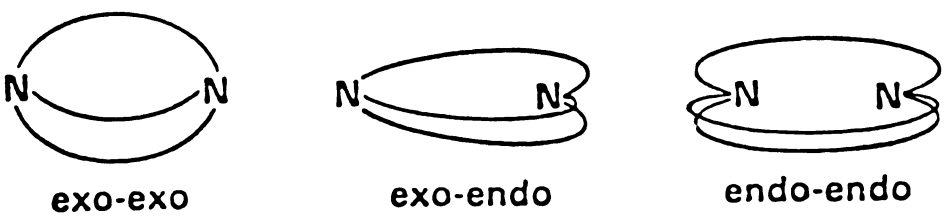

Figure 9. The Configurations of Cryptand C222.

forms in which the lone pairs of the bridgehead nitrogens are directed away from the cavity would not be expected to complex appreciably with metal ions. X-ray analysis of the crystal structures of a number of cryptates showed that the cation is indeed located in the center of the molecular cavity of the macrobicycle in the "in-in" form (62-65).

In addition to preparation of the macrobicyclic ligands, Lehn and co-workers also synthesized tricyclic

cryptands (50, 55, 57), and in several papers, have described the properties of these compounds. The cavity of the tricyclic ligands can be cylindrical or spherical as represented in Figure 10. The cylindrical ligands are formed by two macrocycle linked through two bridges, and contain three cavities, two on the top and the bottom, and the third in the center. The size of the cavities can be changed, by varying the size of the macrocycles and the length of bridges.

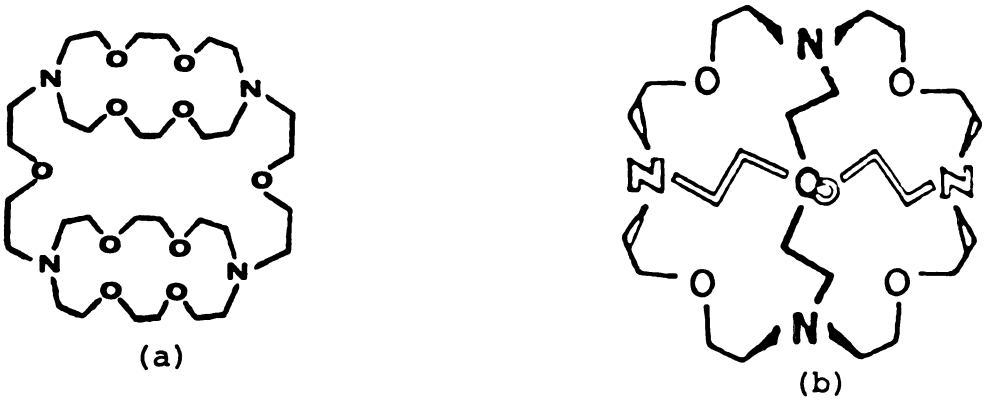

Figure 10. The Structures of (a) Cylindrical, and (b) Spherical Macrotricyclic Cryptands.

As shown in Figure 11 these ligands can form mononuclear or binuclear complexes. In a binuclear cryptate the two macrocycles each serve as a receptor site for a cation. Values of log of stability constants for successive formation of mononuclear and binuclear [3]-cryptates of alkali and alkaline earth metal cations have been determined in methanol/water mixture by Lehn and Simon using ion selective electrodes (68). Their results

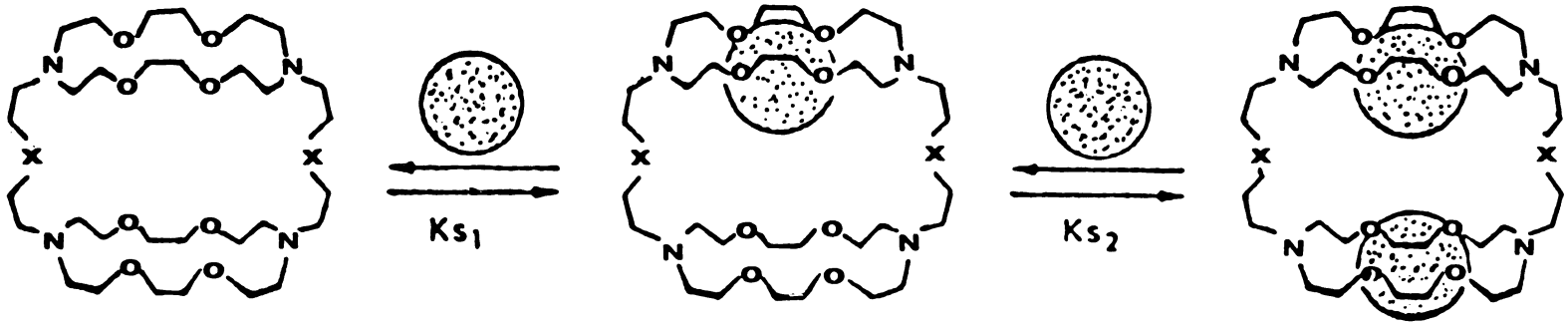

Figure 11. Successive Formation of Mononuclear and Binuclear Cryptate of Cylindrical Macrocyclic Cryptand (Lehn).

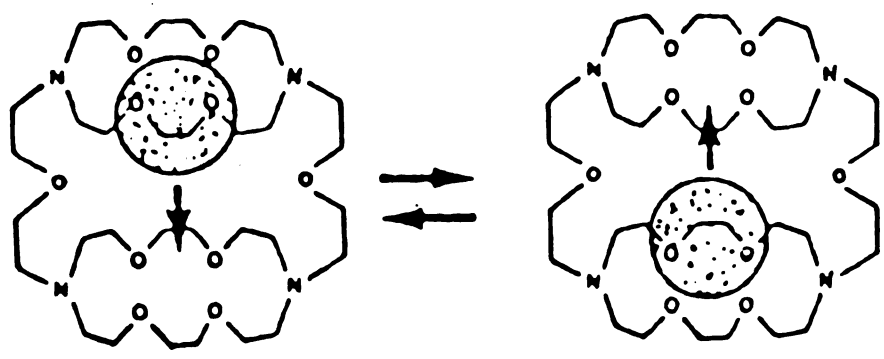

Figure 12. Intramolecular Cation Exchange Process in Mononuclear Complexes of Cylindrical Cryptand (Lehn).

showed that the first formation constant of the inclusion complex of a given ion is somewhat larger than the second one. This indicates that the inclusion of the second ion is almost as easy as that of the first one.

In mononuclear complexes of [3]-cryptates an intromolecular cation exchange may occur in which the cation exchanges between two sites. The cation exchange rate between two rings inside the cavity of a [3]-cryptate has been studied by ^{13}C NMR technique (68). The spectral changes showed an internal cation exchange between binding sites on two rings inside the cavity of the ligand as represented in Figure 12.

The spherical macrotricyclic ligands contain a single central cavity (Figure 10-b) and these ligands should be especially well suited for the alkali and alkaline metal cations which are spherical in shape. Ligands containing spherical cavity were prepared by Graf and Lehn (50). They complexed K^+, Rb^+, Cs^+, NH_4^+ and Ba^{2+} ions. These compounds also form very stable complexes with anions. The halide complexes are reported to be quite stable in water (50).

E. Thermodynamics of Cation-Macrocyclic Interaction

Thermodynamics in solution of macrocyclic polyether complexes has been extensively studied during the last ten years (3, 6, 10, 69). Most of the studies have been carried out in water, water/methanol or methanolic solutions

(47), consequently little is known at the present time about the thermodynamics of complexation in nonaqueous solvents.

The equilibrium constant for the complexation of the Cs^+ ion by C222 has been studied as a function of temperature in acetone, propylene carbonate, and N,N-dimethylformamide solutions using ^{133}Cs NMR techinque (54). The ΔH°_c and ΔS°_c values, obtained in this work, showed that the complex is enthalpy stabilized but entropy destablized. Thermodynamics of complexation of Cs^+ ion with large macrocyclic polyethers, dibenzo-30-Crown-10, dibenzo-24-Crown-8, and dibenzo-21-Crown-7 have been studied in five nonaqueous solvents by ^{133}Cs NMR technique (70). It was found that the stability of the 1:1 complexes formed between Cs^+ ion and these ligands increases with decreasing temperature and in all cases negative ΔH°_c and ΔS°_c values characterize the formation of such complexes. It was concluded that as the cyclic polyether ring size increases, the entropy of complexation becomes more negative, suggesting that significant conformational changes of the ligand may be important in the formation of these complexes.

An excellent interpretation of the enthalpic and entropic contributions for complexation in aqueous solutions has been discussed by Kauffmann and co-workers (71).

The stability constant (K_f) of the complex is related to the net changes of free energy, ΔG°, enthalpy, ΔH°, and entropy, ΔS°, according to the well known equation:

$$-RT \ln K = \Delta G^\circ = \Delta H^\circ - T\Delta S^\circ.$$

From these functions important conclusions may be taken about the various factors governing complex formation, such as solvation effects, the character of the coordinate bond, and the changes of the structure often taking place during complex formation.

Stability constants, from which the ΔG° values are calculated, provide a direct measure of the extent of complexing in solution. The measured enthalpy change for a cation-ligand reaction in solutions reflects (a) the bond energy of the cation-donor atom bonds, (b) solvation energy of the reactants and products, (c) the contribution arises from changes in ion-solvent interaction beyond the first solvation or ligation shell , (d) changes in interbinding sites repulsions. Several factors contribute to ΔS°, including (1) ligand and cation desolvation, (2) solvation of the complex, (3) translational entropy loss on formation of a single complex from two species, (4) changes in ligand internal entropy upon complexation caused by orientation and conformational changes.

The cyclic polyethers form much more stable complexes than do their corresponding open chain analogs. Morf et al. (72) and Izatt et al. (47) have compared log K values for the reactions of some macrocyclic ligands and their open chain analogs with K^+, Na^+, Ba^{2+}, and Cu^{2+} ions. As illustrated in Table 3 the stability constants

Table 3. Comparison of Stability Constants of Metal Cation Complexes of Macrocyclic Ligands with Their Open Chain Analogs (72,47)

Ligand	Cation	Solvent	Log K_f (at 25°C)
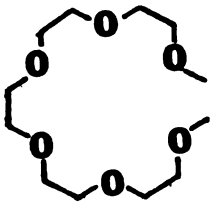	K^+	MeOH (99 Wt. %) H_2O (1 Wt. %)	2.27
	Na^+	"	1.0
	Ba^{2+}	"	2.51
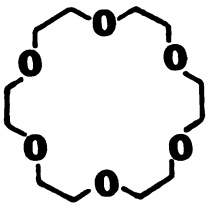	K^+	"	6.05
	Na^+	"	4.33
	Ba^{2+}	"	7.0
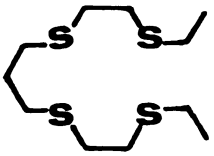	Cu^{2+}	MeOH (80 Wt. %) H_2O (20 Wt. %)	1.15
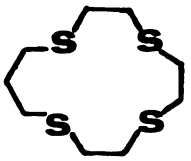	Cu^{2+}	MeOH (80 Wt. %) H_2O (20 Wt. %)	3.48
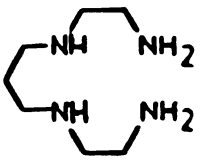	Cu^{2+}	H_2O	20.1
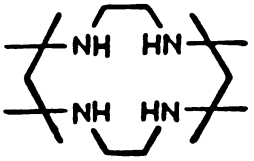	Cu^{2+}	H_2O	28.0
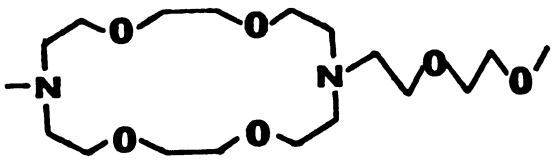	Ba^{2+}	H_2O	4.80
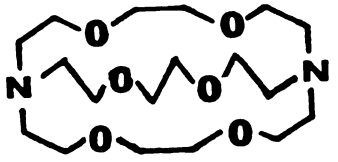	Ba^{2+}	H_2O	9.50

of open chain ligands are several orders of magnitude lower than those of their cyclic analogs.

In order to emphasize the greater stability of macrocyclic complexes over the non-cyclic ones, the term "macrocyclic effect" was used by Cabbiness and Margerum (73). The macrocyclic effect is a Gibbs energy term, referring to the following reaction:

$$\underset{\text{non-cyclic}}{(ML)^{n+}} + \underset{\text{macrocyclic}}{L'} \rightarrow \underset{\text{macrocyclic}}{(ML')^{n+}} + \underset{\text{non-cyclic}}{L}$$

and the enhanced stability of the macrocyclic complex may have its origins in both enthalpy and entropy terms (52).

The macrocyclic effect has been explained in terms of entropy factors which oppose complete envelopment of cations by acyclic polyethers (73). The linear polyether does not envelope the cation as completely as the cyclic one because of electrostatic repulsion between its terminal groups and the unfavorable entropy change involved in forcing the linear into an almost cyclic structure. Although this effect was originally explained in terms of entropy factors which oppose complete envelopment of cations by acyclic polyethers, however, studies on macrocyclic tetramines (74, 75) and tetrasulfide systems (76) revealed that the thermodynamic parameter (ΔH), coupled with ligand solvation effects, often play a greater role in the origin of the macrocyclic effect.

The enhancement of the stability of cryptate complexes over the crown complexes has been observed by Lehn and co-workers (21). The increase in complex stability of bicyclic ligand over monocyclic ligands which is even larger than the macrocyclic effect is called "cryptate effect" or "macrobicyclic effect" (21). This effect is also illustrated in Table 3.

F. Nuclear Magnetic Resonance

a. Introduction

Solutions of alkali metal cation complexes have been studied by various experimental techniques. Potentiometric measurements have been done by Frensdorff (10) and Lehn and co-workers (2) for determination of formation constants of alkali ion complexes with many macrocyclic ligands. In recent years, however, nuclear magnetic resonance spectroscopy, as well as infrared and Raman spectroscopy have become powerful techniques for the study of the solvation phenomena and of complexation reaction in both aqueous and nonaqueous media (16, 77-85).

Since nuclear magnetic resonance measurements are specific for each nucleus, they can be used for quantitative and qualitative determinations of the species in solutions. Proton, ^{13}C, and alkali metal NMR studies have provided much detailed information about the nature of cation complexation by crowns and cryptands. Proton and ^{13}NMR techniques can be used for ellucidation of structure

in solution as demonstrated, for example, by the work of Live and Chan (32) who were able to show the solution structures of complexes of some of the crown ethers.

Nuclear magnetic resonance of the alkali cations and the thallium ion have been used extensively for studying ionic solvation, ionic association, preferential solvation of alkali cations and thallium ion and in complex formation with a variety of ligands, particularly macrocyclic ligands in aqueous as well as nonaqueous solvents. A review of the alkali metal NMR has been published by Popov (77). An older review of the use of the NMR for the study of ions in different solvents has been published by Amis and Hinton (86).

b. Chemical shift measurements of alkali metal nuclei

Since the alkali metal chemical shifts are very sensitive to the immediate environment of the corresponding metal ion in solutions, they have been used for the studies of ion-ion, ion-solvent and ion-ligand interactions (77). For nuclei with an adequate NMR sensitivity, observation of signals at low enough concentrations to allow determination of stability constants should be possible as demonstrated by Dewitte et al. for ^{133}Cs (87).

All of the alkali metals possess at least one isotope with a magnetic nucleus, i.e., ^{7}Li, ^{23}Na, ^{39}K, ^{87}Rb, and ^{133}Cs. The nuclear properties of the alkali elements are given in Table 4. In all cases the spin is

Table 4. Nuclear Properties of Alkali and Thallium Nuclei.

	^{7}Li	^{23}Na	^{39}K	^{87}Rb	^{133}Cs	^{205}Tl
Nuclear spin (in units of $h/2\pi$)	3/2	3/2	3/2	3/2	7/2	1/2
Magnetic moment μ (in multiples of the nuclear magneton, $eh/4\pi MC$)	3.2560	2.2101	0.3909	2.7414	2.5642	1.612
Relative sensitivity to ^{1}H at constant field	0.294	9.27×10^{-2}	5.08×10^{-4}	0.177	4.74×10^{-2}	0.192
Natural abundance (%)	42.57	100	93.08	72.8	100	70.48
Resonance frequency at 14.09 kilogauss field (MHz)	23.315	15.868	2.800	19.630	7.864	34.611

greater than $\frac{1}{2}$ and, therefore, the nuclei have a quadrupole moment and consequently, the resonance lines cannot be narrow. In practice, however, due to the extremely rapid and generally random molecular motions which averages the local magnetic and electric fields to very small values, with the exception of ^{87}Rb, the resonance lines are narrow and, in the case of ^{7}Li and ^{133}Cs the natural linewidth are less than 1 Hz (16). Therefore in most cases the chemical shifts can be measured precisely.

The position of a nuclear magnetic resonance signal is determined by the total shiedling that the nucleus under investigation receives from various sources. This shielding is expressed by the screening constant, σ. A general formula for σ has been developed by Ramsey (88). According to Ramsey's equation the screening constant is the sum of the various diamagnetic and paramagnetic terms: $\sigma = \sigma_p + \sigma_d$.

Saika and Slichter (89) divided the screening constant into three independent contributions represented by:

$$\sigma = \sigma_d + \sigma_p + \sigma_0$$

The σ_d term (shielding factor) is related to the local diamagnetic currents in the molecule and arises from the induced magnetic field due to the circulation of electrons around the nucleus; σ_p is the paramagnetic term (deshielding factor) and is usually the dominant term, and

it arises from the interaction of ground state with excited electronic states in the presence of a magnetic field. Contributions from other atoms to the shielding of the resonant nucleus are contained in σ_0. Unless one is considering proton shifts, σ_0 can be ignored. For the heavier nuclei, σ_p is so much larger than σ_d that the later term can be ignored (90).

Kondo and Yamashita (91) suggested that the paramagnetic shift term is caused by the repulsive forces between the closed shell of the ions. These forces act over a short range and compete with electrostatic attractions which tend to reduce the separation of ions containing opposite charges. The paramagnetic term for an alkali nucleus can be written according to the following equation:

$$\sigma_p = -16\ \alpha^2\ \langle r^{-3}\rangle_{np}\ (\Delta E)^{-1}_{np}\ S^2$$

in which α is a constant = $\frac{e^2}{2mC^2}$ where m and e are the mass and charge of the electron respectively, $\langle r^{-3}\rangle_{np}$ is the expectation value for the outermost P-electron of the element, $(\Delta E)^{-1}_{np}$ is the average mean excitation energy from the np to the (n+1)p orbital, and S is the overlap integral between P orbital of the alkali ion and the neighboring ions.

Deverell and Richards (92) who modified the theory of Kondo and Yamashita, provided a qualitative interpretation of cation chemical shift in solutions. They suggested that the chemical shift at concentration c, relative to

the free ion can be written as:

$$\sigma = -16\ \alpha^2 \langle r_i^{-3} \rangle_{np}\ (\Delta E)_{np}^{-1}\ [\sum_j \Lambda_{i-j}^c + (\Lambda_{i-H_2O}^c - \Lambda_{i-H_2O}^\circ)]$$

where Λ_{i-j}^c refers to the appropriate sum of the overlap integrals for the orbital of the central ion (i) and all other ions present in solution which may have the same charge or the opposite charge of the central ion. The $\Lambda_{i-H_2O}^c - \Lambda_{i-H_2O}^\circ$ indicates changes in the effect of solvent-ion overlap integrals. Since $\langle r_i^{-3} \rangle_{np}$ and $(\Delta E)_{np}^{-1}$ both increase with increasing atomic number (93), the magnitude, and therefore the relative importance of σ_p increases in going from Li^+ ion to Cs^+ ion. Since the range of the chemical shifts varies directly with the atomic number of the alkali nucleus, the NMR measurements are particularly sensitive in the case of cesium-133 nucleus. In addition the narrowness of the resonance line permits very accurate determinations of the chemical shifts.

C. Thallium-205 NMR Measurement

The thallium ion has been proposed as a probe of the role of the alkali ions in biological systems (94) because its chemistry is analogous to that of the K^+ ion (95). The ionic radii of K^+ and Tl^+ ions are similar (1.33 and 1.40 A° respectively) (96), and the chemical properties of these two ions are sufficiently alike that Tl^+ can replace K^+ in several enzymes without loss of

activity (96). The NMR properties of ^{205}Tl are given in Table 4. Thallium-205 is an ideal NMR probe for studies of ionic solvation, ionic association, and complex formation in aqueous as well as nonaqueous solvents, because the change in its resonance frequency is very sensitive to its chemical surrounding, and it has a spin = $\frac{1}{2}$, high natural abundance, and high sensitivity. The solvent dependent chemical shift of ^{205}Tl is much larger than alkali nuclei. For example the change in its resonance frequency in going from water to pyridine is approximately 782 ppm. By comparison, with the change in chemical shift of ^{23}Na in these two solvents which is about 1.26 ppm (81). Therefore, the greater sensitivity of the thallous chemical shift to the environment of the ion makes it a better system than alkali metal ions as regards of subtle changes in its environment.

Chemical shift measurements of ^{205}Tl have been made by Freeman et al. (97, 98) for different thallium salts in aqueous solutions.

Bacon and Reeves (99) who studied the spin-lattice relaxation of ^{205}Tl, reported that the spin-lattice relaxation rate and the spin-spin relaxation rate (R_2) of the thallous ion are very sensitive to the disolved oxygen in aqueous solutions. It was found, however, that the relaxation rates are independent of the anion, the concentration, and isotope substitution in the solvent (i.e., D_2O for H_2O) or in the resonant nuclei (i.e., ^{203}Tl for ^{205}Tl). In addition, chemical shift measurements have

been made and the effects of the addition of complexing agents (ethylendiamine and 0-phenanthroline) on the chemical shift and relaxation of thallous ion in aqueous solution have been discussed by Chan and Reeves (100).

Zink et al. (101-103) studied preferential solvation and the solvent dependence of the thallium-205 using ^{205}Tl NMR technique. They found that the solvent dependence chemical shift of the thallous ion is over 2600 ppm depending on the particular thallium salt and solvent under study, and it correlates linearly with the relative solvating ability of the solvents for Tl^+ ion.

Solvation of the thallous ion in dilute solutions of several binary solvent systems was studied by Briggs and Hinton (84, 85) by ^{205}Tl NMR spectroscopy. An attempt was made to separate solvation effects related to the Lewis basicity of the solvents from the structural changes in the solvation sphere. It was found that Tl^+ ion is preferentially solvated by DMSO rather than pyridine, despite the latter's greater electron-donating ability. This was explained in terms of structural effect or strict effect related to the size of pyridine molecule. Dimethylsulfoxide is known to be associated in the pure liquid due to dipolar interactions through S-O bond (104). Introduction of pyridine into neat DMSO results in the break up of the polymeric structure of the latter via a dipole interaction, resulting in an enhancement of donicity of DMSO in the mixture (104). In

addition, pyridine is more structured in mixed solvent system than in the pure solutions, and thus less able to solvate the ions when mixed with other solvents (85).

Thallium-205 NMR method has been used by several researchers for studies of the complexes of Tl^+ ion with antibiotic ionophores such as, nonactin, monactin, dinactin (105) and valinomycin (96). Srivanavit and co-workers (106) determined the stability constants of thallium complexes relative to formation constants of other univalent cations complexes for a number of macrocyclic crown ethers in various solvents using NMR techniques. The effect of the solvents on the binding constants was discussed in terms of solvation of the ions and the ligand.

CHAPTER II

EXPERIMENTAL PART

A. Synthesis and Purification of Ligands

a. Synthesis of 1,4,7-trithia-12-Crown-4 (TT12C4)

The complexing agent 1,4,7-trithia-12-Crown-4 was prepared in a manner similar to that reported by Bradshaw and co-workers (42). This material was synthesized from Bis(2-chloroethyl) ether (Aldrich) and Bis(2-mercaptoethyl) sulfide (K and K) as illustrated in the following reaction

$$ClCH_2\text{-}CH_2\text{-}O\text{-}CH_2\text{-}CH_2Cl + HS\text{-}CH_2\text{-}CH_2\text{-}S\text{-}CH_2\text{-}CH_2\text{-}SH$$

$$\xrightarrow[C_2H_5OH]{NaOH} 2NaCl + 2H_2O +$$

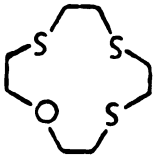

A solution of sodium hydroxide was prepared by dissolving 12.5 gram of sodium hydroxide (Dark Brothers) in 400 ml of ethanol and was placed in a large three-necked round bottom flask. An equimolar mixture of the Bis(2-chloroethyl) ether (0.11 mole, 15.75 gram) and Bis(2-mercaptoethyl) sulfur (0.11 mole, 17.1 gram) was dissolved in 300 ml of ethanol and added dropwise to the NaOH solution over a long period of time (about 6 hours). The reaction flask was equipped with a mechanical stirrer as well as with a nitrogen gas inlet and outlet. In order to increase the yield of the product the reaction was carried out at high dilution with vigorous stirring, under a nitrogen atmosphere. Once the two solutions were

completely mixed, the reaction mixture was refluxed for about 8 hours and then was allowed to cool to room temperature. The excess base was neutralized with hydrochloric acid, and then the resulting mixture was filtered. The solvent was removed using the Rotovap-R Büchi. The residual viscous liquid was extracted with three 200 ml of diethyl ether. The combined ether extracts were dried over anhydrous magnesium sulfate and then filtered. After removal of the ether and recrystallization of the remaining yellow solid in benzene, the pure product was obtained. Following the purification by recrystallization, the ligand was dried under vacuum over barium oxide (Fisher Scientific Co.) for 3 days at room temperature. Its melting point (measured on the Fisher Johns Melting Point apparatus) was found to be 91°C which is identical to the literature value (42). A 0.1M solution of TT12C4 in deuterated chloroform (Aldrich) was used and the chemical shifts for three kinds of hydrogen (a, b, and c, Figure 1) were measured relative to TMS (Merck Co.) as an internal standard. The NMR assignments were exactly the same as reported by Bradshaw (42).

b. Purification of commercial ligands

Eighteen-Crown-six (18C6) was obtained from the Parish Chemical Company. The ligand was purified by forming a complex with acetonitrile (Matheson, Coleman and Bell) (107). The fine white crystals of the 18C6.MeCN

complex were dried under vacuum for 48 hours to remove the weakly bound MeCN from the complex. The melting point of the purified product was 38-39°C in satisfactory agreement with the reported value of 39°C (107). Dithia-18-Crown-6 was obtained from Parish Chemical Company and required vacuum drying for two days. The complexing agents, dibenzo-24-Crown-8, and dibenzo-21-Crown-7 were received from Parish Chemical Company and they were purified by recrystallization from normal heptane (Mallinckrodt) and then dried under vacuum over barium oxide (Fisher Scientific Co.) for three days. The melting points of the fine white crystals were found to be 114° and 106°C, respectively, which are the same as the literature values (29).

Cryptand-222 (E.M. Laboratories, Inc.) and Cyclo-(tetraethylen-glycol-2,6-Pyridinedicarboxylate) (Parish Chemical Company) were purified by two recrystallizations from n-hexane (Fisher Scientific Co.) and then vacuum dried for several days. Dibenzo-27-Crown-9 (Parish Cehmical Company) was recrystallized from reagent grade n-heptane and dried under vacuum for several days.

B. Salts

Lithium perchlorate (Fisher Scientific Co.) was oven dried at 190°C for several days. Anhydrous silver nitrate (Baker, AR) was dried over P_2O_5 in a vacuum oven at 65°C for one day. Thallium (I) perchlorate (K & K) after purification by recrystallization from deionized

distilled water was dried at 110°C for twenty four hours. Sodium tetraphenylborate (T.J. Baker) was dried in a vacuum oven at 60°C for three days. Cesium thiocyanate (Rocky Mountain Research, Inc.) was recrystallized from methanol and dried under vacuum at 50°C for 48 hours. After drying, the salts were stored in vacuum desicators charged with granulated barium oxide (Fisher Scientific Co.).

C. Solvents

The solvents were purified and dried according to the following procedures: Propylene carbonate (Aldrich), nitromethane (Aldrich), dimethylformamide (Mallinckrodt), dimethylsulfoxide (Fisher), and Pyridine (Fisher) were refluxed over calcium hydride (Fisher) under reduced pressure over night and then fractionally distilled and further dried over freshly activated molecular sieves (Lind type 4A). Molecular sieves were washed with distilled water, then oven dried, and finally activated to 500°C under a flow of dry nitrogen. Acetone (Fisher) was refluxed over calcium sulfate (W.A. Hammond Drierite), fractionally distilled, and dried over activated molecular sieves. Tetrahydrofuran (Baker, analyzed reagent) and acetonitrile (Mallinckrodt) was refluxed over calcium hydride, fractionally distilled and further dried over activated molecular sieves. Tetramethylguanidine (Eastman) was refluxed over granulated barium oxide (Fisher) for about 30

hours and purified by fractional distillation under reduced pressure. Methanol (Fisher or Mallinckrodt) was refluxed over magnesium turnings and iodine for ~ 24 hours and then distilled under nitrogen atmosphere. The distillate was allowed to stand over activated molecular sieves for ~ 20 hours.

All of these solvents were stored in brown glass bottles and transferred in a dry box under a nitrogen atmosphere. Water contents and purity of the solvents were tested either by Karl Fischer titration using an automatic Karl Fischer Aquatest (Photovolt Corp.) titrator or by using a Varian Aerograph Model 490 gas chromatograph with a Porapak Q Column. The water content of the purified solvents was below 100 ppm in all cases.

Acetonitrile-d_3 (Stohler Isotope Chemicals) and dimethylsulfoxide-d_6 (Stohler Isotope Chemicals) were used as received.

D. Instrumental Measurements

Alkali metal and thallium NMR measurements were performed on a highly modified Varian Associate DA-60 spectrometer in the Fourier Transform mode, operating at 23.31, 15.87, 7.87 and 34.61 MHz for ^{7}Li, ^{23}Na, ^{133}Cs and ^{205}Tl respectively. The instrument has a magnetic field of 14 Kilogauss (1.4 Tesla), and it is equipped with a wide-band probe capable of multinuclear operation (108). An external proton field lock was employed to

maintain the field stability. The NMR spectrometer is interfaced to a Nicolet 1083 Computer for data aquisition. Data treatment was done using the Nicolet FT-NMRD program (109). Non spinning 10 mm OD NMR tubes (Wilmad) were used. In the case of studies of temperature dependences of the ^{133}Cs chemical shifts the temperature was monitored using a thermocouple housed in a10 mm NMR tube and inserted in the solvent. During measurements a constant temperature was monitored within $\pm$ 1°C. Because the resonance frequency of the reference varies with the temperature an insulated reference tube (110) was used. In order to reach the equilibrium temperature, each sample tube was left in the probe for ~ 15 minutes before any measurement.

Chemical shifts obtained for the different metal nuclei were referenced to 0.31 M aqueous solutions of $TlNO_3$ for ^{205}Tl, 3.0 M $LiClO_4$ for ^{7}Li, 0.5 M CsBr for ^{133}Cs, and 3.0 M NaCl for ^{23}Na NMR measurements. However, all the chemical shifts for sodium-23, Cesium-133, and thallium-205 reported in this thesis are ultimately referenced to infinitely dilute aqueous solutions of the Na^+, Cs^+ and Tl^+ ions. All reported data are also corrected for differences in the bulk volume diamagnetic susceptibility of the solvent (111, 112). The following equation was used to make these corrections.

$$\delta_{corr} = \delta_{obs} + \frac{2\pi}{3} (X_v^r - X_v^s) \qquad (1)$$

where δ_{corr} and δ_{obs} are the corrected and observed

Table 5. Diamagnetic Susceptibility Correction on DA-60 for Various Solvents

Solvent	Bulk Volume Diamagnetic Susceptibility$\times 10^6$	Correction (ppm)
Acetone (AC)	-0.460	-0.545
Acetonitrile (AN)	-0.534	-0.390
Dimethylformamide (DMF)	-0.500	-0.308
Dimethylsulfoxide (DMSO)	-0.605	-0.241
Methanol (MeOH)	-0.515	-0.429
Nitromethane (NM)	-0.391	-0.689
Propylen Carbonate (PC)	-0.634	-0.180
Pyridine (PY)	-0.612	-0.226
Tetramethylguanidine (TMG)	-0.590	-0.272
Water	-0.720	-0.000

chemical shifts, respectively, and X_v^r and X_v^s are the bulk volume diamagnetic susceptibilities of the reference (aqueous) and sample (nonaqueous) solvents. Since the concentration of added salt was low in all cases, no correction for the contribution of the salt to the magnetic susceptibility of the solution was applied in these studies. The magnitude of the correction for various solvents is shown in Table 5.

For the mixed solvents, the volume diamagnetic susceptibility of a given mixture was calculated by the following equation (113)

$$X_V^{min} = \frac{V_A}{V_A + V_B} \cdot X_V^A + \frac{V_B}{V_A + V_B} \cdot X_V^B \qquad (2)$$

where X_V^{min} is the calculated volume susceptibility of the mixture, V_A and V_B are the volumes of solvents A and B respectively, X_A and X_B are the volume diamagnetic susceptibilities of the pure solvents A and B respectively. Downfield (paramagnetic) chemical shifts from the reference are designated as positive.

The PMR spectra were obtained at 25°C on a Varian T-60 spectrometer. Spinning 5 mm NMR tubes (Wilmad) were used. Chemical shifts were measured relative to TMS (Merck Co.) as internal standard. The shifts reported in this thesis are given in ppm at a magnetic field of 14.09 KG.

E. Sample Preparation

All samples were weighed out into volumetric flasks using an analytical balance. In view of the hydroscopicity of the nonaqueous solvents and of the reagents, all of the solutions were prepared in a dry box under a nitrogen atmosphere. The mixed solvents were prepared by taking a certain volume of a solvent and mixing with the second solvent to give the desired volume percent of the binary solvent. Solutions containing both salt and ligand were usually prepared (if the ligand was soluble enough) by mixing appropriate columns of stock solutions followed by dilution to the mark with pure solvent or solvent mixture. When the ligands were only sparsely soluble, the samples were prepared by weighing out the various amounts of the complexing ligand into a 2 ml volumetric flask followed by dilution with the metal ion solution. After dissolution of the ligand, the solutions were transferred to 10 mm NMR tubes, capped, and wrapped with teflon tape to prevent both contamination by atmospheric water and solvent evaporation.

In the case of studies of competitive solvation of Cs^+ ion in water-nonaqueous mixed solvents, the solutions were prepared by weighing a snap cap vial, adding the desired volume of one solvent, weighing, then adding the desired volume of another solvent and weighing again. Knowing these weights, the number of moles of each solvent and the resultant mole fraction were calculated. The

appropriate amount of cesium salts were weighed out into a 2 ml volumetric flask and the desired solvent mixture was added to the mark.

F. Data Handling

Chemical shift data obtained from complexation studies were analyzed on a CDC-6500 computer using a non-linear curve fitting program, KINFIT (114) to obtain the formation constant of complexes. A linear least squares program was used to obtain the enthalpies and entropies of complexation.

CHAPTER III

MULTINUCLEAR MAGNETIC RESONANCE STUDY OF COMPLEXATION OF Na^+, Cs^+, Tl^+, Li^+ AND Ag^+ IONS BY THIA-CROWN AND CROWN ETHERS IN NONAQUEOUS SOLVENTS

A. Introduction

Since the synthesis of macrocyclic polyethers by Pedersen (1), the properties of these ligands and their complexes have been under active investigation because of the possible chemical and biological applications of their unusual ion complexation and transport effects. For these applications one needs the knowledge of the effect of solvent, cation, anion, and ligand parameters on the complexation reactions between the metal ions and macrocyclic ligands.

It has been found (14, 56, 115-117) that nuclear magnetic resonance of alkali nuclei, such as ^{7}Li, ^{23}Na, and ^{133}Cs, is one of the most powerful techniques for the complexation studies of corresponding ions with macrocyclic ligands in nonaqueous as well as in aqueous solutions. Thallium-205 NMR has also become an important probe for investigation of solvation phenomena, solution structure, and complexation of the thallous ion. The thallium-205 chemical shift is very solvent dependent and it is very sensitive to small changes in the chemical environment of the Tl^{+} ion. Both the chemical shift and the line width of the nuclear resonances of alkali metal ion nuclei and $^{205}Tl^{+}$ ion give useful information about the ion-ligand, ion-solvent, and ion-ion interactions.

The work presented here deals with the use of alkali metal nuclei, thallium-205, and proton NMR techniques

which not only provide the binding constants of the different complexes but they also give useful information on the effects of the solvent, the cation type, the type of the donor atoms, and the ring size of the macrocyclic ligands. In this chapter we will compare the ability of DT18C6 and 18C6, to form complexes with thallium, sodium and cesium ions in several nonaqueous solvents. We also describe the complexation strength of TT12C4 with silver and lithium ions in nonaqueous solvents. A comparison of the ion-binding properties of the macrocycles TT12C4 and 12C4 to lithium ion in a wide variety of nonaqueous solvents will be made.

B. Results and Discussion

1. Complexation of Na^+ ion by DT18C6

The sodium-23 chemical shift-mole ratio data are given in Table 6. The variation of the sodium-23 chemical shift as a function of DT18C6/Na^+ in various nonaqueous solvents is shown in Figures 13 and 14. It is obvious that the solvent plays an important role in the complexation process. For example, except for DMSO solutions, the sodium ion resonance shifts upfield or downfield (depending on the solvent) with the increasing concentration of the macrocycle until a certain mole ratio of Ligand/Na^+ is reached. The more pronounced curvature in the mole ratio plot in NM solution (Figure 13) compared to those of other solvents is an indication of a stronger

Table 6. Mole Ratio - Chemical Shift Data for Sodium Tetraphenylborate in the Presence of DT18C6 in Various Solvents

AN[a]		NM[b]		AC[b]		PC[c]		DMF[d]		DMSO[e]	
L/Na^+	δ (ppm)	L/Na^+	δ (ppm)	L/Na^+	δ (ppm)	L/Na^+	δ (ppm)	L/Na^+	δ (ppm)	L/Na^+	δ (ppm
0.00	-7.58	0.00	-14.04	0.00	-7.95	0.00	-9.10	0.00	-4.51	0.00	-0.06
0.50	-6.92	0.52	- 9.50	0.31	-7.77	0.34	-8.70	0.28	-4.61	0.29	-0.04
0.80	-6.77	0.79	- 7.23	0.50	-7.72	0.47	-8.56	0.61	-4.70	0.58	-0.34
1.02	-6.50	0.98	- 5.39	0.85	-7.69	0.68	-8.19	0.77	-4.70	0.77	-0.17
1.20	-6.35	1.24	- 4.70	1.03	-7.63	0.77	-8.31	1.01	-4.73	0.90	-0.36
1.54	-6.31	1.47	- 4.24	1.25	-7.60	1.03	-8.06	1.20	-4.84	1.13	0.01
1.98	-6.16	1.96	- 4.46	1.47	-7.61	1.27	-8.01	1.50	-4.81	1.56	-0.57
2.54	-6.08	3.06	- 4.16	2.05	-7.57	1.57	-7.94	1.91	-4.84	2.17	-0.37
3.02	-6.08	3.06	- 4.16	2.51	-7.57	2.08	-7.74	2.46	-4.87	2.79	-0.38
4.05	-6.07	4.12	- 4.08	3.16	-7.53	2.46	-7.51	3.29	-4.89		
						3.31	-7.47				

[a]Concentration of $NaB\phi_4$ = 0.05M.

[b]Concentration of $NaB\phi_4$ = 0.025M

[c]Concentration of $NaB\phi_4$ = 0.021M

[d]Concentration of $NaB\phi_4$ = 0.02M

[e]Concentration of $NaB\phi_4$ = 0.005M

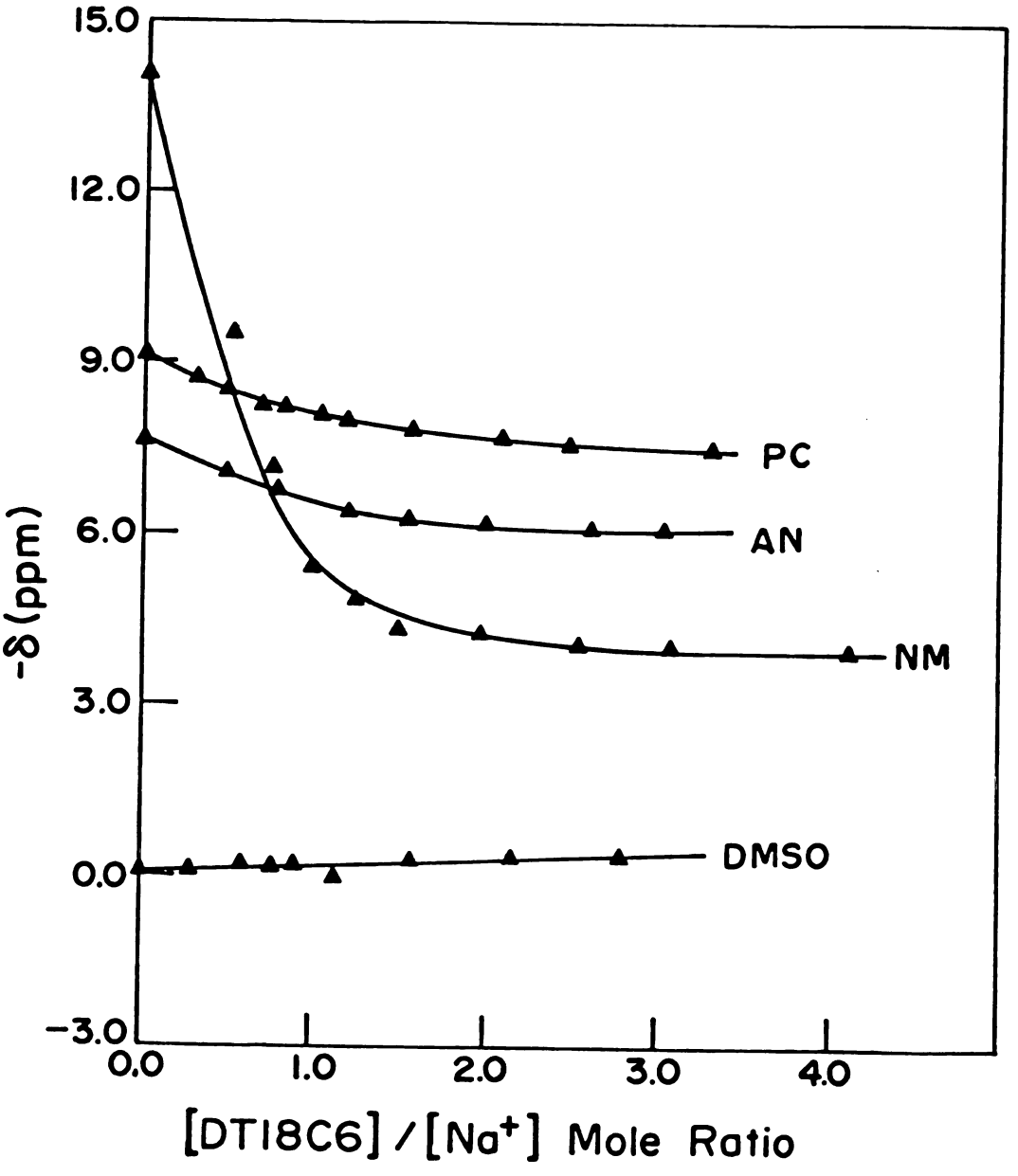

Figure 13. Chemical shifts of sodium-23 as a function of DT18C6/Na^+ mole ratio in various solvents.

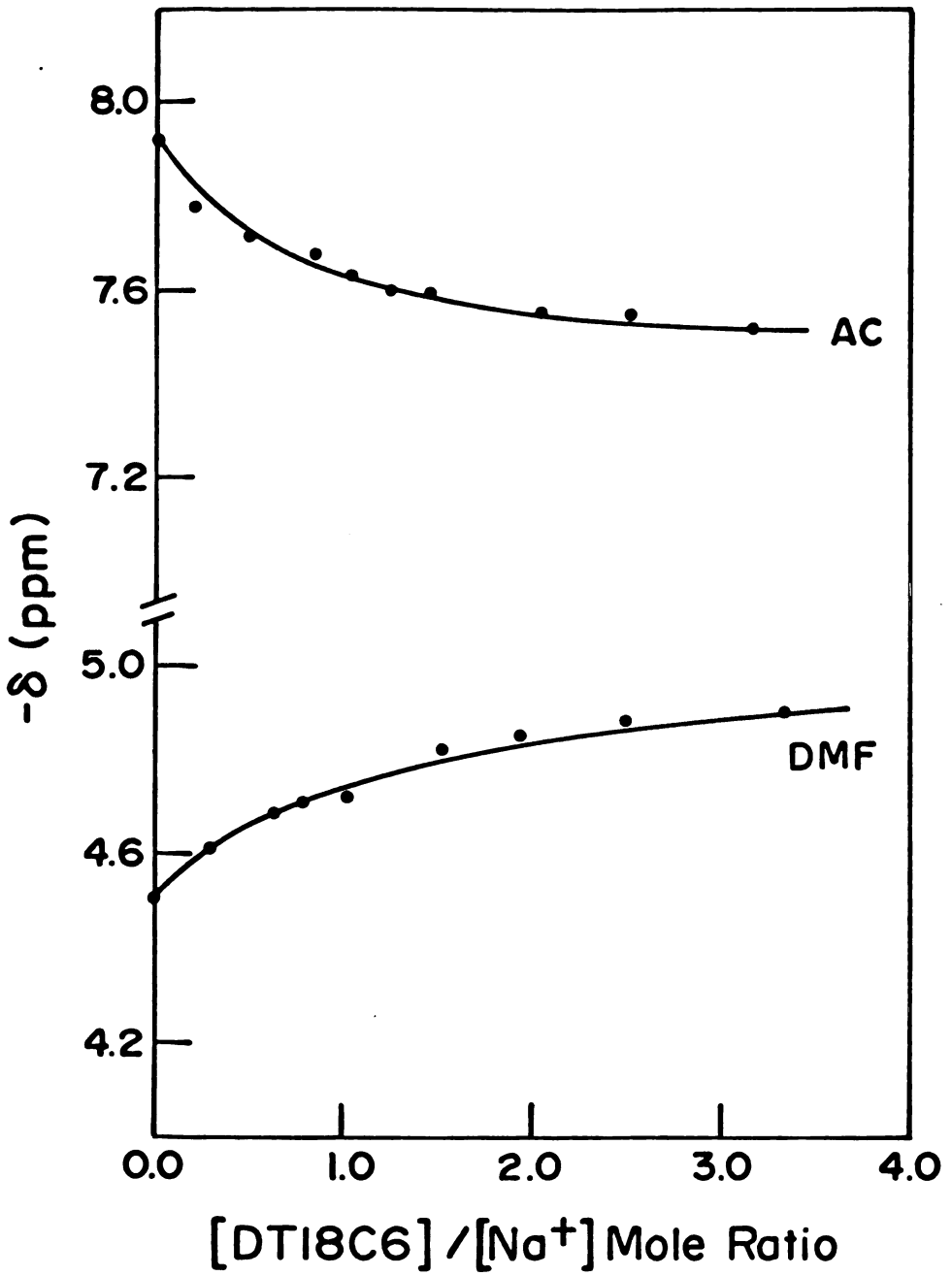

Figure 14. Sodium-23 chemical shifts vs. DT18C6/Na^+ mole ratio in AC and DMF.

interaction between Na^+ and DT18C6 in NM than in all other solvents. As shown in Figure 13 the frequency of the ^{23}Na resonance in DMSO is essentially independent of the DT18C6/Na^+ mole ratio. Therefore, there is no evidence for the formation of a complex in this solvent.

The variation of the chemical shift with Ligand/Na^+ mole ratio was used to obtain the formation constants of $(DT18C6 \cdot Na)^+$ complex. Assuming that only cation-ligand interactions are important and the rate of exchange of the metal ion between the two sites (free cation in the bulk solution and the complexed cation) is fast to the NMR time scale, the observed chemical shift is related to those of the free cation and the complexed cation by the following equation

$$\delta_{obs} = \delta_M X_M + \delta_{ML} X_{ML} \qquad (1)$$

where δ_{obs} is the observed chemical shift, X_M and X_{ML} are the fractions of the cation in the free and complex states and δ_M and δ_{ML} are the chemical shifts characteristic of the two environments. Given that $X_M = C_M/C_M^t$ the following expression can be derived

$$\delta_{obs} = \frac{C_M}{C_M^t} (\delta_M - \delta_{ML}) + \delta_{ML} \qquad (2)$$

where C_M and C_M^t are the concentrations of free metal ion and total metal ion. The stability constant is defined as the equilibrium constant (in lit/mole) for the following reaction

$$M^+ + L \rightleftharpoons ML^+ \qquad (3)$$

where M^+ and L represent uncomplexed cation and ligand, and ML^+ is a 1:1 (metal ion : ligand) complex. The concentration equilibrium constant is given by the usual expression

$$K_f = \frac{[ML^+]}{[M^+][L]} = \frac{C_{ML}}{C_M C_L} \tag{4}$$

where C_{ML}, C_M, and C_L are the molar equilibrium concentrations of the complex, free cation, and free ligand respectively. By a simple algebraic substitution, the above expression may be rewritten in the form of

$$K_f = \frac{C_M^t - C_M}{C_M(C_L^t - C_M^t + C_M)} \tag{5}$$

where C_L^t is the total concentration of the ligand Using the mass balance equations, we can derive equation (6)

$$\delta_{obs} = [(K_f C_M^t - K_f C_L^t - 1) \pm (K_f^2 C_L^{t\,2} + K_f^2 C_M^{t\,2} - 2K_f^2 C_M^t C_L^t + 2K_f C_L^t + 2K_f C_M^t + 1)^{\frac{1}{2}}](\frac{\delta_M - \delta_{ML}}{2K_f C_M^t}) + \delta_{ML} \tag{6}$$

which relates the observed chemical shift to the formation constant (K_f), the total metal cation the ligand concentration (C_M^t and C_L^t respectively), the chemical shift of the free cation (δ_M), and the chemical shift of the complexed cation (δ_{ML}). Since δ_{obs}, C_M^t, C_L^t are known and the value of δ_M can be measured, using the metal salt solution with no ligand, equation (6) contains two unknown parameters,

δ_{ML} and K_f. A nonlinear least-squares program KINFIT is used to solve the expression by using the experimental parameters, δ_{obs}, C_M^t, C_L^t and δ_M and adjusting K_f and δ_{ML} values until the calculated chemical shifts correspond to the experimental values within the error limits of the measurement. The results of the above calculations for $(DT18C6 \cdot Na)^+$ system in various solvents are given in Table 9.

The data collected in Table 9 show that the stability constants of $(DT18C6.Na)^+$ complex among various solvents decrease in the order NM > AC > PC > AN > DMF > DMSO. This behavior reflects the much stronger cation solvation by DMSO and DMF, compared to other solvents, with which the polyether has to compete.

Various scales of the solvating ability of solvents have been suggested. A quantitative measure of the solvating power of solvents is provided by the so-called "donor number", D.N, which seems to agree quite well with the behaviour of alkali cation complexes in nonaqueous solutions. The donor number which has been proposed by Gutmann (118) is defined as the negative enthalpy value (in K.cal/Mole) for the 1:1 adduct formation between antimony pentachloride and the solvent molecules in 1,2-dichloroethane as an inert solvent

$$S + SbCl_5 \xrightarrow{1,2\text{-DCE}} S.SbCl_5$$

$$\text{Donor Number} \equiv -\Delta H_{S.SbCl_5} \text{ (K cal/Mole)}$$

The Gutman donor numbers and the dielectric constants as well as the structural formula of the non-aqueous solvents are shown in Table 7. Generally, we expect that in solvents with high donor ability and dielectric constant the stability constant of the complex should decrease due to the competition between the ligand and the solvent molecules for the metal ion. The results obtained in this work fit this generality.

As illustrated in Table 9 the resonance frequency of the complexed $^{23}Na^{+}$ ion is solvent dependent which indicates that the metal ion is only partially insulated from the solvent and the solvent molecules can still interact with the vacant coordination sites of the complexed cation.

2. Complexation of Cs^{+} ion by DT18C6

The cesium-133 chemical shift-mole ratio data for complexation of cesium ion by DT18C6 in acetone, propylene carbonate, nitromethane, and dimethylsulfoxide are shown in Table 8. Figure 15 shows the mole ratio plots for the $(DT18C6.Cs)^{+}$ complex in various solvents. In all cases the plots show little curvature with no observable break at any mole ratio, which indicates the existence of a very weak interaction between the cesium ion and the ligand. In the case of acetone, propylene carbonate and nitromethane solutions, the plots of chemical shifts versus ligand to metal ion mole ratios

Table 7. Structure, Gutmann Donor Number, and Dielectric Constant of Certain Solvents

Solvent	Structure	Gutmann Donor Number[a]	Dielectric Constant
Nitromethane (NM)	$H_3C\text{-}NO_2$	2.7	35.9
Acetonitrile (AN)	$H_3C\text{-}CN$	14.1	37.5
Propylene Carbonate (PC) (1,2-propandiol cyclic carbonate)	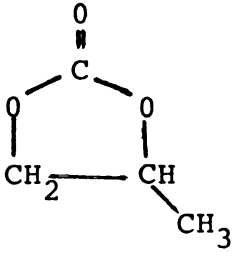	15.1	65.0
Acetone (AC)	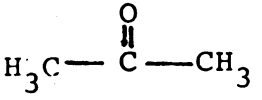	17.0	20.7
Methanol (MeOH)	$H_3C - OH$	25.7	32.7
Dimethylformamide (DMF)	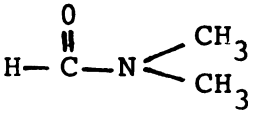	26.6	36.1
Dimethylsulfoxide (DMSO)	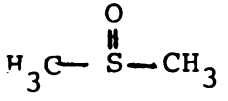	29.8	45.0

Table 7 (continued)

Solvent	Structure	Gutmann Donor Number[a]	Dielectric Constant
Pyridine (PY)	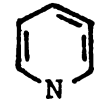	33.1	12.3
Tetramethylguanidine (TMG)	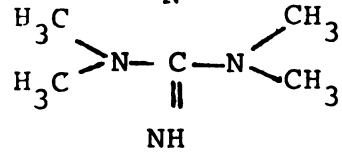	-	11.0
Water	H_2O[b]	~ 33	78.5

[a] Reference 118.

[b] Reference 113.

Table 8. Mole Ratio - Chemical Shift Data for CsSCN in the Presence of DT18C6 in Various Nonaqueous Solvents

AC[a]		PC[b]		NM[c]		DMSO[c]	
L/Cs^+	δ (ppm)	L/Cs^+	δ (ppm)	L/Cs^+	δ (ppm)	L/Cs^+	δ (ppm)
0.00	-13.75	0.00	-34.44	0.00	-57.57	0.00	66.97
0.28	-12.90	0.22	-33.97	0.32	-55.87	0.34	67.05
0.54	-12.27	0.30	-33.81	0.64	-54.41	0.58	66.97
0.88	-11.30	0.53	-33.35	0.96	-53.00	1.02	66.97
1.01	-11.27	0.61	-33.20	1.17	-51.91	1.14	66.97
1.23	-10.64	0.79	-32.65	1.62	-49.74	1.52	66.90
1.57	-10.03	0.91	-32.50	1.89	-48.57	1.82	66.98
2.02	- 9.17	1.02	-32.30	2.38	-46.24	2.30	67.06
2.57	- 7.85	1.33	-31.61	2.89	-44.62	2.90	66.82
3.02	- 7.15	1.77	-30.87	3.70	-41.83		
3.97	- 5.30	2.18	-30.10				
		3.01	-28.70				

[a]Concentration of salt = 0.025M

[b]Concentration of salt = 0.014M

[c]Concentration of salt = 0.005M

Figure 15. Cesium-133 chemical shifts vs. DT18C6/Cs^+ mole ratio in various solvents.

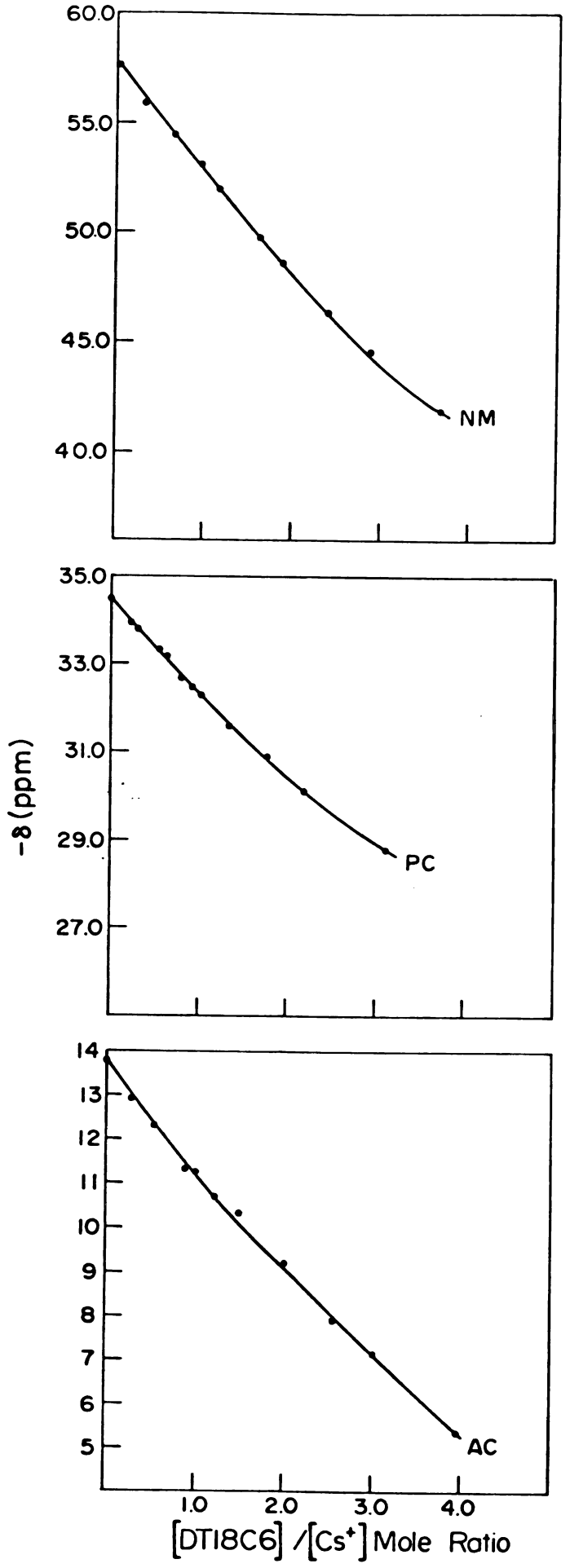
60.0
55.0
50.0
45.0
40.0
NM
35.0
33.0
31.0
29.0
27.0
PC
14
13
12
11
10
9
8
7
6
5
AC
-δ (ppm)
1.0
2.0
3.0
4.0
[DT18C6] / [Cs+] Mole Ratio

(Figure 15) show that complexation of Cs^+ ion by the ligand yielded paramagnetic shift, resulting from an increase in the electron density around the cesium ion. In the case of dimethylsulfoxide, however, which is a solvent with high donor ability (DN = 29.8), no chemical shift variation results as the Ligand/Cs^+ mole ratio is increased (see Table 8).

The stability constants and the limiting chemical shifts for $(DT18C6.Cs)^+$ are listed in Table 10. Since the cesium ion is rather weakly solvated because of its low charge density, the stability of the complex is only marginally dependent on the nature of the solvent. The large difference between the limiting chemical shift of the complex is a good indication that the complexed cation remains exposed to the solvent molecules.

3. Complexation of Tl^+ ion by DT18C6

The complexation between thallous ion and 1,10-dithia-18-Crown-6 was studied in nitromethane, acetone, acetonitrile, dimethylformamide, and 1,1,3,3-tetramethylguanidine. The measured thallium-205 chemical shifts at different Ligand/Tl^+ mole ratios are given in Table 11. The mole ratio plots for the complexation in various solvents are illustrated in Figure 16.

No significant variation in the chemical shift of thallium-205 is observed upon addition of ligand to the thallous salt in the case of tetramethyguanidine which

Table 9. Log of Formation constants and the Limiting Chemical Shifts of $(DT18C6.Na)^+$ Complex in Various Solvents at 32 ± 1°C.

Solvent	Log K_f	δ_{lim} (ppm)
Nitromethane	3.25 ± 0.15	-4.39 ± 0.10
Acetone	2.42 ± 0.48	-7.91 ± 0.08
Propylene Carbonate	1.87 ± 0.10	-7.43 ± 0.14
Acetonitrile	1.82 ± 0.10	-6.29 ± 0.05
Dimethylformamide	1.52 ± 0.21	-5.06 ± 0.09
Dimethylsulfoxide	~ 0	-

Table 10. Log of Stability Constants and the Limiting Chemical Shifts of $(DT18C6.Cs)^+$ Complex in Various Solvents at 32 ± 1°C.

Solvent	Log K_f	δ_{lim} (ppm)
Nitromethane	1.16 ± 0.07	16.9 ± 9.0
Acetonitrile[a]	0.97 ± 0.27	94.1 ± 3.0
Propylene Carbonate	0.96 ± 0.24	-24.2 ± 6.6
Acetone	0.61 ± 0.09	65.2 ± 3.8
Dimethylformamide[a]	0.56 ± 0.29	2.10 ± 1.27
Dimethylsulfoxide	0	-

[a] Reference (119).

Table 11. Mole Ratio - Chemical Shift Data for $TlClO_4$ in the Presence of DT18C6 in Various Nonaqueous Solvents

AC[a]		NM[b]		DMF[a]		AN[c]		TMG[d]	
L/Tl^+	δ (ppm)	L/Tl^+	δ (ppm)	L/Tl^+	δ (ppm)	L/Tl^+	δ (ppm)	L/Tl^+	δ (ppm)
0.00	-209.18	0.00	-354.71	0.00	130.30	0.00	-214.91	0.00	106.63
0.74	115.05	1.05	237.37	0.54	132.15	1.00	322.52	0.57	109.45
1.00	177.36	1.19	238.34	0.76	133.21	1.20	283.63	0.89	110.77
1.18	216.16	1.26	237.19	0.98	133.82	1.55	274.02	0.98	110.94
1.53	261.21	1.60	234.72	1.23	135.77	1.95	272.34	1.75	110.15
2.06	228.55	1.91	234.38	1.53	136.20	2.45	272.09	2.41	111.03
2.53	300.98	2.38	235.40	2.04	137.53	2.95	272.34	3.04	111.59
2.93	306.72	3.14	235.61	3.26	140.80	3.95	272.96	3.67	112.80
4.23	317.21	4.41	235.17	4.10	142.56	5.00	273.29	4.24	113.86
5.49	321.82	6.10	236.32						

[a]Concentration of $TlClO_4$ = 0.01M

[b]Concentration of $TlClO_4$ = 0.006M

[c]Concentration of $TlClO_4$ = 0.02M

[d]Concentration of $TlClO_4$ = 0.014M

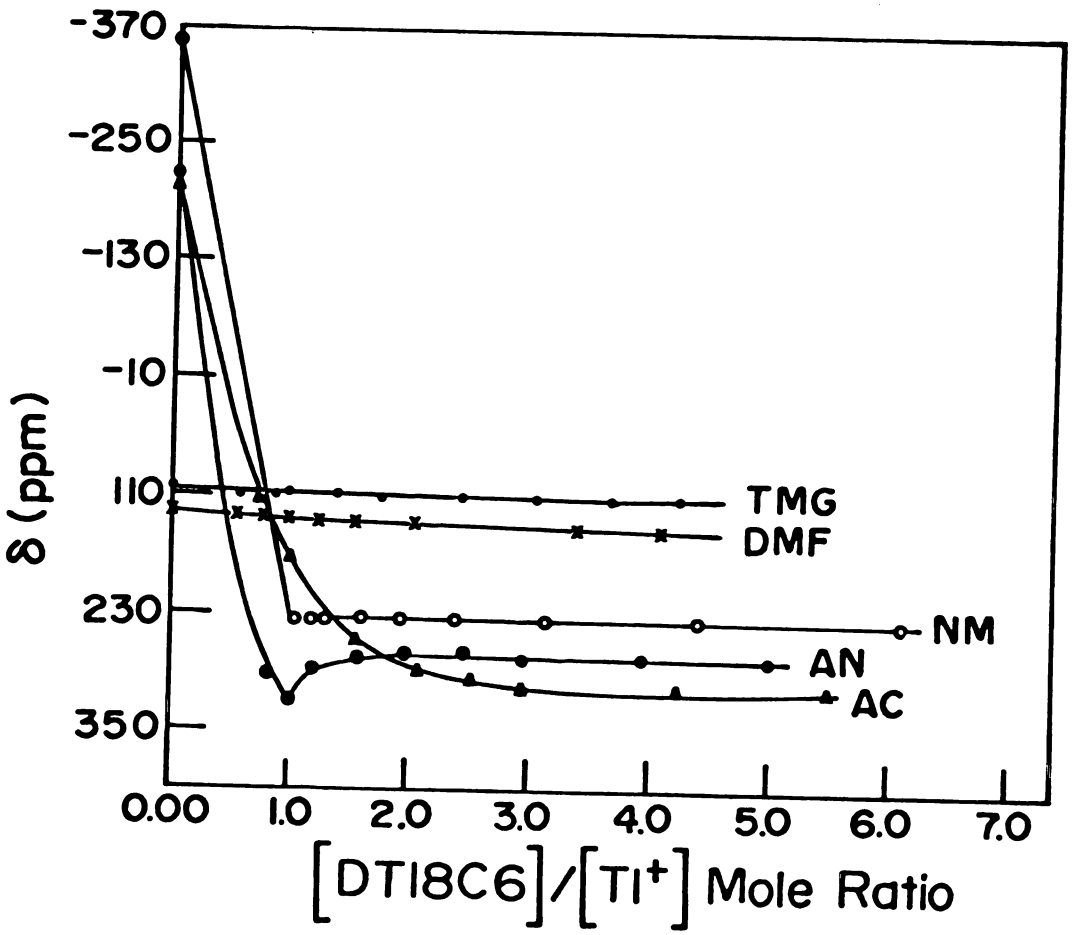

Figure 16. Thallium-205 chemical shifts vs. DT18C6/Tl^+ mole ratio in various solvents.

would be expected to have a high donor ability. On the other hand, in solvent of weak donor ability such as nitromethane (DN = 2.7), the resonance frequency of the ^{205}Tl is strongly affected by addition of the ligand, and the mole ratio plot consists of two straight lines intersecting at 1:1 mole ratio. This behavior indicates the existence of a very strong interaction between the thallium ion and the ligand. In such cases the formation constants cannot be determined and we can only conclude that the log K_f > 5. A gradual shift is observed in dimethyformamide solutions which could be due to the formation of a weak complex.

It is interesting to note that in acetonitrile solutions as the DT18C6/Tl^+ mole ratio increases from 0 to 1 the ^{205}Tl resonance shifts upfield, then further addition of the ligand gives a downfield shift. Beyond the mole ratio of 2, the resonance seems to level off to a constant value. This behavior clearly indicates a two-step complexation reaction, first the formation of a 1:1 complex and then the addition of a second molecule of the ligand gives a 2:1 (ligand:metal ion) sandwich complex.

The formation constants for the $(DT18C6 \cdot Tl)^+$ complex in various solvents are listed in Table 13. The results show that the variations of the solvent can produce a significant change in the binding properties of the ligand.

4. Complexation of the Tl^+ ion with 18C6

Table 12 summarizes the results obtained in the study of complexation of the Tl^+ ion by 18-Crown-6 in various non-aqueous solvents. The plots of the thallous ion chemical shifts versus the 18C6/Tl^+ mole ratio are shown in Figure 17. Depending on the nature of the solvent, the thallium-205 resonance shifts upfield or downfield with the increasing concentration of macrocyclic ligand. The more pronounced break in the DMF curve, compared to that in the DMSO curve, is a good indication of a stronger polyether complex formation in DMF than DMSO solutions. The behavior in acetone solutions shows that two complexes may be formed. Indeed only the slight upward drift of the chemical shifts beyond the 1:1 mole ratio can be used as an evidence for the formation of 2:1 complex, but the data do not permit determination of K_2. The data collected in Table 13 show that the stability constants of the complex are much lower in dimethylsulfoxide and dimethylformamide solutions than in nitromethane, acetonitrile and acetone solutions. These results reflects the much stronger cation solvation by the DMSO and DMF molecules, compared to the other solvents.

5. Complexing of the Li^+ ion by TT12C4

The results of our lithium-7 NMR studies for the interaction between Li^+ ion and macrocyclic ligand, 1,4,7-trithia-12-Crown-4, are tabulated in Table 14. The lithium-7 chemical shifts as a function of TT12C4/Li^+

Table 12. Mole Ratio - Chemical Shift Data for 18C6 Complex with Tl^+ ion in Various Solvents

DMSO[a]		AC[b]		DMF[b]		AN[a]		NM[c]	
L/Tl^+	δ(ppm)	L/Tl^+	δ(ppm)	L/Tl^+	δ(ppm)	L/Tl^+	δ(ppm)	L/Tl^+	δ(ppm)
0.00	328.44	0.00	-204.07	0.00	159.05	0.00	-214.81	0.00	-360.19
0.25	299.17	0.19	-199.87	0.17	118.48	0.30	-194.26	0.85	-197.41
0.50	239.94	0.44	-193.58	0.34	79.27	0.64	-173.46	0.98	-170.16
0.65	212.50	0.59	-189.61	0.70	4.31	0.88	-156.17	1.02	-170.60
0.90	162.60	0.79	-183.88	0.79	-11.57	0.91	-153.26	1.20	-164.87
0.98	148.40	0.95	-181.32	1.00	-45.34	1.05	-147.09	1.48	-164.16
1.09	125.91	1.08	-181.41	1.15	-73.46	1.18	-146.74	1.90	-163.81
1.36	93.64	1.42	-181.67	1.49	-83.07	1.62	-146.61	2.33	-164.34
1.67	65.07	1.70	-181.94	2.10	-91.19	1.97	-146.66	2.97	-164.42
1.96	38.89	2.04	-182.07	3.14	-98.42	2.59	-146.88	3.63	-164.25
2.16	28.07	2.33	-182.20	4.09	-97.71	3.13	-147.10	5.68	-164.17
2.63	4.59	2.86	-182.99	5.18	-98.59	4.06	-147.41		
2.87	-4.67	3.37	-183.35	7.00	-97.86				
3.47	-13.52	4.45	-184.41						
3.79	-27.06	6.05	-185.20						
4.31	-35.79	7.55	-187.58						
4.80	-42.93								
5.87	-53.25								
6.79	-59.07								
7.85	-63.92								

[a]Concentration of $TlClO_4$ = 0.02M; [b]Concentration of $TlClO_4$ = 0.01M; [c]Concentration of $TlClO_4$ = 0.006M.

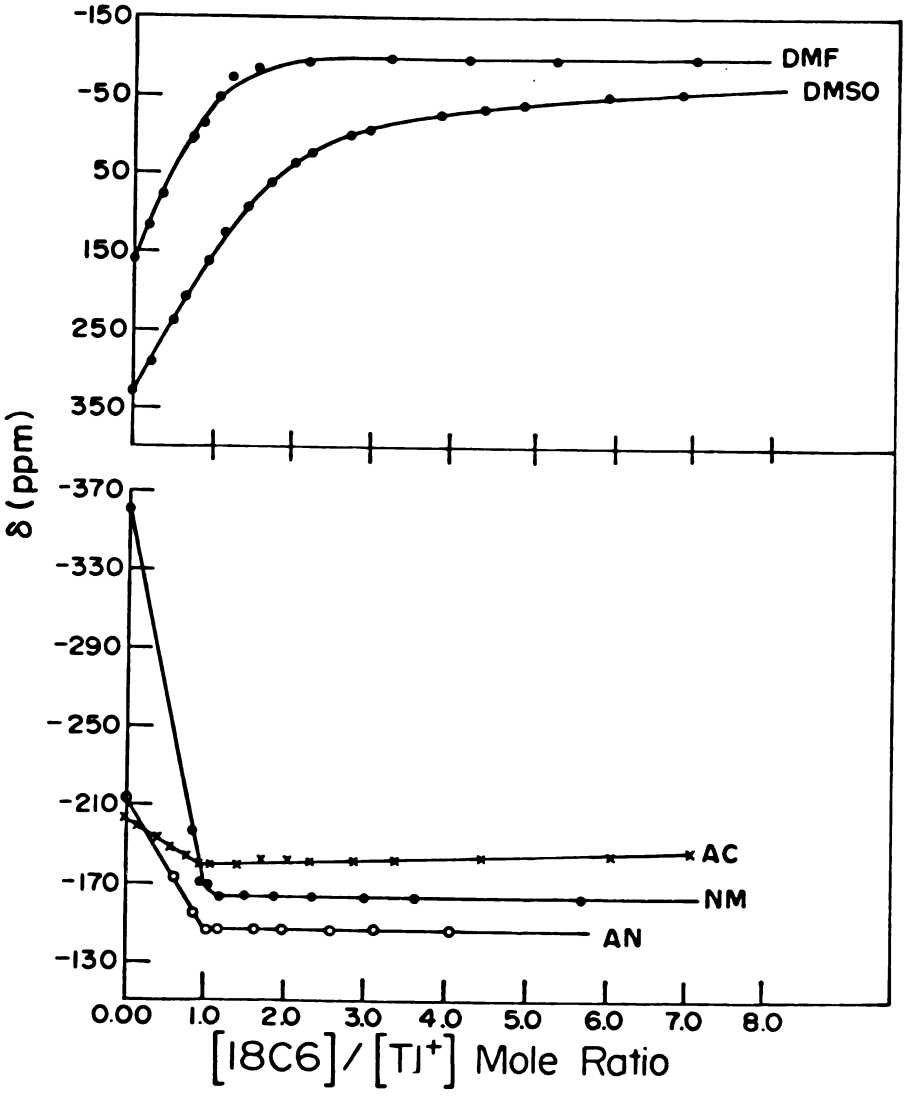

Figure 17. Thallium-205 chemical shifts vs. 18C6/Tl^+ mole ratio in various solvents.

Table 13. Stability Constants of Thallium (I) Complexes with Dithia-18C6 and 18C6 in Various Non-aqueous Solvents

Solvent	Log K_f	
	DT18C6	18C6
Nitromethane	> 5	> 5
Acetonitrile	> 5	> 5
Acetone	2.97 ± 0.01	> 5
Dimethylformamide	1.24 ± 0.01	3.35 ± 0.06
Dimethysulfoxide	~ 0	1.92 ± 0.01
Tetramethylguanidine	~ 0	-

Table 14. Mole Ratio-Chemical Shift Data for $LiClO_4$ (0.02M) in the Presence of TT12C4 in Various Solvents at 30°C.

PY		AC		DMSO		NM	
L/Li^+	δ (ppm)	L/Li^+	δ (ppm)	L/Li^+	δ (ppm)	L/Li^+	δ (ppm)
0.00	2.40	0.00	0.88	0.00	-0.96	0.00	0.16
0.40	2.43	0.33	0.97	0.19	-1.05	0.32	0.22
0.55	2.43	0.50	0.99	0.56	-0.96	0.57	0.22
0.80	2.36	0.70	1.00	0.72	-0.96	0.75	0.22
0.83	2.41	0.88	1.02	0.83	-.096	1.00	0.25
0.98	2.46	1.00	0.98	1.11	-0.96	1.24	0.25
1.20	2.36	1.25	1.00	1.23	-0.94	1.50	0.27
1.44	2.29	1.50	0.99	1.83	-0.94	2.00	0.27
2.00	2.38	2.00	0.97	2.36	-0.96	2.50	0.30
2.25	2.41	2.30	0.96	2.66	-1.07	2.66	0.30
2.50	2.39	2.50	1.01	2.99	-1.04		
3.00	2.36	3.10	1.00				

Table 14 (continued)

AN		PC		THF	
L/Li^+	δ (ppm)	L/Li^+	δ (ppm)	L/Li^+	δ (ppm)
0.00	-2.38	0.00	-0.64	0.00	-0.72
0.50	-2.44	0.30	-0.60	0.50	-0.71
0.75	-2.49	0.50	-0.61	1.00	-0.77
0.88	-2.44	0.75	-0.59	1.50	-0.88
1.00	-2.49	1.00	-0.61	2.00	-0.77
1.25	-2.55	1.25	-0.63	2.50	-0.88
1.50	-2.54	1.50	-0.62		
2.00	-2.54	2.00	-0.60		
2.50	-2.58	2.50	-0.63		
		3.00	-0.64		

mole ratios in seven nonaqueous solvents are plotted in Figure 18. It is seen that in all cases, the frequency of the lithium-7 resonance is almost independent of the Ligand/Li^+ mole ratio which suggests that the immediate environment of the lithium ion is not changed upon addition of the ligand. It is evident, therefore, that the interaction between lithium ion and TT12C4 is not appreciable. At least two factors play an important role in causing this behaviour. The first is the large size of the sulfur atom compared to the oxygen atom, which results in a decrease in the ligand cavity size and in an alteration of the ring conformational energies. On the other hand, complexing of Li^+ is weakened appreciably by the sulfur substitution in the polyether ring due to the smaller negative charge on the donor atom. In addition, the Li^+ ion is relatively largely solvated and it may be more difficult to strip the solvent molecules from the Li^+ ion than from the larger cations.

6. Complexation of the Ag^+ ion by TT12C4

Complexing of silver ion by TT12C4 was studied in acetonitrile-d_3, dimethysulfoxide-d_6 and pyridine solutions using proton NMR technique. The chemical shifts for three kinds of hydrogen a, b, and c (Figure 19) of the thiacrown ether were determined relative to the TMS as an internal standard. The results of these studies are given in Table 15 and the plots of the ^1H chemical shift as a

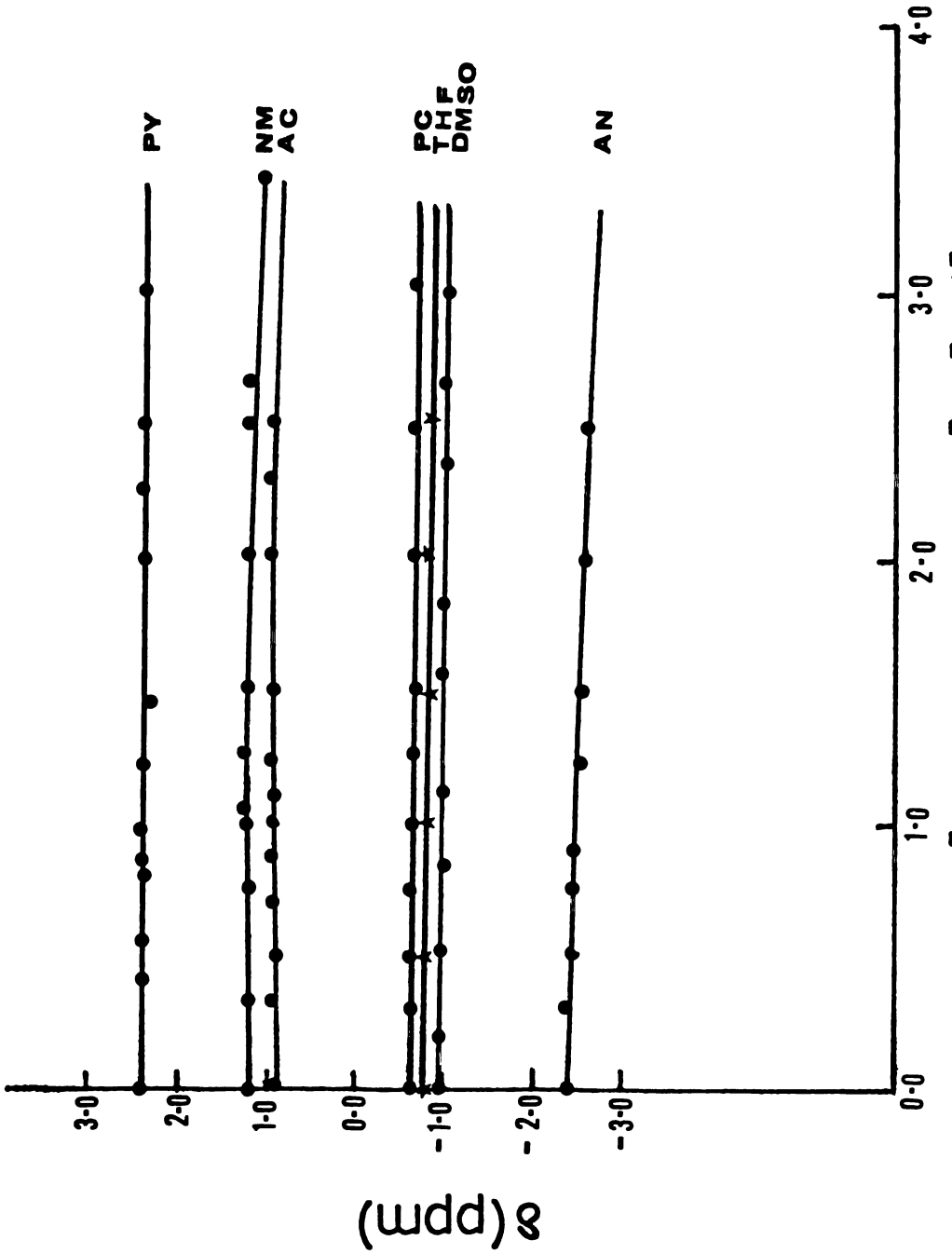

Figure 18. Lithium-7 chemical shifts vs. TT12C4/Li^+ mole ratio in nonaqueous solvents.

Table 15. Hydrogen Chemical Shift Data for TT12C4 in the Presence of Ag^+ ion in Various Solvents

Solvent	Ag^+/L	δ_{Ha} (ppm)	δ_{Hb} (ppm)	δ_{Hc} (ppm)
AN-d_3 [a]	0.00	2.77	2.63	3.63
	0.50	2.88	2.75	3.58
	0.78	2.90	2.77	3.55
	1.26	2.93	2.80	3.52
	1.52	2.92	2.80	3.52
	1.94	2.92	2.80	3.50
	2.50	2.93	2.80	3.52
	3.40	2.92	2.80	3.50
Py [b]	0.00	2.83	2.60	3.50
	0.48	2.87	2.67	3.52
	1.10	2.90	2.70	3.53
	1.60	2.90	2.70	3.53
	2.00	2.90	2.72	3.53
DMSO-d_6 [a]	0.00	2.77	2.60	3.55
	0.50	2.85	2.72	3.50
	0.87	2.90	2.78	3.48
	1.00	2.90	2.80	3.48
	1.14	2.92	2.82	3.48
	1.52	2.92	2.82	3.48
	2.18	2.93	2.83	3.48
	2.50	2.93	2.83	3.48
	3.00	2.93	2.83	3.48

[a] Concentration of TT12C4 = 0.05M.

[b] Concentration of TT12C4 = 0.10M.

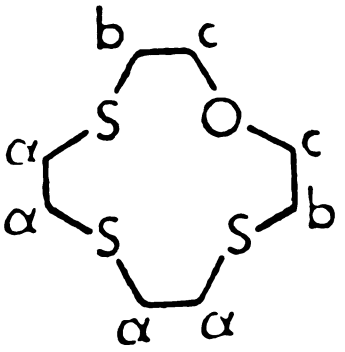

Figure 19. Structural formula of 1,4,7-trithia-12-Crown-4

of Ag^+/TT12C4 mole ratio for various kinds of hydrogen are shown in Figure 20. The chemical shifts for different types of hydrogen (a, b, and c) are falling in the order of $H_b > H_a > H_c$, and the most pronounced shifts are observed for the H_b protons. These data clearly show that there is a definite interaction between the Ag^+ ion and TT12C4.

Chemical shifts observed for the various protons may be the result of small differences in their magnetic environment which in turn are sensitive to conformational changes.

C. Comparison of the Results

The results obtained in this work, demonstrate the weaker complexing strength of 1,10-dithia-18-Crown-6 than 18-Crown-6 for the sodium, cesium and thallium ions (Table 16). Two factors seem to be important in causing this loss of stability. The first is the larger size of the sulfur atom compared to the oxygen atom, which results

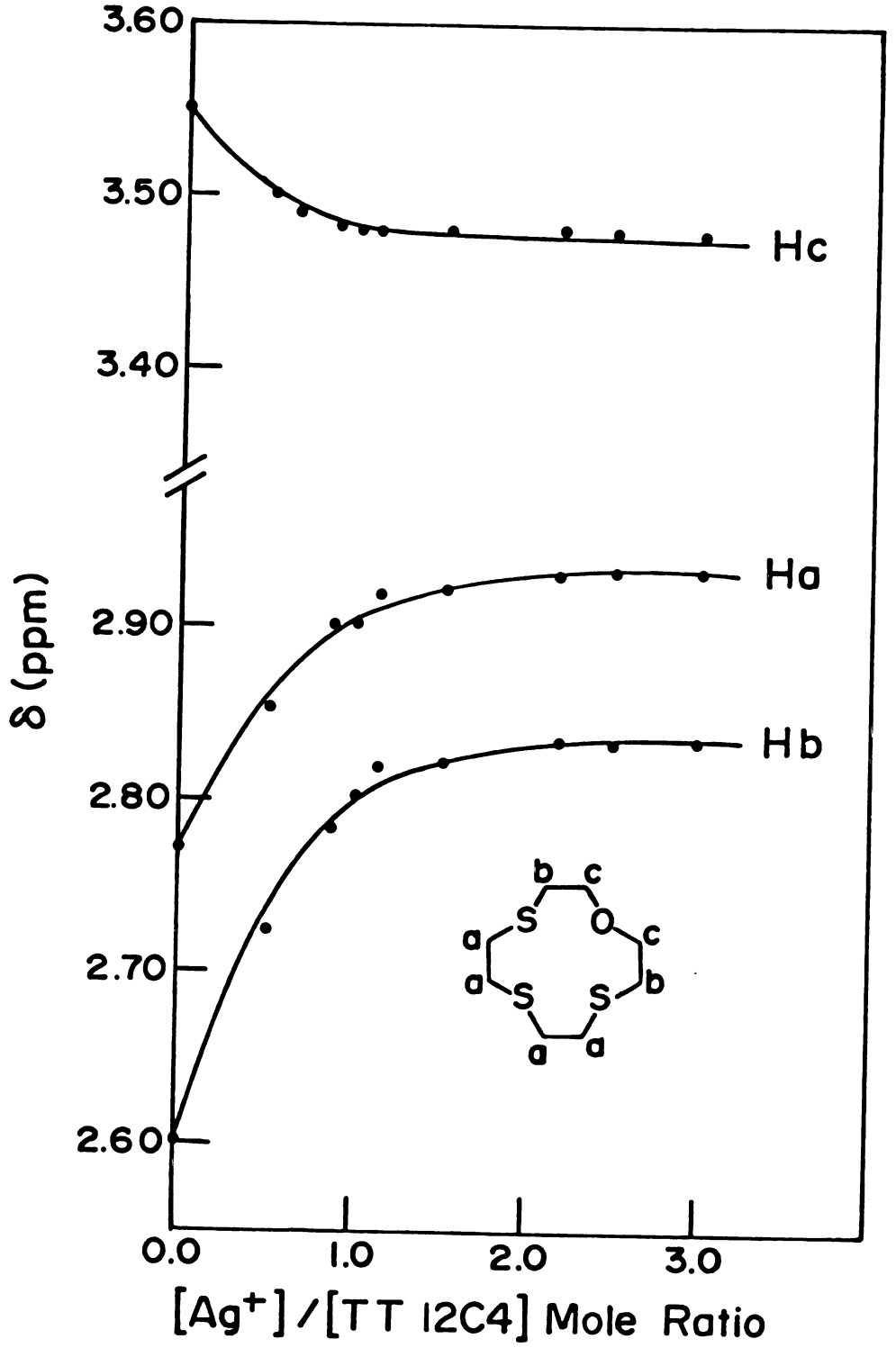

Figure 20. The variation of the proton chemical shift of the three different protons of TT12C4 with the Ag^+/TT12C4 mole ratio in DMSO-d_6.

Table 16. Stability Constants of the Sodium, Cesium, and Thallium (I) Complexes with DT18C6 and 18C6 Crown Ethers in Various Solvents

	log K_f					
	DT18C6			18C6		
Solvent	Na^+	Cs^+	Tl^+	$Na^{+(a)}$	$Cs^{+(b)}$	Tl^+
Nitromethane	3.25±0.15	1.16±0.07	> 5	> 4	-	> 5
Acetone	2.42±0.48	0.61±0.09	2.98±0.02	> 4	> 5	> 5
Propylene Carbonate	1.87±0.11	0.96±0.24	-	> 4	4.14±0.19	-
Acetonitrile	1.82±0.10	0.97±0.27	> 5	3.80±0.20	> 5	> 5
Dimethylformamide	1.52±0.21	0.56±0.29	1.24±0.01	2.23±0.04	3.93±0.15	3.35±0.06
Dimethylsulfoxide	~0	~0	~0	1.41±0.07	3.04±0.04	1.92±0.01

(a) Reference 120.

(b) Reference 26. Both CsL and CsL_2 complexes are formed; only the values of K_1 are given here.

in a decrease in ligand cavity size. The second is lower electronegativity of the sulfur atoms compared to the oxygen atoms, which results in a decrease in electrostatic interaction between metal cation and the donor atoms.

Complexation studies of the cesium ion with 18C6 were performed by Mei (36) in various nonaqueous solvents. Both 1:1 and 2:1 (ligand:metal) complexes are formed in all solvents studied. The weakest complex was found in DMSO solutions, K_1 = 1100 $\pm$ 100 and K_2 = 1.00 $\pm$ 0.4. Complexing of Na^+ by 18-Crown-6 was studied by Lin (120) in various organic solvents. For comparison purposes, the results of this work and Mei's studies are included in Table 16.

The comparison of our results obtained from sodium-23 and cesium-133 NMR studies on the complexation of Na^+ and Cs^+ ions by DT18C6 in various solvents with Mei's and Lin's results show some evidence of stronger interactions of these ions with 18C6 than with DT18C6. Although DT18C6 prefers binding with the thallium (I) ion rather than the alkali metal ions a decrease in the complexation strength is still observed when the sulfur substituted ligand is used. Pearson's hard-soft acid-base theory (121) does not seem to explain the complexation strength observed for the thallium ion. According to the Pearson's theory, the soft acid, thallium ion, should prefer to bind to ligands containing sulfur atoms (soft base) rather than ligands possessing oxygen atoms (hard base). From size

consideration, however, the thallium ion may prefer to form a stronger complex with 18C6 than with DT18C6. It is probable, therefore, that a primary reason for the lower stability of the complexes formed between DT18C6 and thallium ion, is that this cation is too large to fit into the ligand cavity since the hole in the macrocycle is smaller when the sulfur atom is a donor than when the oxygen atom is a donor (10). It would be expected, therefore, that the metal ion does not fit into the cavity but it may lie above the plane of the ligand ring. On the other hand, the cavity of 18C6 does accommodate the Tl^+ ion because its ionic diameter (2.80 A°) is close to that of the 18C6 cavity.

Comparison of the data obtained from thallium-205, sodium-23 and cesium-133 NMR studies in various solvents (Table 16) shows that the stability of the appropriate complexes is falling in the order $(DT18C6 \cdot Tl)^+ > (DT18C6 \cdot Na)^+ > (DT18C6 \cdot Cs)^+$ regardless of the solvent in which the complexation takes place. This seems reasonable because the thallium ion is capable of forming ionic bonds with the oxygen atoms and (partially) covalent bonds with the sulfur atoms, whereas the sodium and cesium ions form only ionic bond. An exception, however is observed in the case of complexation of Na^+ and Tl^+ ions by DT18C6 in dimethylformamide solutions in which the stability of the $(DT18C6 \cdot Tl)^+$ complex is lower than that of the

$(DT18C6 \cdot Na)^+$ complex. A possible reason for such an exception may be due to the poorer solvating ability of dimethylformamide for the sodium ion than for the thallium ion. Since dimethylformamide posseses a nitrogen atom (soft base), it may prefer to solvate the Tl^+ ion (soft acid) rather than the Na^+ ion (hard acid).

Although the sodium ion (higher charge density compared to the Cs^+ ion) is probably more solvated than the cesium ion, it forms a stronger complex with DT18C6. Probably the lower stability of the $(DT18C6 \cdot Cs)^+$ complex is due to the fact that the cation is too large (cation diameter = 3.34 A°) to match the ligand cavity. On the other hand, the cavity size of the ligand may accommodate well the sodium ion (cation diameter = 1.90).

The results obtained with lithium-7 NMR studies on the complexation of the Li^+ ion by TT12C4 in acetonitrile, dimethylsufloxide, tetrahydrofuran, propylene carbonate, nitromethane, acetone, and pyridine solutions show that the interaction between lithium ion and TT12C4 in these solvents is not strong. Complexation of lithium ion with 12C4 in various solvents was studied by Smetana (117) using lithium-7 NMR technique. Some of his results are given in the following Table. As we expect, comparison of these data with our results shows that the interaction between Li^+ with 12C4 is much higher than the interaction of this ion with TT12C4 in various nonaqueous solvents.

Table 17. Stability Constants of $(Li \cdot 12C4)^+$ Complex in Different Solvents

Solvent	log K_1	log K_2
NM	4	1.57
AN	4.25	
AC	1.62	
PY	0.70	
DMSO	0	

These results are not unexpected, since the cavity size of TT12C4 is so small that a metal ion could not be located in it. Likewise the electronegativity of the oxygen is higher than that of sulfur which makes the C-S bond less ionic than the C-0 bond.

Comparison of the data from the proton NMR studies on the complexation of the silver ion by TT12C4 is AN-d_3, DMSO-d_6 and pyridine with the results of lithium-7 NMR measurements shows some evidence of stronger interaction between silver ion and TT12C4 than the interaction of lithium ion with this ligand in nonaqueous solvents. This seems reasonable because the Ag^+ ion is capable to form ionic bond with oxygen atom and more covalent bonds with sulfur atoms than the lithium ion. Therefore the covalent bonding plays an important role in the Ag^+ complexes of polyethers containing sulfur atoms. In general substitution of sulfur atom for oxygen atom in the polyether ring reduces affinity for Tl^+ and alkali metal ions but greatly increases the binding to silver ion.

CHAPTER IV

THERMODYNAMIC STUDIES OF THE COMPLEXATION OF DIBENZO-27-CROWN-9 AND DIBENZO-24-CROWN-8 WITH CESIUM ION IN VARIOUS NONAQUEOUS SOLVENTS

A. INTRODUCTION

While the properties of macrocyclic polyethers and their alkali complexes have been under active investigation during the past several years, it seems, however, that most of the attention has been focused on alkali cation complexes with small crown ethers and, in particular, on 18-Crown-6 and its derivatives. Few thermodynamic studies have been reported for the reaction of metal ions with large macrocyclic crown ethers (i.e., larger than 18-Crown-6) despite the very interesting properties of these ligands. Therefore, little is known of their complex forming ability. Izatt and co-workers (9, 122) determined the thermodynamic quantities (ΔG_c°, ΔS_c°, and ΔH_c°) for the complexes of alkali and alkaline earth cations with 21-Crown-7, dibenzo-24-Crown-8, and dibenzo-27-Crown-9 in methanol or methanol-water mixtures by calorimetric technique.

The present study reports the use of the cesium-133 NMR study of the Cs^+ ion complexation by large macrocyclic crown ethers, dibenzo-27-Crown-9 and dibenzo-24-Crown-8 in various nonaqueous solvents, and shows how the thermodynamic parameters for the complexation process is affected by the nature of the medium, the cavity size, and the number of donor atoms in the polyether ring.

B. Complexation of Cs^+ ion by DB27C9

a. Effect of the solvent on the stability of the $(DB27C9 \cdot Cs)^+$ complex

Cesium-133 chemical shifts were measured as a function of DB27C9/Cs^+ mole ratio for the $(DB27C9 \cdot Cs)^+$ system in dimethylsulfoxide, dimethylformamide, methanol, propylene carbonate, acetonitrile, pyridine, acetone and nitromethane solutions at 30°C. The cesium-133 NMR chemical shift-mole ratio data are given in Tables 18-26. The variation of the ^{133}Cs chemical shifts as a function of the DB27C9/Cs^+ mole ratio in various solvents is shown in Figures 21 and 22.

The chemical shift-mole ratio plots were analyzed by a computer fit of the data to the equation relating the observed chemical shift to the formation constant of the complex as described in Chapter III. The stability constants and the limiting chemical shifts for the $(DB27C9 \cdot Cs)^+$ complex in various solvents at 30°C are listed in Table 27.

A change of solvent would be expected to result in changes in the complex stability, especially when the cation and ligand are strongly solvated. As mentioned in the first chapter, the solvation of the ligand and metal cation are influenced by the donor ability and dielectric constant of the solvents as well as by the shape and size of the solvent molecules. However, it has been shown that

the donor ability of a solvent plays the most important role in the behavior of alkali complexes in nonaqueous solvents (16).

It is seen that (Table 27) the formation constants of the $(DB27C9 \cdot Cs)^+$ complex are much lower in dimethylsulfoxide and dimethylformamide solutions than in the other solvents. Dimethylsulfoxide (D·N = 29.8) and dimethylformamide (DN = 26.6) with high donor abilities can solvate Cs^+ ion quite strongly and, therefore, compete with the ligand for the cesium ion. Therefore in these solvents the formation of the $(DB27C9 \cdot Cs)^+$ complex is weakened. These results are consistent with the previous studies of the solvation of the Cs^+ ion by different solvents which showed that DMSO and DMF are much more strongly solvating solvents than the other solvents used in this investigation (11). It is interesting to note that although DMF and NM have comparable dielectric constants (Table 27), the formation constant of the complex in NM, a poor donor solvent, is much higher than DMF which has a larger donor number.

Pyridine seems to be an exceptional solvent. Although it has a high donor number (DN = 33.1), the formation constant of $(DB27C9 \cdot Cs)^+$ complex in this solvent is surprisingly high. Similar behaviors for the pyridine solutions of alkali cation-crown ether complexes have been observed by Mei (11), Shamsipur (70), and Smetana (117)

in our laboratory. A possible explanation for this exception may be the relatively poor solvating ability of pyridine for alkali cations. Since pyridine is a nitrogen donor and, therefore, a "soft base", it may not solvate strongly the alkali metal ions which are relatively "hard acids" (121).

b. Thermodynamic parameters for the complexation of Cs^+ ion by DB27C9

In order to have a better understanding of the thermodynamic behavior of $(DB27C9 \cdot Cs)^+$ system, we conducted the complexation studies of Cs^+ ion by the macrocyclic ligand, DB27C9, in various nonaqueous solvents at different temperatures. The chemical shifts of the cesium-133 resonance were measured as a function of $DB27C9/Cs^+$ mole ratios at various temperatures in dimethylformamide, propylene carbonate, nitromethane, acetonitrile, acetone, pyridine, and methanol solutions. In all cases studied here, only one resonance of the metal ion was observed (regardless of the Lig/Cs^+ mole ratio and the temperature), which indicates a fast exchange between the two cationic sites (i.e. free ion in the bulk solution and the complexed ion).

The data obtained from these studies are given in Tables 18-25. Figures 23-30 show the variations of the cesium-133 chemical shifts as a function of $DB27C9/Cs^+$ mole ratios at different temperatures in the above

Table 18. Mole Ratio - Chemical Shift Data for CsSCN (0.005M) in the Presence of DB27C9 in NM at Various Temperatures.

L/Cs^+	Temperature °C					
	30	40	50	61	75	90
0.00	-59.13	-60.52	-61.76	-63.39	-65.87	-67.50
0.16	-55.71	-56.87	-57.65	-59.51	-60.98	-63.24
0.36	-51.57	-52.92	-53.77	-55.17	-57.11	-59.66
0.56	-47.18	-48.03	-38.89	-50.29	-52.00	-54.93
0.88	-42.14	-42.84	-93.77	-45.24	-47.42	-50.21
1.04	-40.75	-41.52	-42.37	-43.69	-45.55	-48.35
1.20	-40.28	-40.90	-41.60	-42.91	-44.93	-47.07
1.38	-40.05	-40.52	-41.14	-42.30	-43.76	-45.86
1.64	-39.81	-40.44	-40.74	-41.75	-43.29	-45.09
1.94	-39.81	-40.12	-40.67	-41.45	-43.23	-44.47
2.38	-39.73	-40.13	-40.51	-41.29	-42.68	-44.08
3.40	-39.66	-40.05	-40.44	-41.06	-42.14	-43.61

Table 19. Mole Ratio - Chemical Shift Data for CsSCN (0.005M) in the Presence of DB27C9 in DMF at Different Temperatures.

L/Cs^+	Temperature °C					
	-10	0	10	20	30	40
0.00	5.94	4.32	2.22	0.28	- 1.19	- 2.43
0.27	- 0.64	- 1.40	- 2.04	- 3.13	- 3.75	- 4.60
0.49	- 4.91	- 4.99	- 4.99	- 5.07	- 5.53	- 5.69
0.71	- 8.09	- 8.01	- 7.39	- 7.08	- 7.01	- 7.01
0.84	- 9.64	- 9.33	- 8.56	- 7.78	- 7.71	- 7.40
1.00	-12.28	-11.67	-10.35	- 9.41	- 9.10	- 8.63
1.24	-14.38	-13.98	-12.13	-10.88	-10.43	- 9.64
1.59	-16.55	-15.69	-14.61	-12.59	-11.97	-11.20
2.14	-18.56	-17.78	-16.32	-14.76	-13.84	-12.98
2.53	-19.34	-18.60	-17.40	-15.93	-14.92	-13.83
3.33	-20.27	-19.96	-19.10	-17.63	-16.86	-15.30
5.39	-21.67	-21.36	-20.81	-19.96	-19.18	-18.10

Table 20. Mole Ratio - Chemical Shift Data for CsSCN (0.005M) in the Presence of DB27C9 in PC at Various Temperatures.

L/Cs^+	Temperature °C					
	12	30	40	46	57	65
0.00	-35.21	-37.54	-38.32	-39.01	-40.25	-41.49
0.16	-34.59	-36.91	-37.54	-38.01	-39.40	-40.87
0.45	-33.81	-35.68	-36.14	-36.69	-38.07	-39.47
0.63	-33.43	-35.13	-35.52	-36.22	-37.22	-39.01
0.80	-33.12	-34.67	-35.36	-35.52	-37.07	-38.31
0.98	-32.66	-34.28	-34.59	-35.06	-36.13	-37.61
1.29	-32.48	-33.66	-34.28	-34.44	-35.44	-36.68
1.57	-32.41	-33.58	-34.05	-34.13	-35.13	-36.37
1.98	-32.26	-33.43	-33.74	-33.98	-34.82	-36.21
2.49	-32.42	-33.39	-33.55	-33.81	-34.44	-35.75
3.12	-32.34	-33.35	-33.51	-33.65	-34.28	-35.52

Table 21. Mole Ratio - Chemical Shift Data for CsSCN (0.005M) in the Presence of DB27C9 in AN at Various Temperatures.

L/Cs^+	Temperature °C					
	9	17	30	45	63	77
0.00	35.26	34.01	30.92	28.90	25.41	22.70
0.16	28.35	26.88	24.72	22.78	19.98	18.12
0.39	13.39	12.45	10.81	10.29	9.28	8.89
0.55	8.12	7.49	6.48	5.87	5.71	5.56
0.82	- 5.92	- 5.61	- 5.38	- 4.68	- 3.28	- 2.35
1.08	-11.34	-11.03	-10.41	- 9.33	- 7.55	- 6.15
1.20	-12.89	-12.51	-12.58	-11.65	- 9.64	- 8.09
1.41	-13.44	-13.92	-13.75	-13.37	-12.27	-10.80
1.63	-13.91	-14.14	-14.22	-13.99	-13.05	-11.81
2.02	-14.22	-14.60	-15.15	-15.00	-14.37	-13.94
2.53	-14.53	-14.91	-15.30	-15.62	-15.30	-14.76
3.37	-14.60	-15.00	-15.62	-16.08	-16.31	-16.08

Table 22. Mole Ratio - Chemical Shift Data for CsSCN (0.005M) in the Presence of DB27C9 in AC at Different Temperatures

L/Cs^+	Temperature °C				
	20	30	40	55	55
0.00	-18.08	-19.79	-21.20	-22.12	-23.20
0.20	-20.41	-21.97	-22.78	-23.51	-24.60
0.37	-22.43	-23.67	-24.26	-24.83	-25.69
0.57	-24.44	-25.53	-25.92	-26.30	-27.08
0.78	-26.77	-27.55	-27.62	-27.86	-28.32
0.93	-28.01	028.63	-28.52	-28.63	-28.94
1.01	-28.63	-29.10	-29.02	-29.18	-29.41
1.25	-28.94	-29.72	-29.61	-29.80	-29.87
1.60	-29.33	-30.03	-30.11	-30.18	-30.42
2.38	-29.41	-30.19	-30.34	-30.75	-30.96
3.04	-29.41	-30.19	-30.50	-30.80	-31.01
3.99	-29.41	-30.19	-30.58	-30.80	-31.11

Table 23. Mole Ratio - Chemical Shift Data for CsSCN (0.005M) in the Presence of DB27C9 in PY at Various Temperatures.

L/Cs^+	Temperature °C					
	30	48	56	68	82	98
0.00	32.54	29.43	27.89	24.78	22.15	20.21
0.13	26.50	24.09	22.61	20.76	17.88	16.25
0.36	11.22	8.74	8.89	7.34	6.64	6.41
0.76	-10.73	- 8.48	- 9.03	- 8.02	- 6.62	- 4.07
0.89	-14.22	-12.59	-11.66	-10.58	- 8.79	- 5.85
1.05	-17.09	-15.70	-14.77	-13.52	-11.67	- 8.63
1.20	-18.02	-17.01	-16.62	-15.15	-13.44	-10.42
1.64	-18.87	-18.80	-18.64	-18.18	-16.71	-14.23
2.29	-19.18	-19.57	-19.69	-19.73	-18.65	-16.71
2.78	-19.34	-19.80	-19.95	-20.53	-19.34	-17.79
3.95	-19.50	-20.03	-20.26	-20.74	-19.97	-18.87

Table 24. Mole Ratio - Chemical Shift Data for Complexation of Cs^+ by DB27C9 in Methanol at Various Temperatures.

L/Cs^+	Temperature °C				
	25	30	40	50	59
0.00	-46.67	-47.36	-48.92	-50.46	-51.87
0.22	-44.58	-45.43	-46.66	-47.82	-49.69
0.37	-43.18	-49.11	-45.12	-46.76	-47.83
0.59	-41.16	-41.93	-42.64	-44.26	-45.82
0.78	-39.76	-40.77	-41.71	-43.02	-44.88
0.96	-38.83	-39.92	-40.85	-42.01	-43.80
1.08	-38.21	-39.06	-39.99	-41.01	-42.71
1.27	-37.74	-38.44	-39.45	-40.46	-42.09
1.73	-37.43	-37.91	-38.56	-39.53	-41.00
2.39	-37.20	-37.75	-38.21	-39.06	-40.38
3.10	-37.36	-37.75	-38.06	-38.83	-40.15

Note: Concentration of CsSCN = 0.005M.

Table 25. Cesium-133 Data for Complexation of Cs^+ Ion by DB27C9 in Methanol at Various Temperatures [a]

L/Cs^+	Temperature °C			
	16	31	40	47
0.00	-44.50	-46.85	-48.22	-49.46
0.18	-42.80	-44.81	-46.13	-47.21
0.48	-40.23	-41.78	-43.03	-43.95
0.75	-38.22	-39.61	-40.70	-31.47
0.87	-37.29	-38.84	-39.69	-40.54
0.97	-37.06	-38.37	-39.30	-40.08
1.07	-36.75	-38.06	-38.91	-39.69
1.47	-36.20	-37.29	-38.06	-38.68
1.85	-36.05	-37.13	-37.80	-38.37
2.56	-36.05	-36.97	-37.60	-38.14
2.91 [b]	-36.05	-36.97	-37.60	-38.14

[a] Conc. of CsSCN = 0.01M.

[b] Saturated solution of ligand.

Table 26. Mole Ratio Study of DB27C9 with CsSCN (0.005M) in DMSO at 30°C

L/Cs^+	δ (ppm)
0.00	65.04
0.21	63.18
0.46	61.16
0.75	59.23
1.04	57.13
1.17	56.18
1.46	54.10
1.81	51.86
2.29	49.23
3.02	45.19

Table 27. Formation Constants of the $(DB27C9 \cdot Cs)^+$ Complex in Various Solvents at 30°C.

Solvent	D•N[a]	D[b]	Log K_f
Dimethylsulfoxide	29.8	45.0	1.38 ± 0.03
Dimethylformamide	26.6	36.1	2.20 ± 0.01
Propylene Carbonate	15.1	65.0	3.64 ± 0.03
Acetonitrile	14.1	37.5	3.89 ± 0.03
Pyridine	33.1	12.3	4.15 ± 0.02
Acetone	17.0	20.7	4.24 ± 0.15
Nitromethane	2.7	35.9	4.29 ± 0.04

[a] D•N = Gutmann Donor Number.

[b] D = Dielectric Constant.

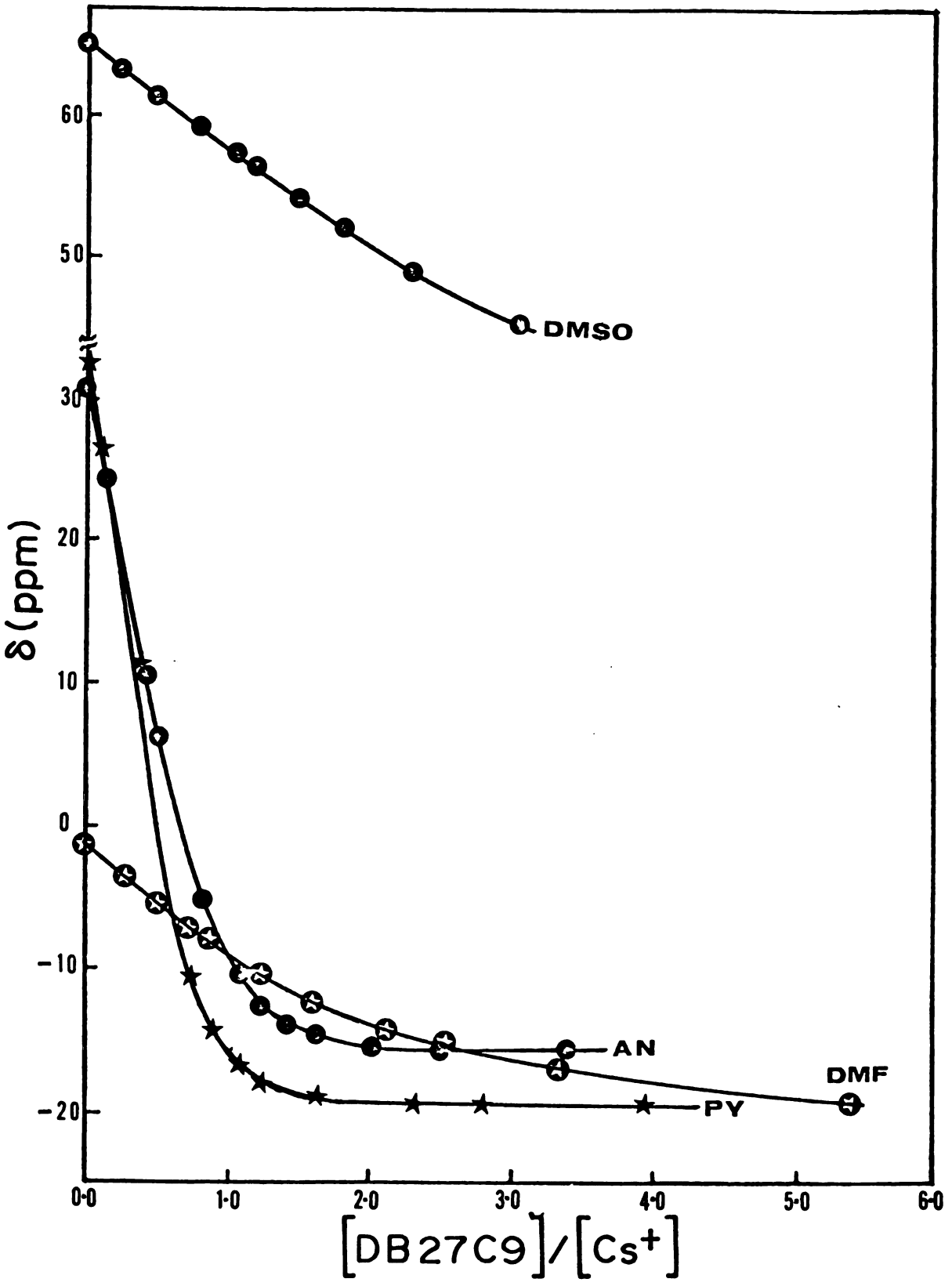

Figure 21. Cesium-133 chemical shift vs. (DB27C9)/$(Cs)^+$ mole ratio in various solvents.

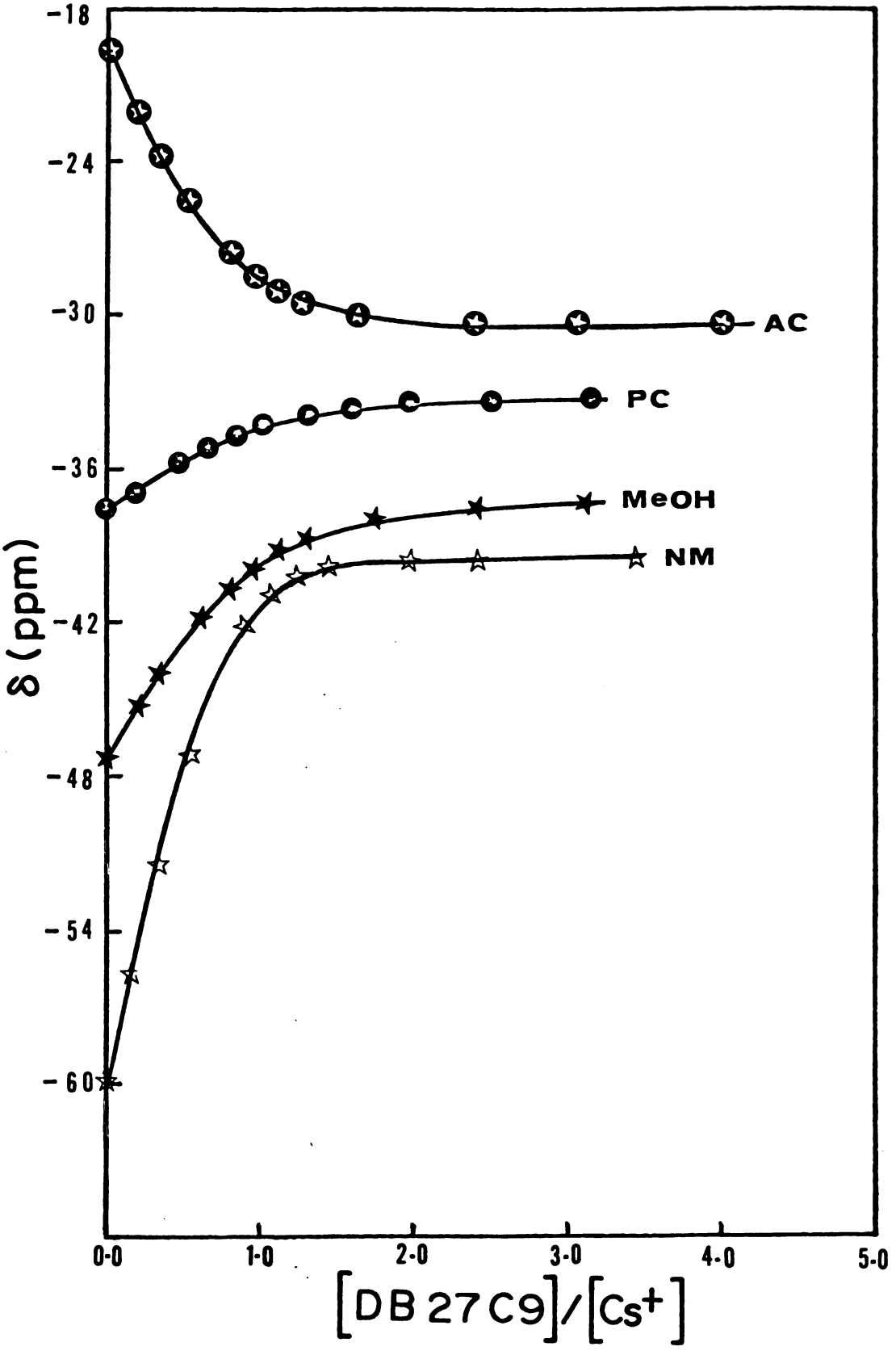

Figure 22. Cesium-133 chemical shifts vs. (DB27C9)/(Cs^+) mole ratio in various solvents.

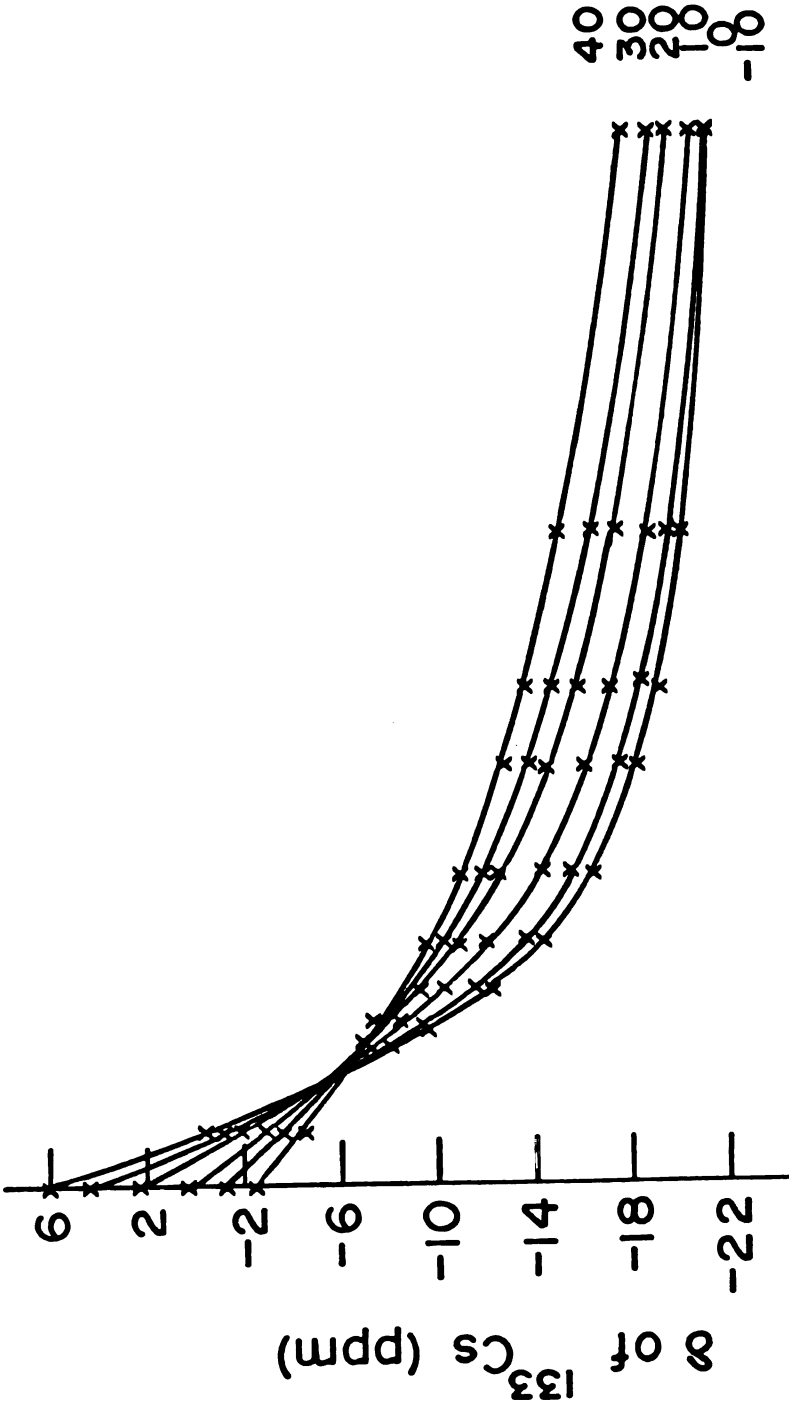

Figure 23. Cesium-133 chemical shift as a function of (DB27C9)/(Cs^+) mole ratio in DMF at different temperatures.

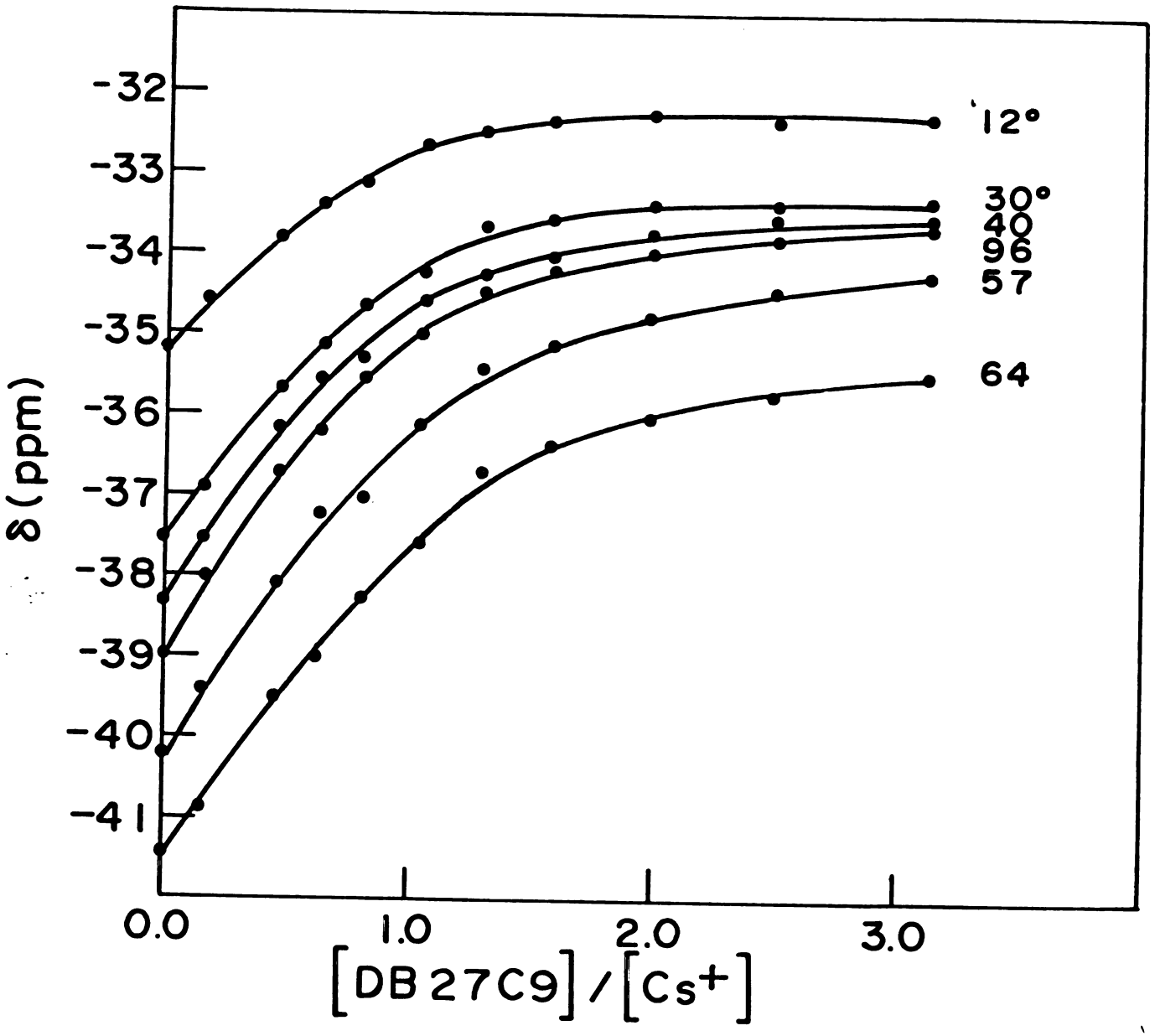

Figure 24. Cesium-133 chemical shift vs. (DB27C9)/(Cs^+) mole ratio in PC at different temperatures.

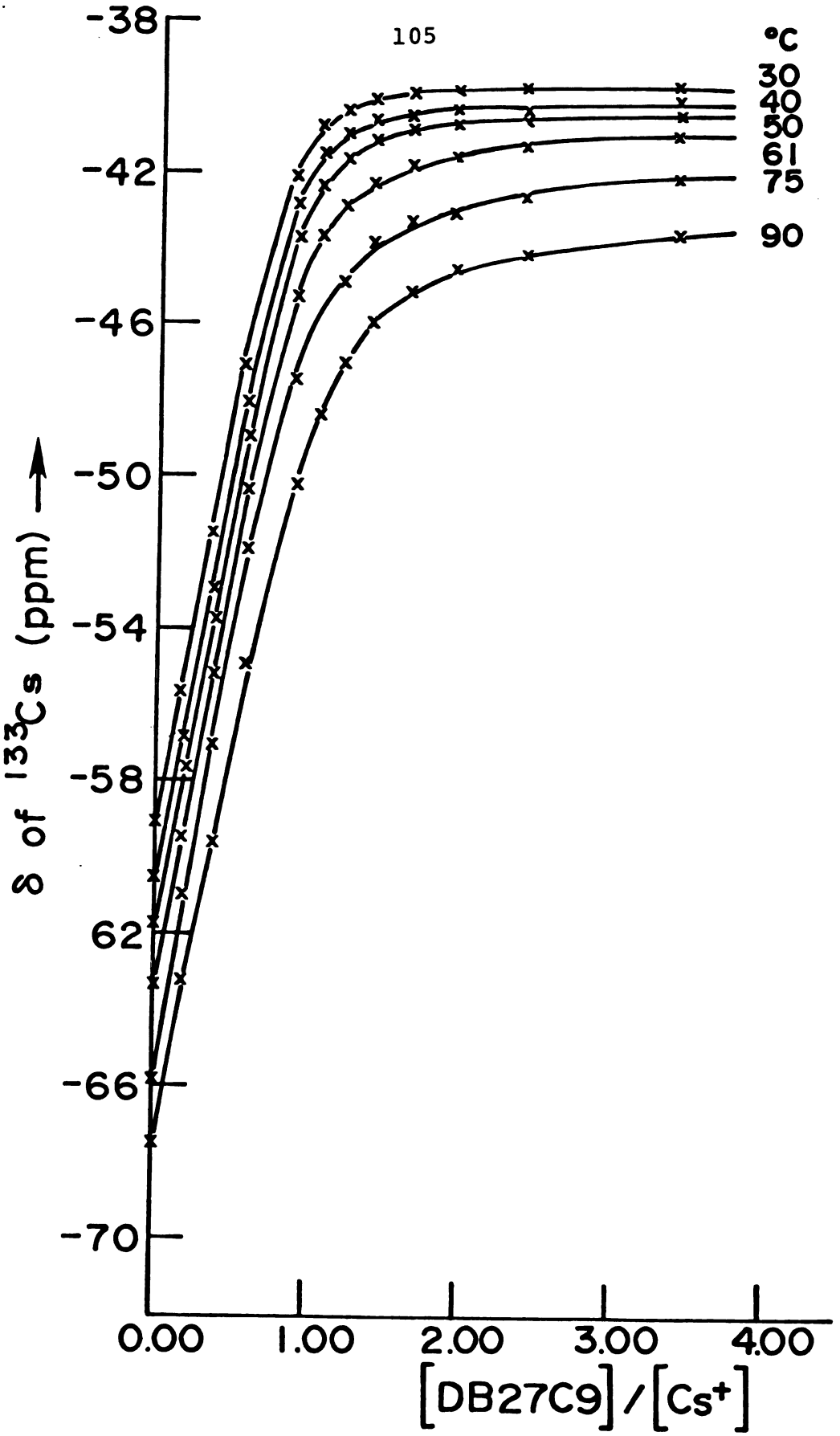

Figure 25. Cesium-133 chemical shift vs. (DB27C9)/(Cs^+) mole ratio in NM at various temperatures.

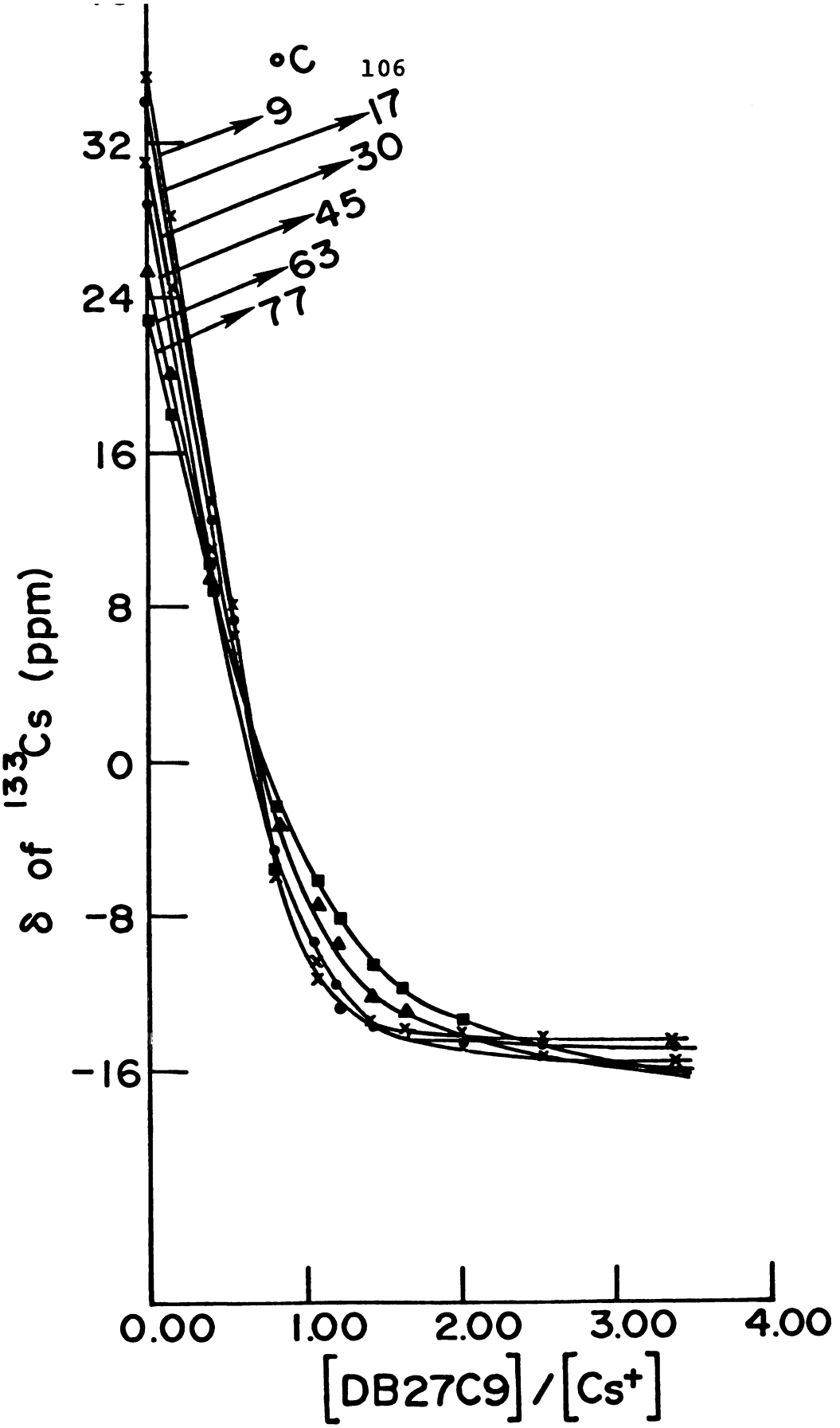

Figure 26. Cesium-133 chemical shift vs. (DB27C9)/(Cs^+) mole ratio in AN at various temperatures.

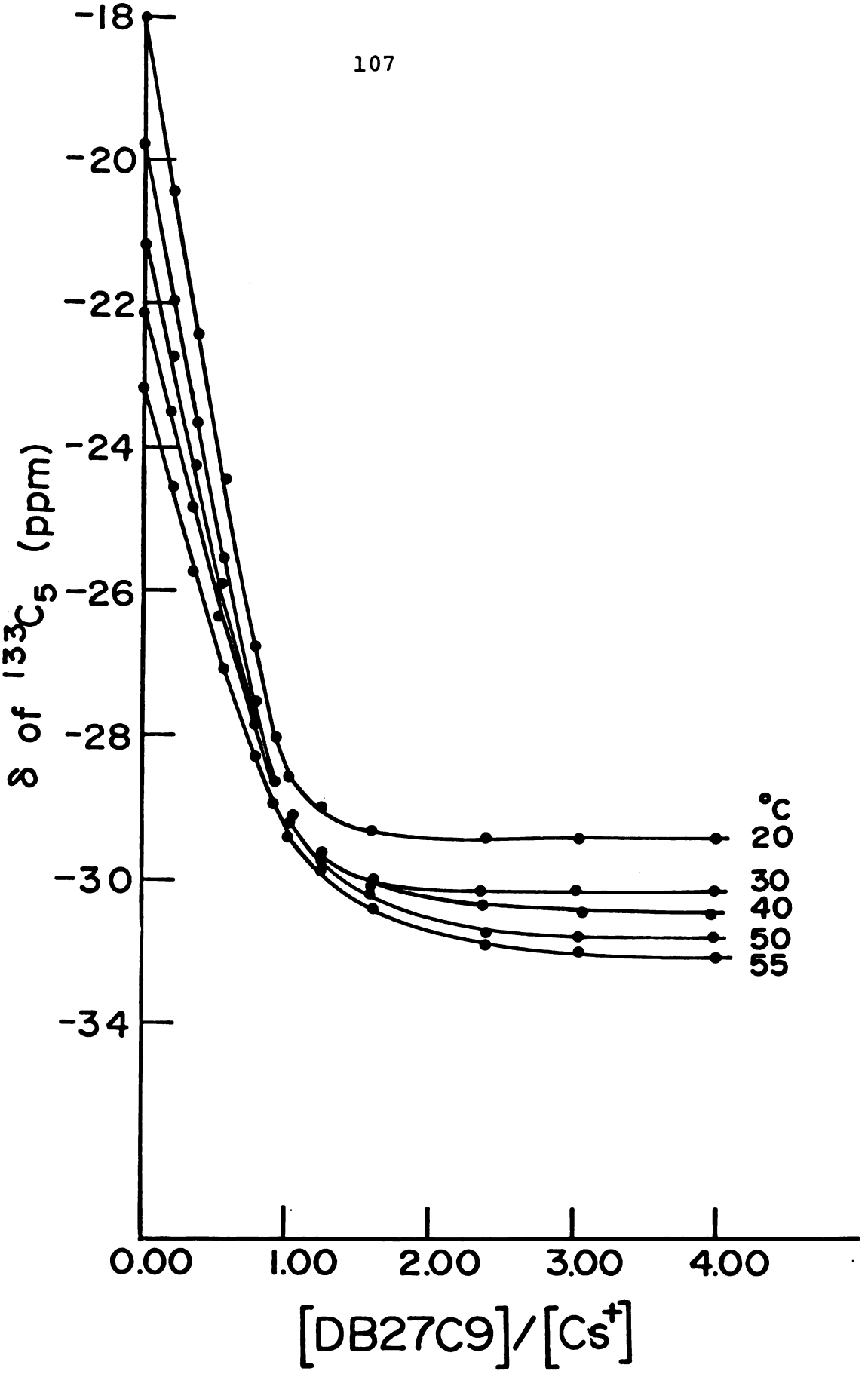

Figure 27. Cesium-133 chemical shift vs. (DB27C9)/(Cs^+) in AC at various temperatures.

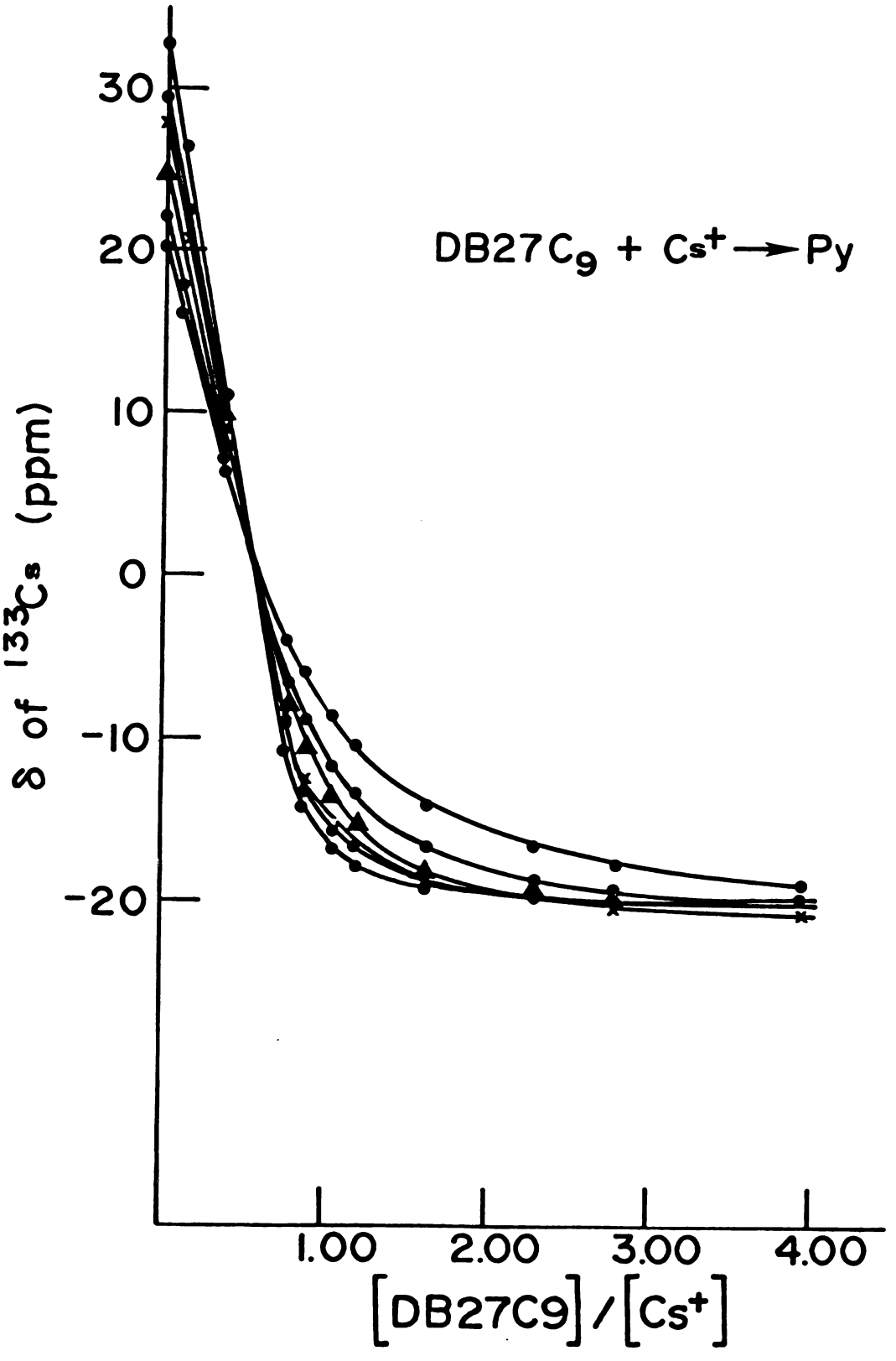

Figure 28. Cesium-133 chemical shift vs. (DB27C9)/(Cs^+) mole ratio in PY at various temperatures.

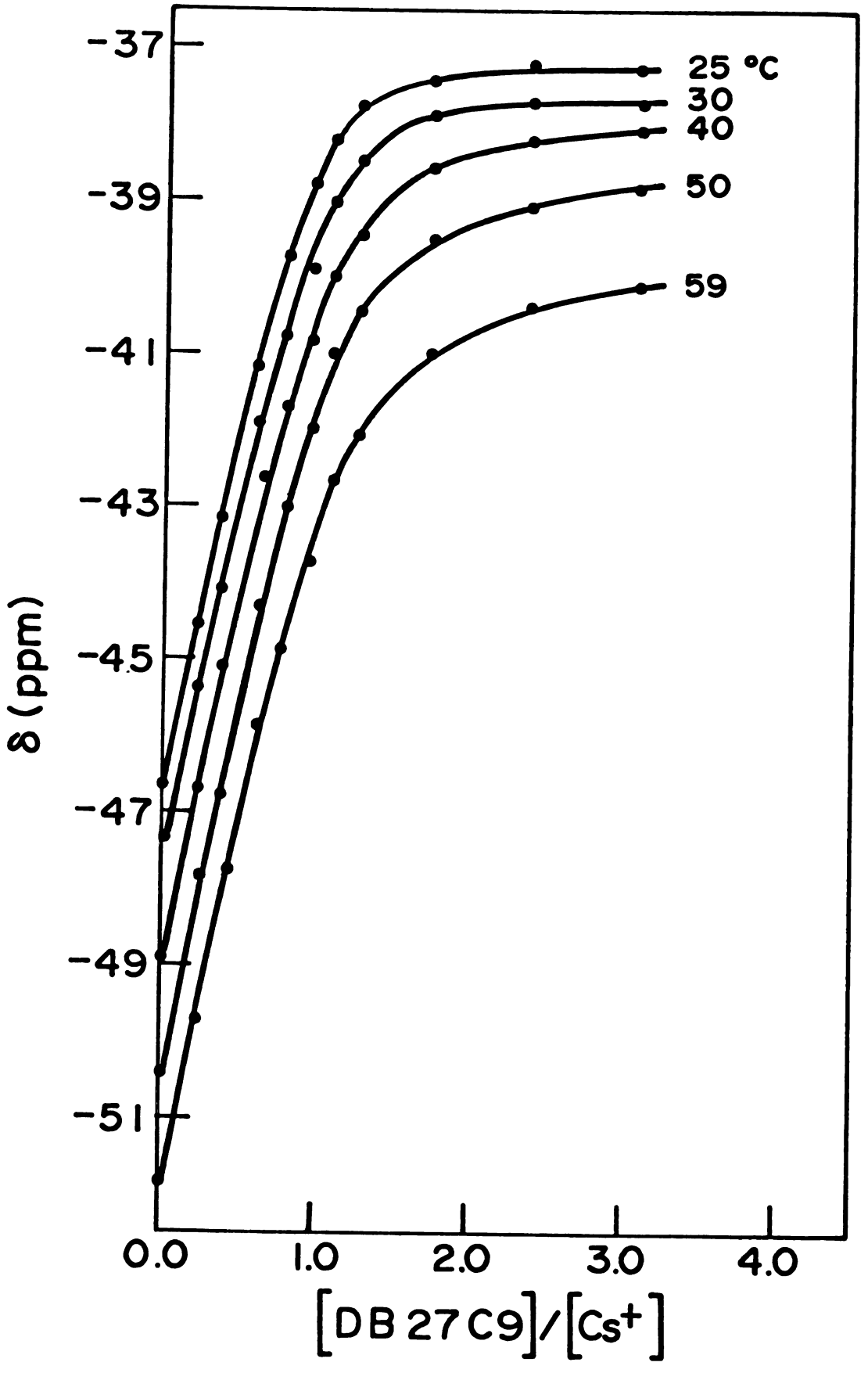

Figure 29. Cesium-133 chemical shift vs. (DB27C9)/(Cs^+) in MeOH at various temperatures.

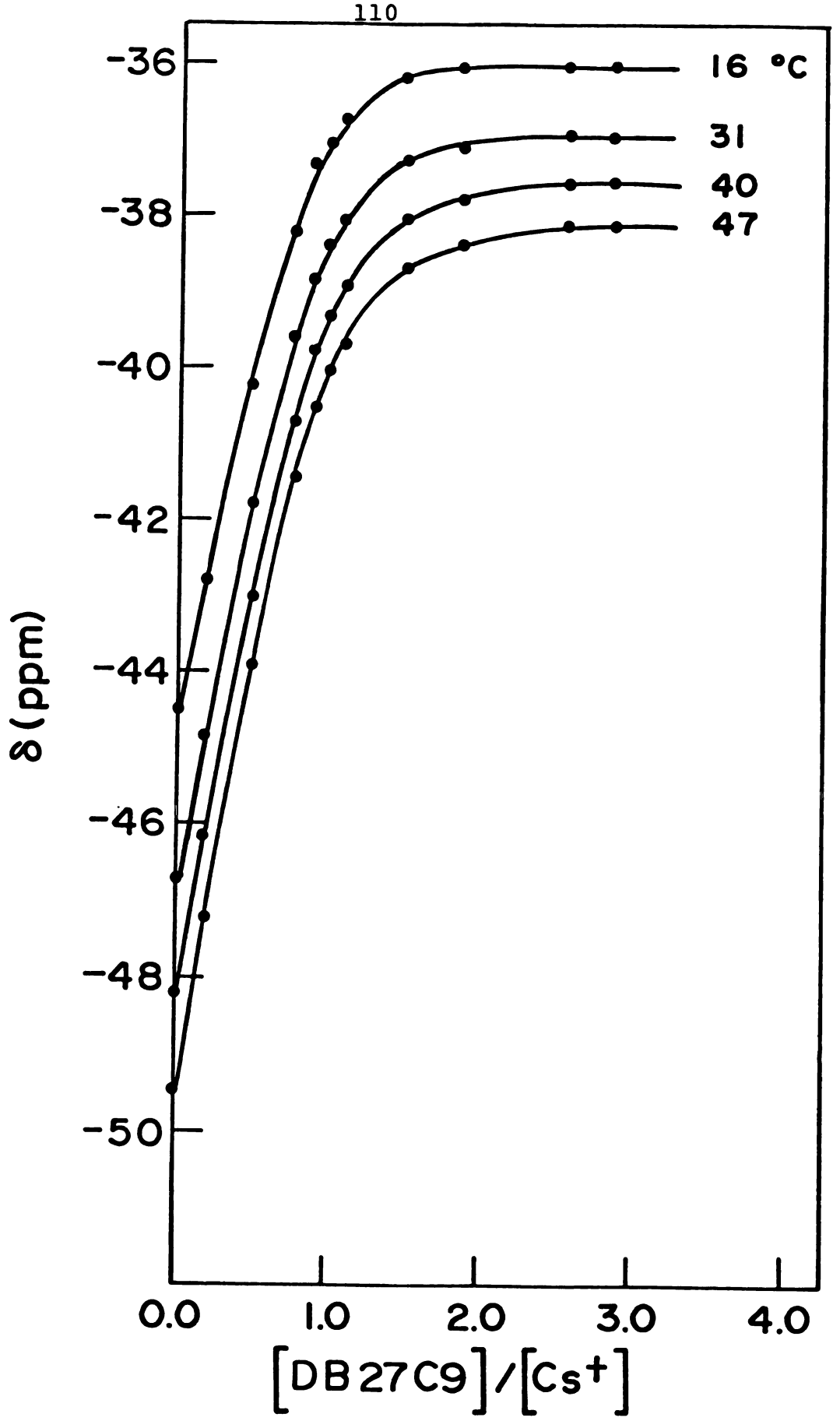

Figure 30. Cesium-133 chemical shift vs. (DB27C9)/(Cs^+) mole ratio in MeOH at various temperatures.

mentioned solvents. It is evident that as the temperature increases the plots show less curvature which indicates the formation of a weaker complex at higher temperatures. This behavior shows that in these solvents the reaction between cesium ion and the ligand is exothermic. The cesium-133 resonance shifts upfield or downfield (depending on the particular solvent) with increasing the concentration of ligand and a clear break at a 1:1 (metal ion:ligand) mole ratio is observed.

The formation constants of $(DB27C9 \cdot Cs)^+$ complex in different solvents at various temperatures were computed by the KINFIT program (page217) and the results are given in Table 28. The data show again that the stability constant increases as the temperature is lowered.

The thermodynamic parameters, ΔG_c°, ΔH_c°, and ΔS_c° values were calculated from variation of the equilibrium constant with temperature using the following well known expressions:

$$\ln K_f = \frac{-\Delta H^\circ}{RT} + \frac{\Delta S^\circ}{R} \qquad (1)$$

$$\Delta G^\circ = -RT \ln K_f$$

Van't Hoff plots of $\ln K_f$ versus $\frac{1}{T}$ for the $(DB27C9 \cdot Cs)^+$ system in various solvents are shown in Figure 31. The enthalpies (ΔH_c°) and the entropies (ΔS_c°) of complexation were obtained from the slopes and intercepts of the plots and the results with the ΔG_c° values

Table 28. Formation Constants of $(DB27C9,Cs)^+$ Complex in Various Solvents at Different Temperatures

Solvent	Temperature (°C)	Log Kf
Dimethylformamide (DMF)	40	2.05 ± 0.01
	30	2.20 ± 0.01
	20	2.33 ± 0.01
	10	2.58 ± 0.01
	0	2.78 ± 0.01
	-10	2.89 ± 0.01
Propylenecarbonate (PC)	64	2.84 ± 0.05
	57	2.95 ± 0.03
	46	3.18 ± 0.03
	40	3.27 ± 0.05
	30	3.64 ± 0.03
	12	> 4
Nitromethane (NM)	90	3.46 ± 0.01
	75	3.48 ± 0.05
	61	3.81 ± 0.02
	50	4.14 ± 0.03
	40	4.24 ± 0.06
	30	4.29 ± 0.04
Acetonitrile (AN)	77	3.09 ± 0.02
	63	3.30 ± 0.02
	45	3.63 ± 0.01
	30	3.89 ± 0.03
	17	4.17 ± 0.04
	9	4.24 ± 0.04
Acetone (AC)	55	3.22 ± 0.04
	50	3.62 ± 0.14
	40	3.88 ± 0.19
	30	4.24 ± 0.15
	20	4.43 ± 0.15

Table 28 (continued)

Solvent	Temperature (°C)	Log Kf
Pyridine (PY)	98	3.08 ± 0.01
	82	3.35 ± 0.02
	68	3.61 ± 0.06
	56	3.78 ± 0.02
	48	3.93 ± 0.02
	30	4.15 ± 0.02
Methanol	59	3.22 ± 0.04
(Conc. of CsSCN = 0.005M)	50	3.32 ± 0.02
	40	3.46 ± 0.03
	30	3.52 ± 0.09
	25	3.74 ± 0.02
Methanol	47	3.35 ± 0.02
(Conc. of CsSCN = 0.011M)	40	3.40 ± 0.02
	31	3.51 ± 0.04
	16	4.09 ± 0.16

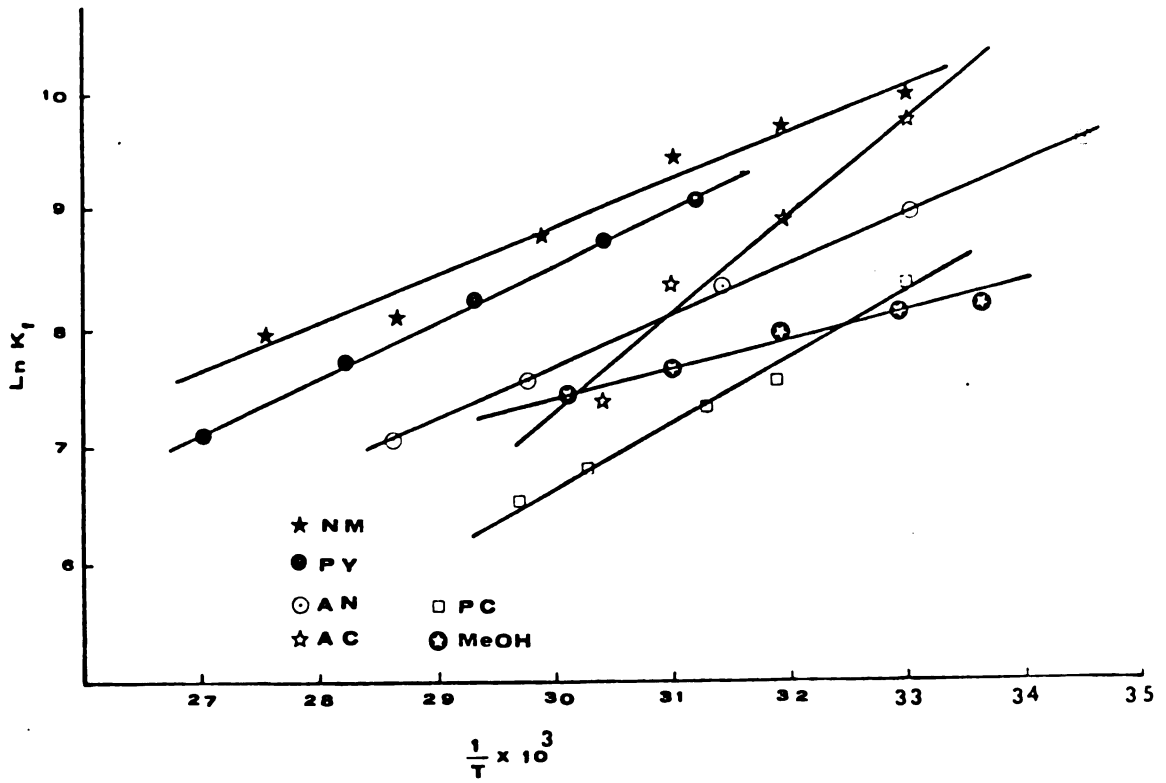

Figure 31. A plot of ln K vs. $\frac{1}{T}$ for the complexation of Cs^+ ion with DB27C9 in various nonaqueous solvents.

(at 30°C) are listed in Table 29. These data indicate that in all cases the $(DB27C9 \cdot Cs)^+$ complex is enthalpy stablized but entropy destabilized, and that both quantities ΔH_c° and ΔS_c°, are quite sensitive to the nature of the solvent.

Of the various factors which contribute to the overall entropy changes (see Chapter I, page 28), it seems that the negative entropy contribution from changes in configurational entropy of the ligand upon complexation may be very pronounced in these cases. The macrocyclic polyether, DB27C9 (contains 9 oxygen atoms in a 27 atom ring) is a representative of the large macrocyclic polyethers, which would be expected to be more flexible than smaller crown ethers. Therefore, a change in the ligand, from a "loose" structure in the free state to a "rigid" structure in the complex state, contributes to the negative entropy changes as a dominant factor.

Quite different ΔS_c° values are observed when the reaction is studied in different solvents (see Table 29) because the rigidity of the free and complexed ligand is different in various solvents. The ΔH_c° values are also solvent dependent since the solvation energies of the Cs^+ ion, the ligand, and of the complex will be different in different solvents.

Table 29. Thermodynamic Parameters for $(DB27C9.Cs)^+$ Complex in Various Nonaqueous Solvents.

Solvent	Log K_f (30°C)	$\Delta G°$ (30°C) (K.Cal/Mole)	$\Delta H°$ (K.Cal/Mole)	$\Delta S°$ (Cal/Mole K°)
Dimethylforamide	2.20 ± 0.01	-3.05 ± 0.01	-7.20 ± 0.37	-13.71 ± 1.19
Methanol	3.52 ± 0.09	-4.88 ± 0.12	-5.09 ± 0.59	- 5.35 ± 1.87
Propylene Carbonate	3.64 ± 0.03	-5.05 ± 0.04	-11.21 ± 0.56	-20.47 ± 1.79
Acetonitrile	3.89 ± 0.03	-5.39 ± 0.04	-7.93 ± 0.42	- 7.95 ± 1.40
Pyridine	4.15 ± 0.05	-5.75 ± 0.07	-9.04 ± 0.52	- 7.10 ± 1.53
Acetone	4.24 ± 0.15	-5.88 ± 0.21	-14.50 ± 1.79	-28.80 ± 5.60
Nitromethane	4.29 ± 0.04	-5.95 ± 0.06	-7.43 ± 0.91	- 4.53 ± 2.78

C. DB24C8 Complex with the Cs^+ ion

The effect of the temperature on the cesium-133 resonance for the $(DB24C8 \cdot Cs)^+$ system was determined at various mole ratios of DB24C8/Cs^+ in dimethylformamide and propylen carbonate solutions. All of the cesium-133 chemical shifts measured at different temperatures are listed in Tables 30 and 31. The chemical shift-mole ratio plots are shown in Figures 32 and 33.

The formation constants of the $(DB24C8 \cdot Cs)^+$ complex at various temperatures are given in Table 32. Plots of ln k versus $\frac{1}{T}$ for the data in this table are shown in Figure 34 and the corresponding thermodynamic parameters are listed in Table 33. Thermodynamic data, show that in both solvents (PC and DMF) the complex is enthalpy stabilized but entropy destabilized, and the enthalpy and entropy values vary with the nature of the solvent. Similar behavior has been observed for $(DB24C8 \cdot Cs)^+$ complex in nitromethane, acetonitrile, acetone, methanol, and pyridine solutions (70). The entropy destabilization of the complex may be explained by the ligand configurational entropy. Dibenzo-24-Crown-8 which is a large macrocyclic ligand should be flexible in the free state, but when it is complexed by the Cs^+ ion it becomes more ordered, and consequently it loses a high degree of freedom in the complexation process.

Table 30. Cesium-133 Chemical Shift Data for Complexation of Cs^+ Ion by DB24C8 in DMF at Various Temperatures

L/Cs^+	Temperature °C					
	0	10	20	30	40	50
0.00	4.16	2.22	0.59	- 1.04	- 2.51	- 3.75
0.25	- 0.55	- 1.74	- 2.28	- 3.13	- 4.21	- 4.99
0.45	- 3.90	- 4.30	- 4.53	- 4.84	- 5.61	- 6.07
0.69	- 7.40	- 6.77	- 6.54	- 6.62	- 6.70	- 7.24
0.84	- 9.41	- 8.32	- 7.94	- 7.55	- 7.55	- 7.94
1.10	-11.81	-10.50	- 9.65	- 9.02	- 8.79	- 8.71
1.45	-14.45	-12.82	-11.58	-10.80	-10.18	-10.02
1.88	-16.40	-15.00	-13.75	-12.67	-11.89	-11.26
2.04	-17.01	-15.46	-14.06	-13.13	-12.12	-11.66
3.08	-19.34	-17.94	-16.77	-15.31	-14.68	-13.83
3.86	-20.56	-19.11	-18.10	-17.01	-15.85	-15.15

Table 31. Cesium-133 Chemical Shift Data for Complexing of Cs^+ Ion by DB24C8 in PC at Various Temperatures

L/Cs^+	Temperature °C					
	20	30	40	50	60	70
0.00	-33.89	-34.98	-36.30	-37.69	-38.61	-39.55
0.18	-33.04	-34.05	-35.36	-36.53	-37.61	-38.70
0.40	-32.42	-33.34	-34.51	-35.60	-36.60	-37.92
0.58	-31.95	-32.88	-33.89	-34.74	-35.99	-37.30
0.82	-31.26	-32.03	-33.12	-33.97	-35.37	-36.14
1.10	-30.71	-31.53	-32.34	-33.20	-34.43	-35.20
1.42	-30.56	-31.14	-32.03	-32.88	-34.04	-34.67
1.92	-30.24	-30.95	-31.80	-32.34	-33.27	-34.20
2.38	-30.40	-30.83	-31.57	-31.95	-32.88	-33.89
3.06	-30.24	-3.075	-31.41	-31.79	-32.65	-33.42
3.88	-30.25	-30.67	-31.33	-31.72	-32.42	-33.19

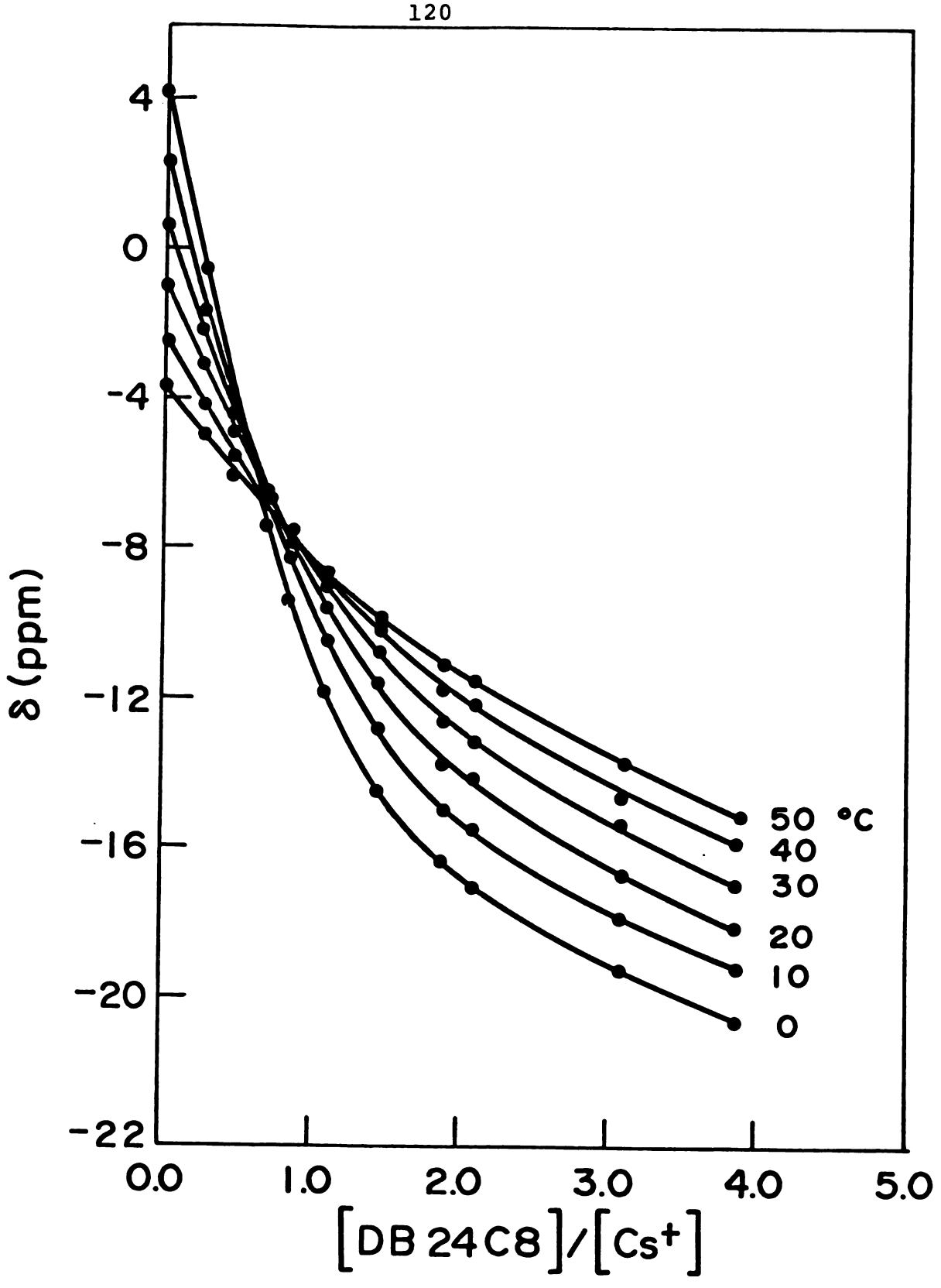

Figure 32. Cesium-133 chemical shift vs. (DB24C8)/(Cs^+) mole ratio in DMF at various temperatures.

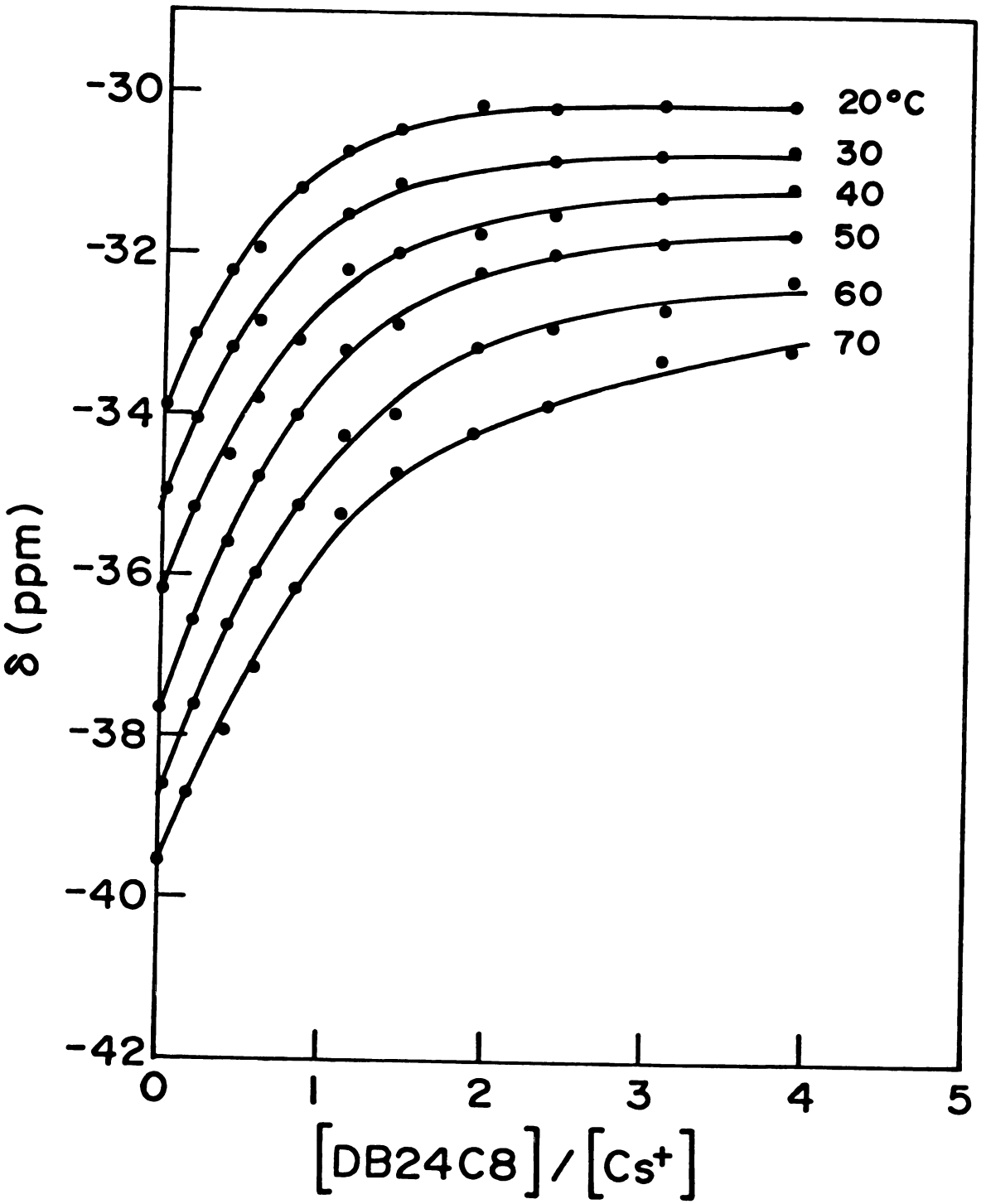

Figure 33. Cesium-133 chemical shift vs. (DB24C8)/(Cs^+) in PC at various temperatures.

Table 32. Stability Constants of $(DB24CB \cdot Cs)^+$ Complex in DMF and PC at Various Temperatures.

Solvent	Temperature (°C)	Log K_f
Dimethylformamide	50	1.89 ± 0.01
	40	2.02 ± 0.01
	30	2.15 ± 0.03
	20	2.32 ± 0.01
	10	2.46 ± 0.03
	0	2.65 ± 0.02
Propylene Carbonate	70	2.70 ± 0.04
	60	2.78 ± 0.02
	50	3.09 ± 0.05
	40	3.12 ± 0.03
	30	3.25 ± 0.04
	20	3.56 ± 0.24

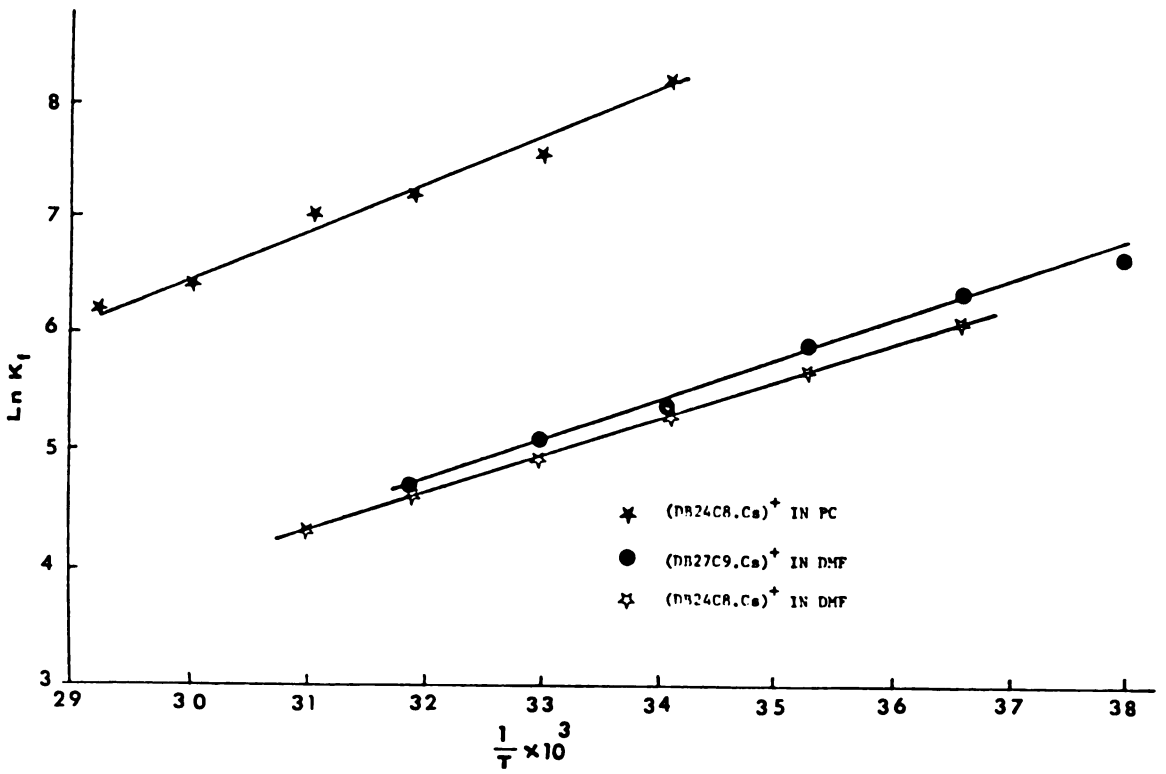

Figure 34. A plot of ln K vs. $\frac{1}{T}$ for the complexation reaction of Cs^+ ion with DB24C8 and DB27C9 in PC and DMF.

Table 33. Thermodynamic Quantities for $(DB24C8 \cdot Cs)^+$ Complex in DMF and PC

Solvent	Log K_f (30°C)	ΔG (30°C) (K Col/Mole)	ΔH° (K Col/Mole)	ΔS° (Cal/Mole K°)
Dimethylformamide	2.15 ± 0.03	-2.98 ± 0.04	-6.12 ± 0.12	-10.29 ± 0.42
Propylene Carbonate	3.25 ± 0.04	-4.51 ± 0.06	-8.11 ± 0.74	-11.39 ± 2.30

D. Comparison of the Thermodynamic Parameters

Thermodynamic parameters obtained for complexing of the Cs^+ ion by dibenzo-27-Crown-9 and dibenzo-24-Crown-8 in various nonaqueous solvents are compared in Table 34. The results are consistent with the change which might be expected from an increase in the cavity size with a consequent increase in the number of donor atoms and in ligand flexibility.

The large differences between the ΔH_c° and ΔS_c° values for these systems suggest that the size of the ligand has a profound effect on the thermodynamic behavior of these complexes. Since in these systems the effects of the metal cation and its charge type on the thermodynamic parameters in the same solvent are the same, therefore the differences in the size of the ligand (consequently the differences in the number of donor atoms and flexibility of the ligand) will be effective in these systems.

It is interesting to note that in all solvents except acetonitrile and methanol the entropy values of the $(DB24C8 \cdot Cs)^+$ complex are less negative than those for the $(DB27C9 \cdot Cs)^+$ complex. It seems reasonable to assume that the dibenzo-27-Crown-9 is a more flexible ligand (because of its larger cavity size) and it undergoes a sizeable deformation upon formation of an inclusion complex, which results in a more negative ΔS_c° value for the complexation reaction.

Table 34. Comparison of thermodynamic quantities for complexation of Cs^+ ion by DB27C9 and DB24C8 in various nonaqueous solvents

Solvent	$(DB27C9 \cdot Cs)^+$			$(DB24C8 \cdot Cs)^+$		
	$\Delta G°(30°C)$ (K.Cal/Mole)	$\Delta H°$ (K.Cal/Mole)	$\Delta S°$ (Cal/Mole.K)	$\Delta G°(30°C)$ (K.Cal/Mole)	$\Delta H°$ (K.Cal/Mole)	$\Delta S°$ (Cal/Mole.K)
DMF	-3.05±0.01	-7.20±0.37	-13.71±1.19	-2.98±0.04	-6.12±0.12	-10.29±0.42
PC	-5.05±0.04	-11.21±0.56	-20.47±1.79	-4.51±0.06	-8.11±0.74	-11.39±2.30
MeOH	-4.88±0.12	-5.09±0.59	- 5.35±1.87	-5.06±0.07	-9.87±0.46	-16.10±1.49 [a]
AN	-5.39±0.04	-7.93±0.42	- 7.95±1.40	-5.47±0.10	-8.12±0.16	- 8.66±0.48
NM	-5.95±0.06	-7.43±0.91	- 4.53±2.78	-5.71±0.11	-6.25±0.10	- 1.79±0.34
PY	-5.75±0.07	-9.04±0.52	- 7.10±1.53	-5.55±0.05	-5.97±0.16	- 1.39±0.46
AC	-5.88±0.21	-14.50±1.79	-28.80±5.60	-5.15±0.13	-11.20±0.52	-20.08±1.71

(a) Reference 70.

Another important point is that in all cases (with the exception of acetonitrile and methanol solutions) the enthalpies of complexation between Cs^+ ion and dibenzo-27-Crown-9 are more negative than those for the corresponding reaction with dibenzo-24-Crown-8. These results may reflect to the increased electrostatic interaction of the Cs^+ ion with dibenzo-27-Crown-9 because of increasing number of interaction sites. On the other hand, the greater flexibility of dibenzo-27-Crown-9 may allow for better enclosure of the cesium ion. In another word, the conformational rearrangement of the ligand upon coordination may occur so as to allow for the greatest interaction between the oxygens of the crown ether and the cation. Such rearrangement has been observed for dibenzo-30-Crown-10 on complexation with K^+ ion as pointed out in Chapter I (page 14). In this case a large deformation of the ligand occurs as it wraps around the potassium ion. It seems reasonable to assume that some wrapping around may occur in the case of complexing of Cs^+ ion by dibenzo-27-Crown-9 which would be expected to result in larger electrostatic energies associated with the Cs^+ donor atoms than in the case of complexing of Cs^+ ion by dibenzo-24-Crown-8. An obvious exception is seen in the case of acetonitrile solutions, probably because it can form a complex in solution with the polyethers, such as that reported with 18-Crown-6 (107). We have no explanation for

the thermodynamic data of the $(DB27C9 \cdot Cs)^+$ system in methanolic solutions. Of course, the role of the ligand solvation on the thermodynamics of complexation cannot be ignored. Since at the present time, the information on the interaction of macrocyclic ligands with the solvent molecules is quite sparse, additional studies on the ligand-solvent interaction are necessary before the thermodynamic behavior of macrocyclic complexes in nonaqueous solvents are understood.

CHAPTER V

CESIUM-133 NMR STUDY OF THE CESIUM ION COMPLEXATION BY CROWN ETHERS AND CRYPTAND-222 IN MIXED NONAQUEOUS SOLVENTS

A. Introduction

While the complexation of macrocyclic ligands with the alkali and alkaline earth cations has been extensively investigated in a wide variety of pure solvents, the complexing ability of the crowns and cryptands in mixed nonaqueous solvents has not been reported previously. Previous measurements of the binding constants of macrocyclic complexes in mixed solvents have been restricted to water/methanol systems.

It was of interest to us to perform some thermodynamic measurements in mixed nonaqueous solvents in order to see how the nature of the medium affects the thermodynamic stability of crown and cryptate complexes.

This chapter reports a study of the Cs^+ ion complexation by macrocyclic ligands C222, DB24C8, and DB27C9 in various mixed nonaqueous solvents. Once again ^{133}Cs NMR was used as the experimental technique.

B. Complexation of the Cs^+ ion by C222

Complexation of the cesium ion with cryptand-222 was studied in AC/DMSO, AN/DMSO, PC/DMSO and PC/DMF binary systems at the probe temperature (32 $\pm$ 1°C). Cesium-133 chemical shifts were determined as a function of C222/Cs^+ mole ratio. The results are listed in Tables 35-38. In

Table 35. Mole Ratio-Chemical Shift Data for CsSCN (0.005M) in the Presence of C222 in DMSO/AC Systems at 32°C.

Pure DMSO		95% DMSO/5% AC		85% DMSO/15% AC		75% DMSO/25% AC	
L/Cs^+	δ (ppm)	L/Cs^+	δ (ppm)	L/Cs^+	δ (ppm)	L/Cs^+	δ (ppm)
0.00	65.12	0.00	65.32	0.00	61.62	0.00	55.69
0.27	66.59	0.22	66.56	0.31	64.57	0.30	58.87
0.55	68.30	0.62	68.97	0.53	65.88	0.54	61.65
0.80	69.93	1.06	72.22	0.71	67.36	0.88	64.76
1.00	70.78	1.64	75.41	0.96	69.53	1.22	67.71
1.55	74.04	2.10	77.80	1.27	71.70	1.78	73.45
1.84	75.35	2.68	80.82	1.76	75.50	2.10	76.24
2.39	77.88	3.02	82.53	2.47	80.08	2.54	78.87
2.65	79.15	4.38	87.96	3.12	83.71	3.50	86.32
3.41	82.49			4.53	90.64	4.02	88.65
4.69	87.38					4.52	91.60

Table 35 (continued)

50% DMSO/50% AC		25% DMSO/75% AC		15% DMSO/85% AC		5% DMSO/95% AC		Pure AC	
L/Cs^+	δ (ppm)	L/Cs^+	δ (ppm)	L/Cs^+	δ (ppm)	L/Cs^+	δ (ppm)	L/Cs^+	δ (ppm)
0.00	47.18	0.00	26.01	0.00	4.25	0.00	-3.31	0.00	-21.58
0.30	53.14	0.24	38.79	0.39	53.26	0.26	31.21	0.24	25.88
0.58	60.28	0.47	55.39	0.55	64.43	0.56	90.95	0.50	69.74
0.90	67.72	0.82	78.89	0.78	91.18	0.82	117.13	0.72	118.47
1.00	69.27	1.12	91.61	1.04	106.23	1.04	136.82	0.96	147.32
1.12	70.59	1.45	103.70	1.29	118.55	1.36	156.83	1.14	159.11
1.32	74.78	1.84	111.53	1.88	140.04	1.60	167.30	1.60	179.81
1.54	78.03	2.12	117.27	2.57	150.35	2.32	173.88	2.02	184.54
2.18	86.33	2.53	125.03	3.33	157.33	2.76	176.91	2.50	186.17
2.44	89.97	3.33	134.57	4.47	16.299	3.48	179.47	3.40	186.93
3.18	97.49	4.59	142.55			4.46	181.71	4.56	188.96
4.78	109.05								

Table 36. Mole Ratio Study of C222 Complex with 0.005M CsSCN in AN/DMSO Systems at 32 C.

Pure AN		80% AN/20 DMSO		60% AN/40% DMSO		40% AN/60% DMSO		20% AN/80% DMSO	
L/Cs^+	δ (ppm)	L/Cs^+	δ (ppm)	L/Cs^+	δ (ppm)	L/Cs^+	δ (ppm)	L/Cs^+	δ (ppm)
0.00	33.16	0.00	41.84	0.00	43.23	0.00	55.78	0.00	61.54
0.22	62.79	0.32	82.93	0.40	74.82	0.41	72.07	0.38	67.50
0.50	117.07	0.54	110.23	0.66	92.74	0.73	80.14	1.04	76.19
0.80	168.95	0.82	131.79	1.00	107.08	1.18	90.37	1.46	81.39
1.06	197.25	1.08	158.00	1.30	120.96	1.45	98.36	1.86	85.26
1.38	204.07	1.30	166.61	1.68	130.11	2.22	111.00	2.44	90.31
1.80	205.16	1.72	175.60	2.16	141.74	2.76	119.06	3.10	95.74
2.32	205.71	2.08	181.42	2.76	149.96	3.31	123.25	3.42	97.99
2.76	205.63	2.66	184.91	3.24	154.31	3.90	128.27	4.10	101.63
3.22	205.70	3.96	188.63	3.90	157.72				
4.49	205.85								

Table 37. Mole Ratio Study of C222 Complex with 0.005M CsSCN in PC/DMSO Binary Mixtures at 32°C.

80% PC/20% DMSO		60% PC/40% DMSO		40% PC/60% DMSO		20% PC/80% DMSO	
L/Cs^+	δ (ppm)	L/Cs^+	δ (ppm)	L/Cs^+	δ (ppm)	L/Cs^+	δ (ppm)
0.00	7.02	0.00	29.90	0.00	45.97	0.00	57.64
0.45	65.02	0.46	56.88	0.29	54.89	0.25	60.75
0.69	90.54	0.82	77.29	0.69	65.67	0.61	65.80
0.96	111.56	1.16	91.94	1.04	74.83	1.27	73.39
1.14	125.52	1.62	107.83	1.43	83.58	1.61	77.81
1.51	138.70	1.92	114.79	1.88	91.25	2.06	81.29
1.96	150.33	2.48	124.79	2.49	99.71	2.53	85.63
2.80	161.19	3.16	133.03	3.04	105.76	3.20	90.91
3.49	165.06	4.20	141.72	4.27	116.15	3.86	94.94
4.08	165.15						

Table 38. Mole Ratio - Chemical Shift Data for CsSCN (0.005M) in the Presence of C222 in DMF/PC Systems at 32°C.

Pure DMF		90% DMF/10% PC		80% DMF/20% PC		70% DMF/30% PC	
L/Cs^+	δ (ppm)	L/Cs^+	δ (ppm)	L/Cs^+	δ (ppm)	L/Cs^+	δ (ppm)
0.00	-1.50	0.00	-3.01	0.00	-5.13	0.00	-7.49
0.33	9.59	0.31	14.28	0.24	11.31	0.26	15.01
0.57	23.09	0.63	30.80	0.55	32.32	0.64	45.63
0.80	30.91	1.00	45.69	0.98	56.52	0.92	61.85
1.08	39.21	1.39	59.96	1.27	67.99	1.32	82.39
1.47	50.46	1.80	70.66	1.82	84.74	1.68	96.97
1.88	61.08	2.20	79.88	2.14	93.66	2.04	106.12
2.59	76.04	2.59	87.87	2.65	103.51	2.44	114.96
3.29	85.12	3.22	98.03	3.39	112.73	3.08	123.33
3.88	92.17	4.04	106.87	4.22	121.42	4.04	132.33
4.78	99.16	4.45	109.28	4.78	125.53	4.62	137.06

Table 38 (continued)

50% DMF/50% PC		30% DMF/70% PC		20% DMF/80% PC		10% DMF/90% PC		Pure PC	
L/Cs^+	δ(ppm)	L/Cs^+	δ(ppm)	L/Cs^+	δ(ppm)	L/Cs^+	δ(ppm)	L/Cs^+	δ(ppm)
0.00	-12.74	0.00	-19.96	0.00	-24.15	0.00	-29.30	0.00	-37.15
0.24	15.48	0.26	21.16	0.26	23.86	0.22	23.04	0.2	14.88
0.57	55.26	0.54	60.01	0.60	69.29	0.48	69.19	0.65	106.41
0.92	85.97	0.98	116.85	0.78	103.42	0.74	113.53	0.98	152.37
1.35	109.86	1.36	141.75	1.22	145.37	1.00	143.78	1.33	168.73
1.49	124.66	1.86	155.08	1.84	164.40	1.36	163.94	1.49	176.41
2.24	135.91	2.12	159.51	2.20	170.19	1.70	171.54	1.84	179.97
2.71	143.21	2.58	163.22	2.54	172.43	2.44	178.52	2.45	182.30
3.41	148.01	3.32	167.26	3.38	175.76	3.24	180.38	2.63	182.53
4.18	153.12	3.98	170.04	3.90	175.92	3.86	181.62	3.41	183.62
4.57	155.22	4.44	170.75	4.64	177.24	4.64	182.09	3.96	184.09
								4.69	184.47

all cases only one resonance of the metal ion was observed, suggesting that the exchange between the two sites (free Cs^+ ion and complexed-Cs^+ ion) is fast compared to the NMR time scale. Graphical representations of the results are shown in Figures 35-39. It is immediately obvious that the nature of the medium plays an important role in the complexation process. For example, as the mole fraction of acetone, acetonitrile, and propylene carbonate in AC/DMSO, AN/DMSO, and PC/DMSO systems is increased, the plots show more pronounced curvature which is evidence for the formation of a stronger complex. Similar behavior is observed in the case of PC/DMF system as the fraction of the propylene carbonate increases.

The values of the formation constants for the cesium-cryptate complex, calculated from the variation of the metal ion chemical shift with the C222/Cs^+ mole ratio, are given in Tables 39-41. The data collected in these tables again show that the values of the stability constant (K_f) of the Cs^+-cryptate increases as the concentration of dimethylsulfoxide and dimethylformamide is lowered. The behavior observed for these systems seems reasonable because solvents with a large donor number, such as dimethylsulfoxide (D·N = 29.8) and dimethylformamide (D·N = 26.6) have fairly large solvating ability for the cesium ion, but solvents with a medium Gutmann donicity, like acetone (D·N = 17.0), acetonitrile (D·N = 14.1), and

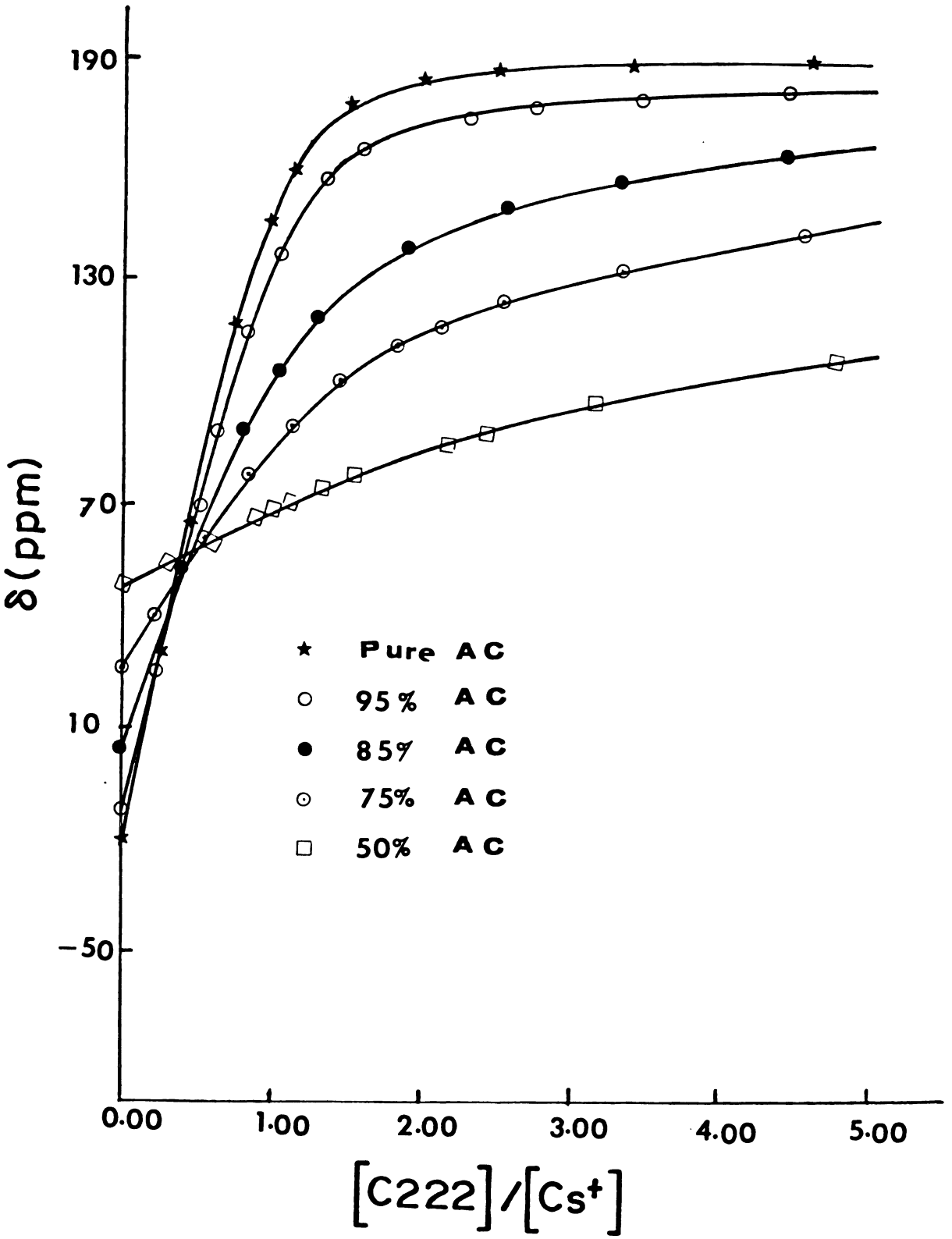

Figure 35. Cesium-133 chemical shifts vs. (C222)/Cs^+) mole ratio in DMSO/AC binary mixtures.

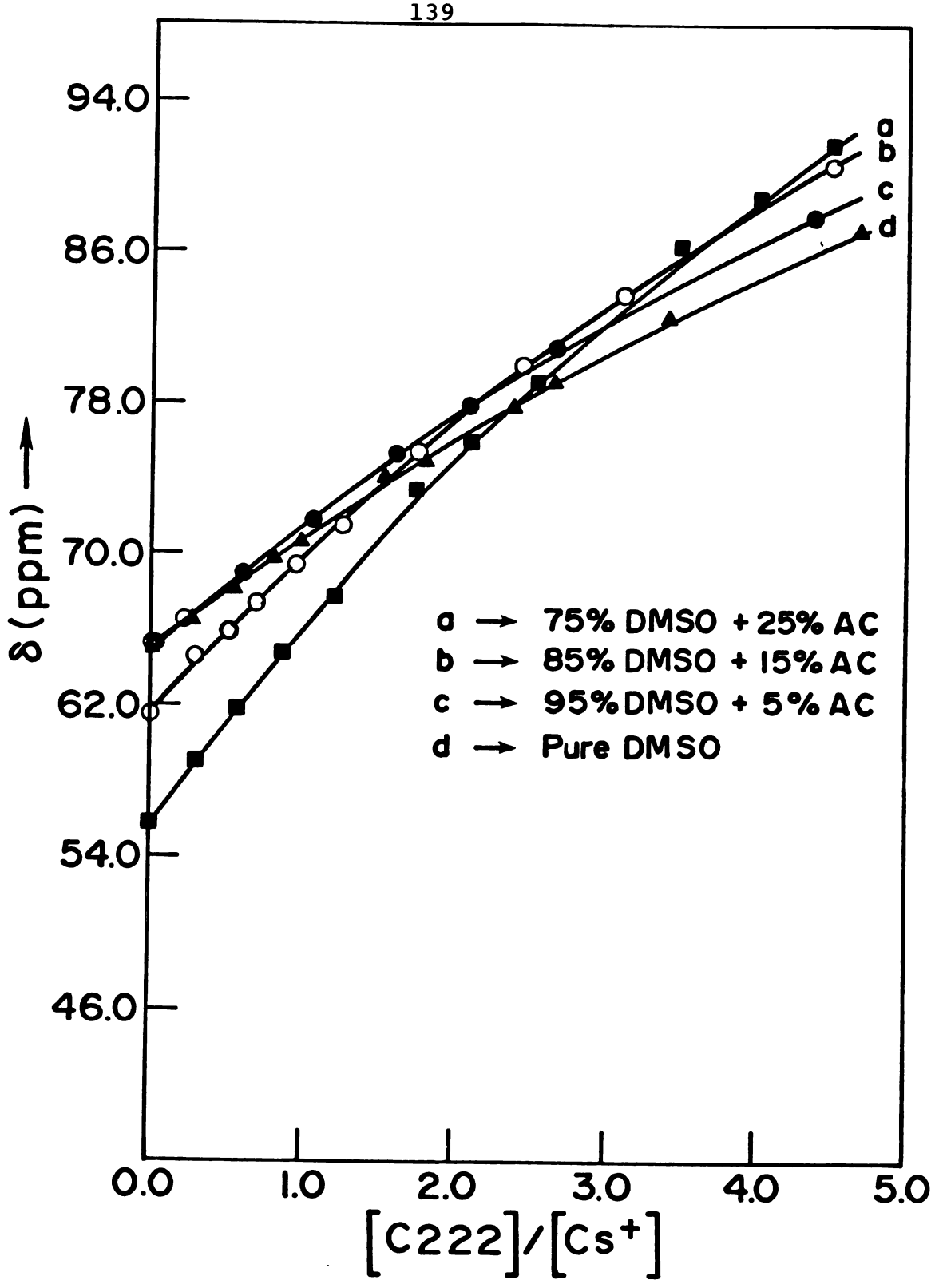

Figure 36. Cesium-133 chemical shifts vs. (C222)/(Cs^+) mole ratio in DMSO/AC binary system.

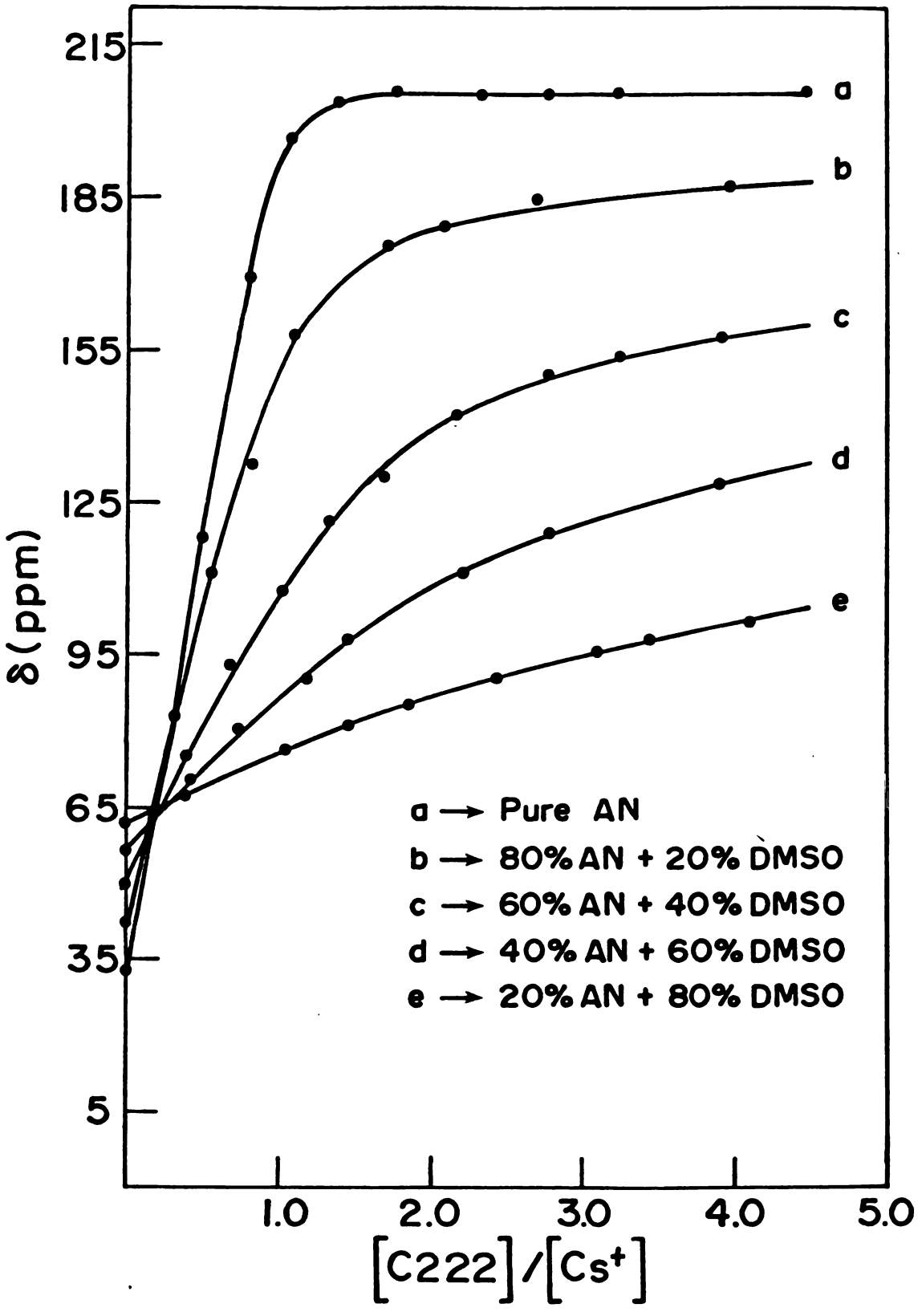

Figure 37. Cesium-133 chemical shifts vs. (C222)/(Cs^+) mole ratio in AN/DMSO binary solutions.

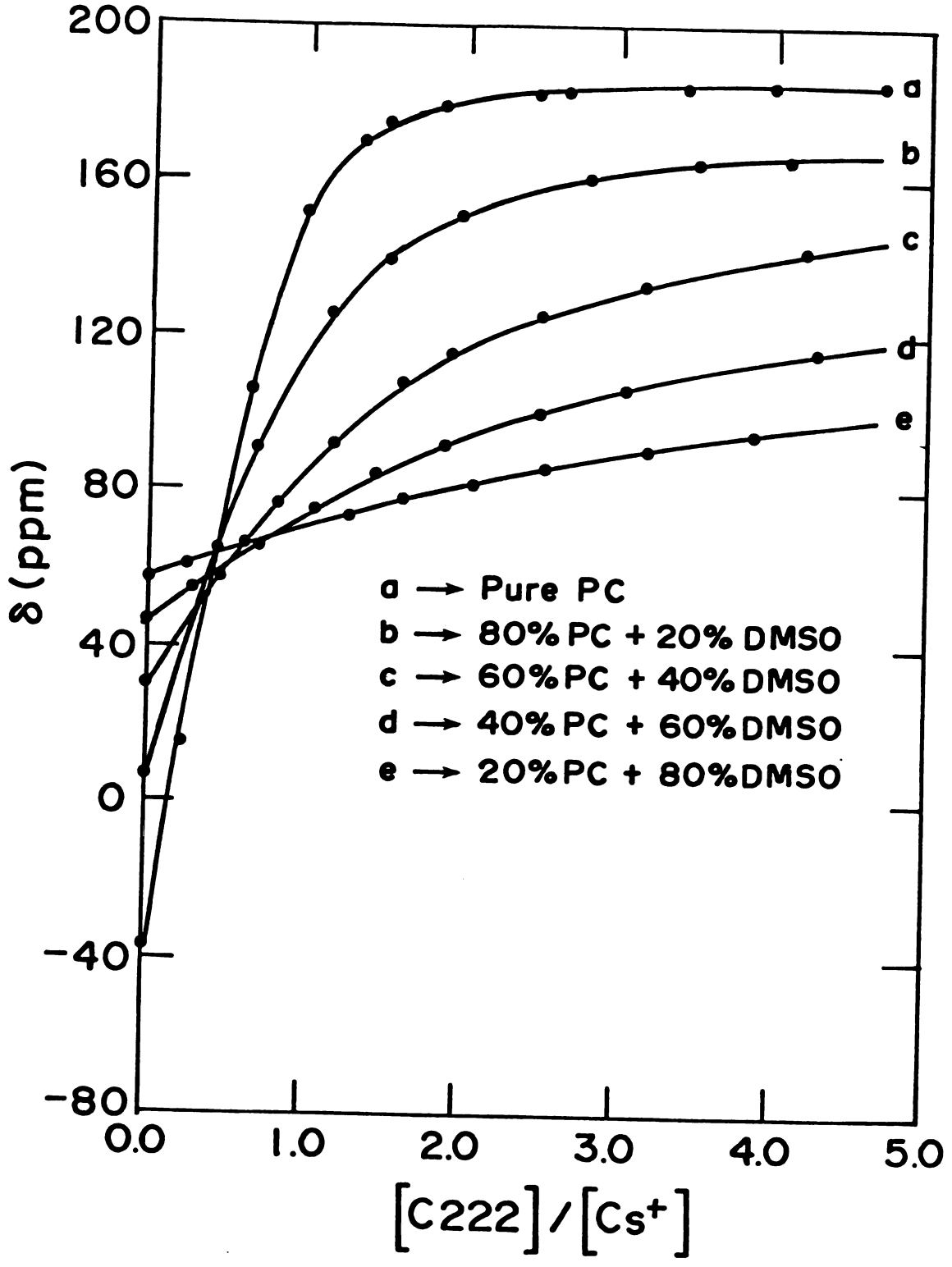

Figure 38. Cesium-133 chemical shifts as a function of $(C222)/(Cs^+)$ mole ratio in PC/DMSO binary mixtures.

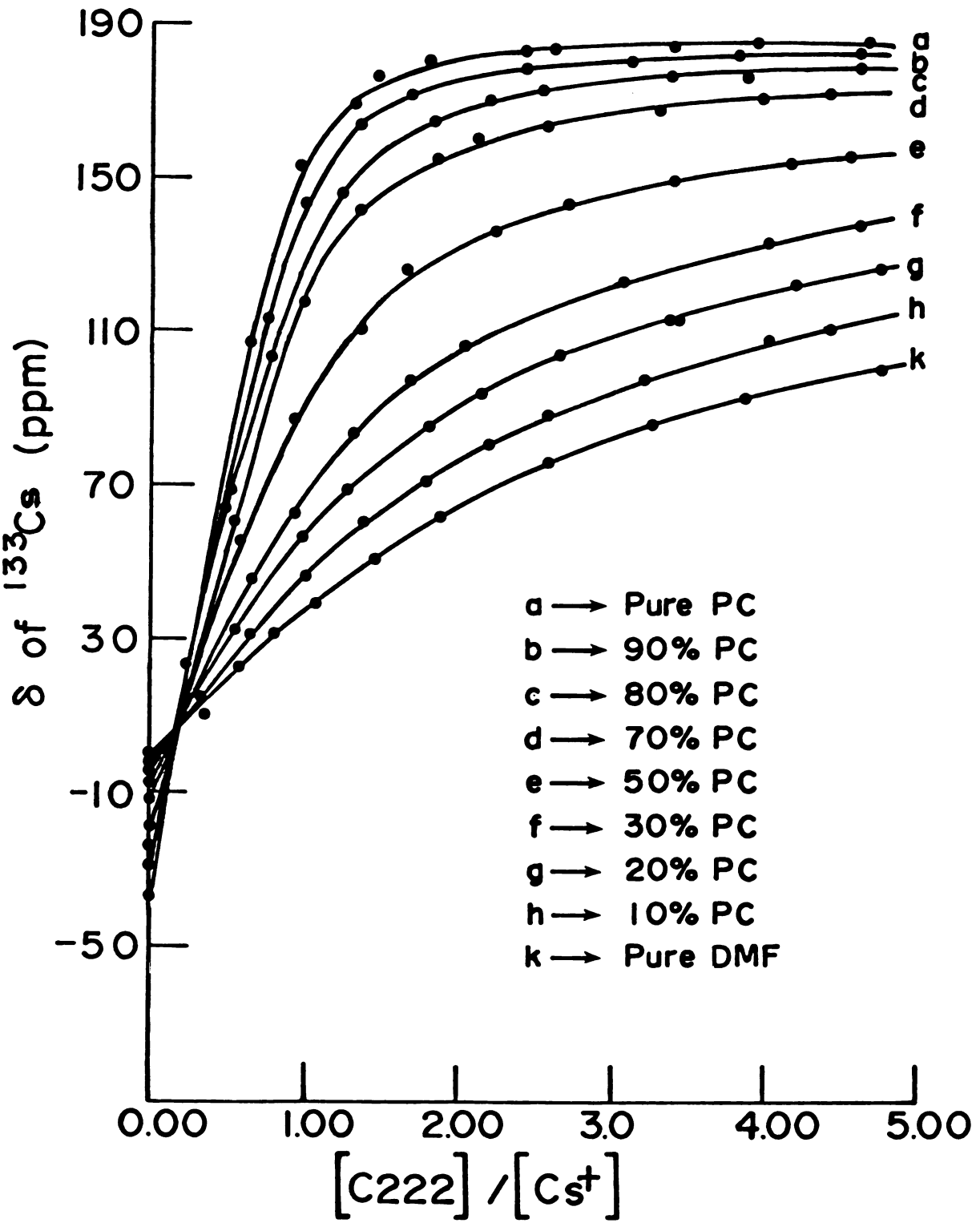

Figure 39. Cesium-133 chemical shifts vs. (C222)/(Cs^+) mole ratio in DMF/PC binary solutions.

Table 39. Log of Formation Constants and Limiting Chemical Shifts for $(C222 \cdot Cs)^+$ Complex in AC and DMSO and Their Mixtures at 32 ± 1°C

Solvent	Log K_f	Limiting Chemical Shift
Pure AC	3.75 ± 0.02	191.1 ± 0.1
95% AC + 5% DMSO	3.28 ± 0.01	187.2 ± 0.2
85% AC + 15% DMSO	2.80 ± 0.01	176.8 ± 0.3
75% AC + 25% DMSO	2.41 ± 0.02	156.7 ± 1.0
50% AC + 50% DMSO	1.80 ± 0.01	155.7 ± 1.5
25% AC + 75% DMSO	1.38 ± 0.04	163.5 ± 7.7
15% AC + 85% DMSO	1.31 ± 0.03	156.1 ± 3.8
5% AC + 95% DMSO	1.25 ± 0.04	143.7 ± 6.0
Pure DMSO	1.19 ± 0.02	154.2 ± 3.4

Table 40. Log of Stability Constants and Limiting Chemical Shifts for $(C222 \cdot Cs)^+$ Complex in Binary Mixed Solvents (at 32 ± 1°C)

Solvent	Log K_f	Limiting Chemical Shift
AN/DMSO System		
Pure DMSO	1.19 ± 0.02	154.0 ± 3.0
20% AN/80% DMSO	1.68 ± 0.02	148.0 ± 3.0
40% AN/60% DMSO	2.05 ± 0.03	167.4 ± 3.0
60% AN/40% DMSO	2.52 ± 0.03	179.4 ± 1.6
80% AN/20% DMSO	3.27 ± 0.02	193.9 ± 0.02
Pure AN	4.71 ± 0.06	206.0 ± 0.3
PC/DMSO System		
20% PC/80% DMSO	1.55 ± 0.04	155.6 ± 5.6
40% PC/60% DMSO	1.94 ± 0.01	159.4 ± 1.2
60% PC/40% DMSO	2.36 ± 0.02	170.8 ± 1.2
80% PC/20% DMSO	3.09 ± 0.07	173.7 ± 1.3
Pure PC	3.90 ± 0.01	186.0 ± 0.1

Table 41. Log of Stability Constants and Limiting Chemical Shifts for $(C222 \cdot Cs)^+$ Complex in PC and DMF and Their Mixture at 32 ± 1°C.

Solvent	Log K_f	Limiting Chemical Shift
Pure PC	3.90 ± 0.01	186.0 ± 0.1
90% PC + 10% DMF	3.65 ± 0.02	184.8 ± 0.2
80% PC + 20% DMF	3.45 ± 0.03	181.1 ± 0.4
70% PC + 30% DMF	3.19 ± 0.01	178.0 ± 0.3
50% PC + 50% DMF	2.80 ± 0.03	169.6 ± 1.2
30% PC + 70% DMF	2.45 ± 0.01	163.8 ± 1.0
20% PC + 80% DMF	2.29 ± 0.01	159.8 ± 0.8
10% PC + 90% DMF	2.14 ± 0.02	154.8 ± 1.9
Pure DMF	2.00 ± 0.02	150.1 ± 3.0

propylene carbonate (D·N = 15.1) have relatively poorer solvating properties towards the cesium ion.

A metal ion which is totally surrounded by the ionophore (ligand) should exhibit a chemical shift independent of the solvent. The chemical shifts of the cesium ion bond to the cryptand-222 in AC/DMSO, AN/DMSO, PC/DMSO, and PC/DMF are listed in Tables 39-41. It is interesting to note that, in all cases, the limiting chemical shifts for the complexed-cesium ion are dependent on the solvent compositions, suggesting that the cesium ion is only partially insulated from the solvent and that the complex exists in the exclusive configuration (11).

C. Complex formation by Cs^+ ion with DB24C8 in DMSO-AC, and PY-MeOH binary systems

In the present work, the influence of the solvent on the stability of the $(DB24C8 \cdot Cs)^+$ complex was investigated. For this purpose, the chemical shift of cesium-133 resonance was measured as a function of DB24C8/Cs^+ mole ratios in dimethylsulfoxide-acetone and pyridine-methanol solutions at 32 $\pm$ 1°C.

The data obtained from these studies are given in Tables 42 and 43. Figures 40-42 show the variation of the ^{133}Cs chemical shifts versus DB24C8/Cs^+ mole ratios at different composition of the solvents. Investigation of these figures shows that in dimethylsulfoxide-acetone

Table 42. Mole Ratio-Chemical Shift Data for CsSCN (0.005M) in the Presence of DB24C8 in AC and DMSO and Their Mixture at 32°C.

Pure AC		85% AC/15% DMSO		70% AC/30% DMSO		50% AC/50% DMSO	
L/Cs^+	δ (ppm)	L/Cs^+	δ (ppm)	L/Cs^+	δ (ppm)	L/Cs^+	δ (ppm)
0.00	-19.89	0.00	13.85	0.00	23.62	0.00	31.72
0.18	-21.61	0.27	8.82	0.22	20.22	0.32	28.36
0.42	-23.47	0.45	6.11	0.46	17.60	0.54	26.40
0.70	-25.40	0.67	2.94	0.76	13.86	0.74	24.62
0.96	-27.18	0.96	0.18	0.82	12.18	1.08	21.91
1.10	-27.34	1.20	-0.194	1.20	9.33	1.32	20.32
1.44	-28.20	1.63	-3.78	1.52	7.13	1.86	17.24
1.75	-28.42	2.27	-5.32	1.94	5.08	2.22	15.60
2.44	-28.58	2.78	-6.07	2.70	2.23	2.64	13.78
3.58	-28.58	3.76	-6.96	3.52	0.41	3.79	10.27

Table 42 (continued)

30% AC/70% DMSO		15% AC/85% DMSO		Pure DMSO	
L/Cs^+	δ (ppm)	L/Cs^+	δ (ppm)	L/Cs^+	δ (ppm)
0.00	55.55	0.00	60.84	0.00	67.13
0.20	53.30	0.22	59.37	0.21	65.20
0.56	48.80	0.45	56.88	0.44	63.10
0.86	46.01	0.73	55.10	0.75	61.01
1.04	44.31	0.92	52.93	1.04	59.30
1.34	41.36	1.00	52.70	1.35	56.97
1.82	37.17	1.53	48.44	1.67	54.88
2.26	34.23	2.12	44.25	2.21	51.71
2.70	31.28	2.76	30.84	2.69	49.37
3.64	26.94	3.65	36.50	3.23	46.51

Table 43. Mole Ratio-Chemical Shift Data for CsSCN (0.005M) in the Presence of DB24C8 in MeOH/PY Systems at 32°C

15% MeOH/85% PY		30% MeOH/70% PY		40% MeOH/60% PY		45% MeOH/55% PY	
L/Cs^+	δ(ppm)	L/Cs^+	δ(ppm)	L/Cs^+	δ(ppm)	L/Cs^+	δ(ppm)
0.00	3.87	0.00	-11.54	0.00	-20.13	0.00	-23.31
0.28	- 4.43	0.30	-17.59	0.24	-22.39	0.18	-24.32
0.44	- 9.63	0.50	-18.73	0.49	-24.17	0.37	-25.56
0.62	-13.11	0.66	-21.14	0.73	-25.87	0.61	-26.41
0.94	-19.16	0.84	-22.84	0.96	-27.27	1.04	-28.42
1.18	-21.80	1.14	-25.25	1.27	-27.96	1.20	-28.66
1.60	-22.88	1.36	-25.94	1.61	-28.36	1.73	-29.20
1.92	-22.94	1.96	-26.64	1.95	-28.59	2.22	-29.36
2.96	-23.35	2.76	-26.88	2.63	-28.89	2.61	-29.51
3.76	-23.50	3.56	-27.03	3.37	-28.74	3.24	-29.43

Table 43 (continued)

50% MeOH/50% PY		60% MeOH/40% PY		65% MeOH/35% PY		70% MeOH/30% PY	
L/Cs^+	δ(ppm)	L/Cs^+	δ(ppm)	L/Cs^+	δ(ppm)	L/Cs^+	δ(ppm)
0.00	-25.77	0.00	-32.19	0.00	-33.61	0.00	-35.88
0.18	-26.70	0.22	-32.04	0.28	-33.14	0.20	-35.18
0.41	-27.47	0.39	-31.80	0.44	-32.92	0.44	-34.72
63	-28.40	0.78	-31.72	0.82	-32.53	0.66	-34.17
0.88	-29.11	0.98	-31.73	1.12	-32.32	0.92	-33.78
1.16	-29.65	1.27	-31.65	1.50	-32.22	1.14	-33.32
1.69	-29.81	1.67	-31.65	1.82	-32.22	1.42	-33.08
2.24	-30.20	2.12	-31.65	2.50	-32.14	2.06	-32.86
2.78	-30.27	2.51	-31.65	3.28	-32.14	2.72	-32.86
3.78	-30.27	3.24	-31.65	3.96	-32.06	3.32	-32.86

Table 43 (continued)

75% MeOH/25% PY		85% MeOH/15% PY		93% MeOH/7% PY	
L/Cs^+	δ (ppm)	L/Cs^+	δ (ppm)	L/Cs^+	δ (ppm)
0.00	-38.05	0.00	-40.96	0.00	-43.94
0.24	-37.12	0.18	-39.87	0.20	-42.45
0.37	-36.58	0.43	-38.71	0.51	-40.37
0.63	-35.65	0.65	-37.47	0.82	-38.43
0.90	-34.64	0.94	-36.39	1.04	-37.42
1.18	-33.94	1.18	-35.61	1.22	-36.34
1.49	-33.71	1.57	-34.84	1.57	-35.79
2.16	-33.40	2.16	-34.37	2.02	-35.48
2.59	-33.48	2.92	-34.37	2.51	-35.10
3.24	-33.32	3.69	-34.37	3.35	-35.10

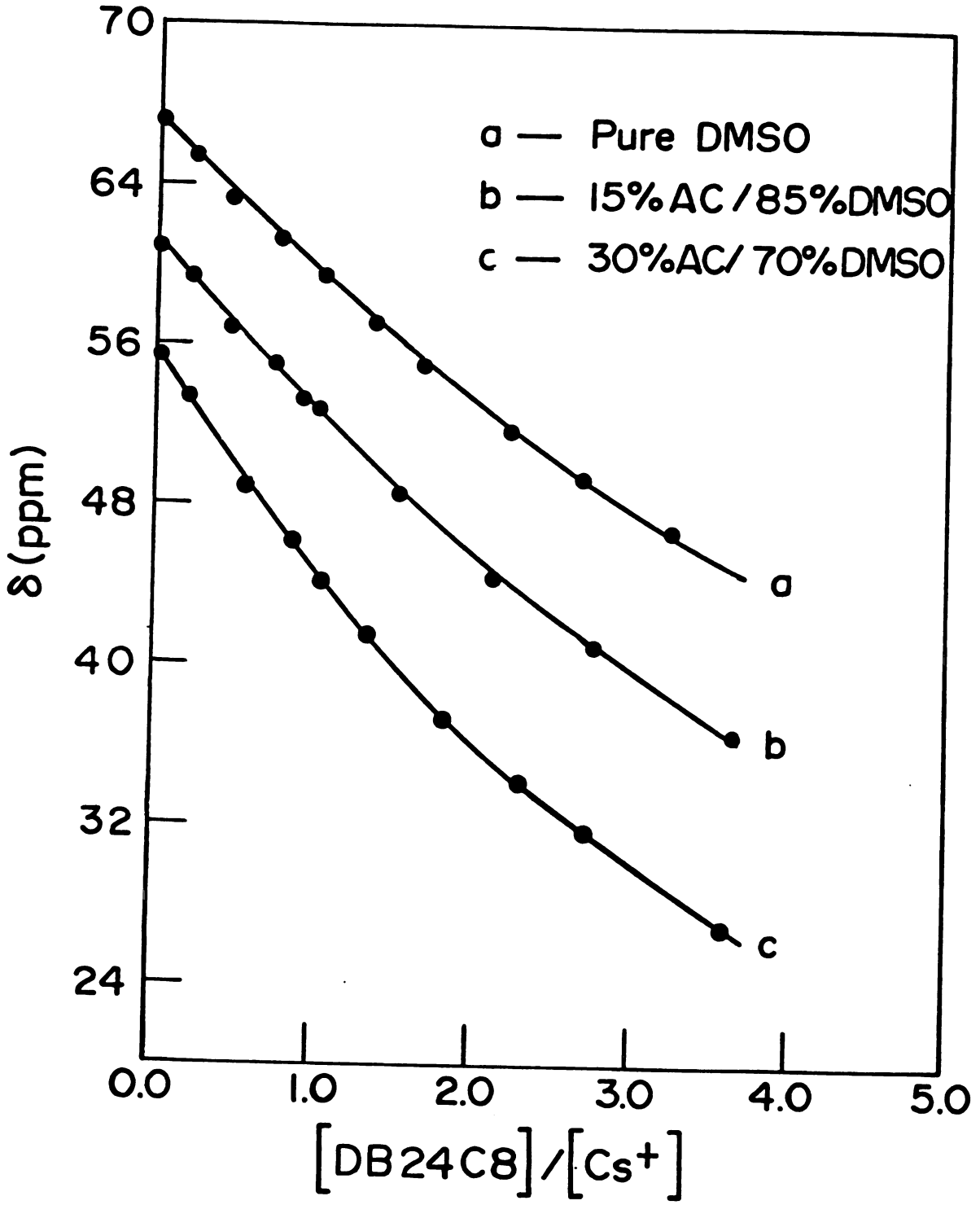

Figure 40. Cesium-133 chemical shifts vs. (DB24C8)/Cs^+) mole ratio in AC/DMSO systems.

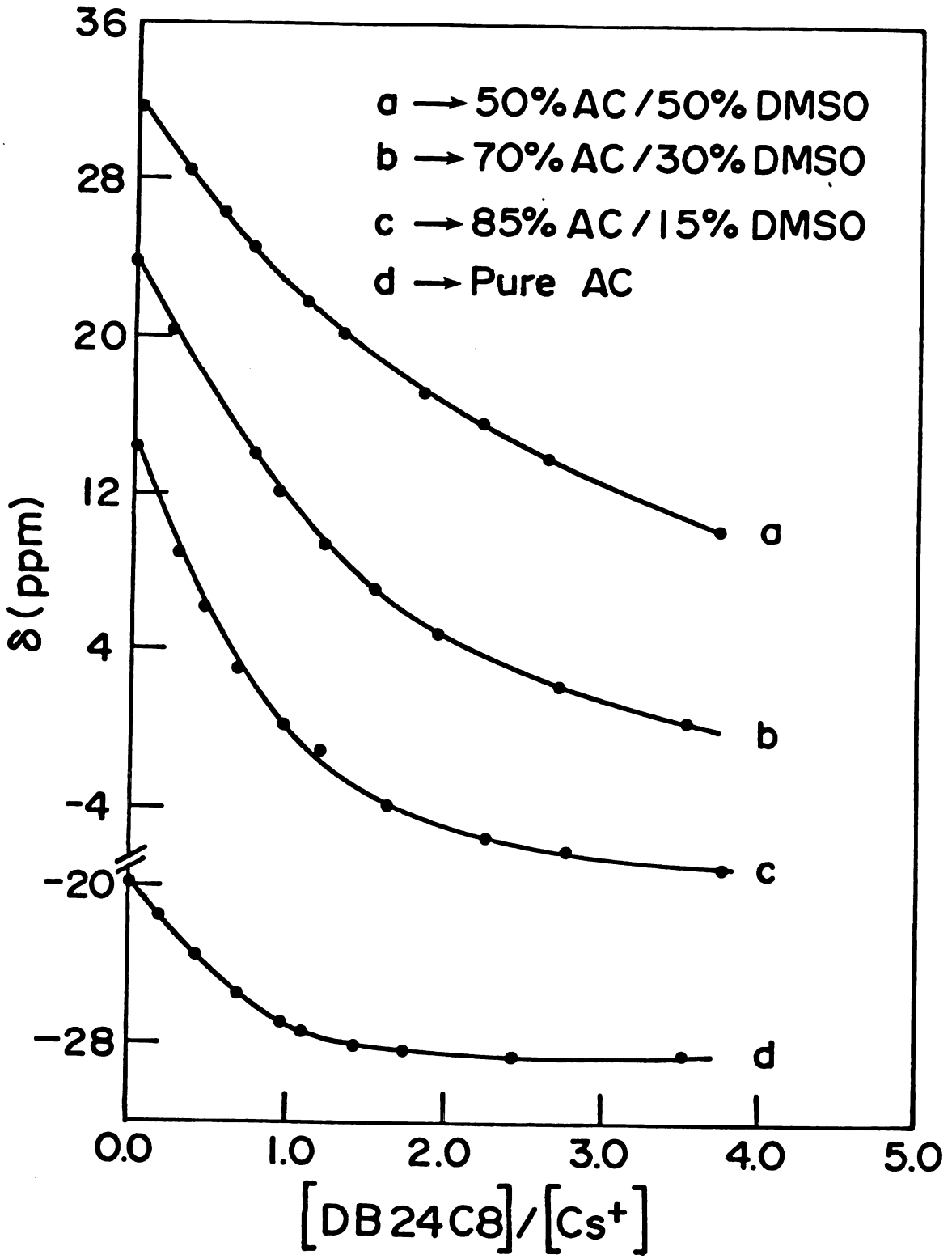

Figure 41. Cesium-133 chemical shifts vs. (DB24C8)/(Cs^+) in AC/DMSO systems.

systems, as the concentration of the dimethylsulfoxide increases the plots show less curvature which implies the formation of a weaker complex at high dimethylsulfoxide concentrations.

It is interesting to note that, the addition of the ligand to a solution of Cs^+ ion in DMSO/AC mixtures always results in an upfield shift. In the PY/MeOH systems, however, the behavior of the chemical shift is quite unexpected. As seen in Figure 42, the variation in the cesium-133 chemical shifts as a function of the mole ratios is not significant in about 50-60 Vol. % of methanol content in PY/MeOH systems. It seems that, the electronic environment of the Cs^+ ion does not change upon complexation in this range of the solvent composition.

The stability constants of the $(DB24C8 \cdot Cs)^+$ complex in DMSO/AC and PY/MeOH systems are listed in Tables 44 and 45. As shown in Table 44 the stability constants of the complex increases with increasing the acetone concentration in the DMSO/AC mixtures. In the case of PY/MeOH systems, however, there does not seem to be a simple relation between the stability of the complex and the solvent composition.

Discussion

The variation of the formation constants of the $(C222 \cdot Cs)^+$ complex as a function of solvent composition in acetone-dimethylsulfoxide, acetonitrile-dimethysulfoxide,

Figure 42. Cesium-133 chemical shifts as a function of (DB24C8)/(Cs^+) mole ratio in methanol-pyridine binary solutions.

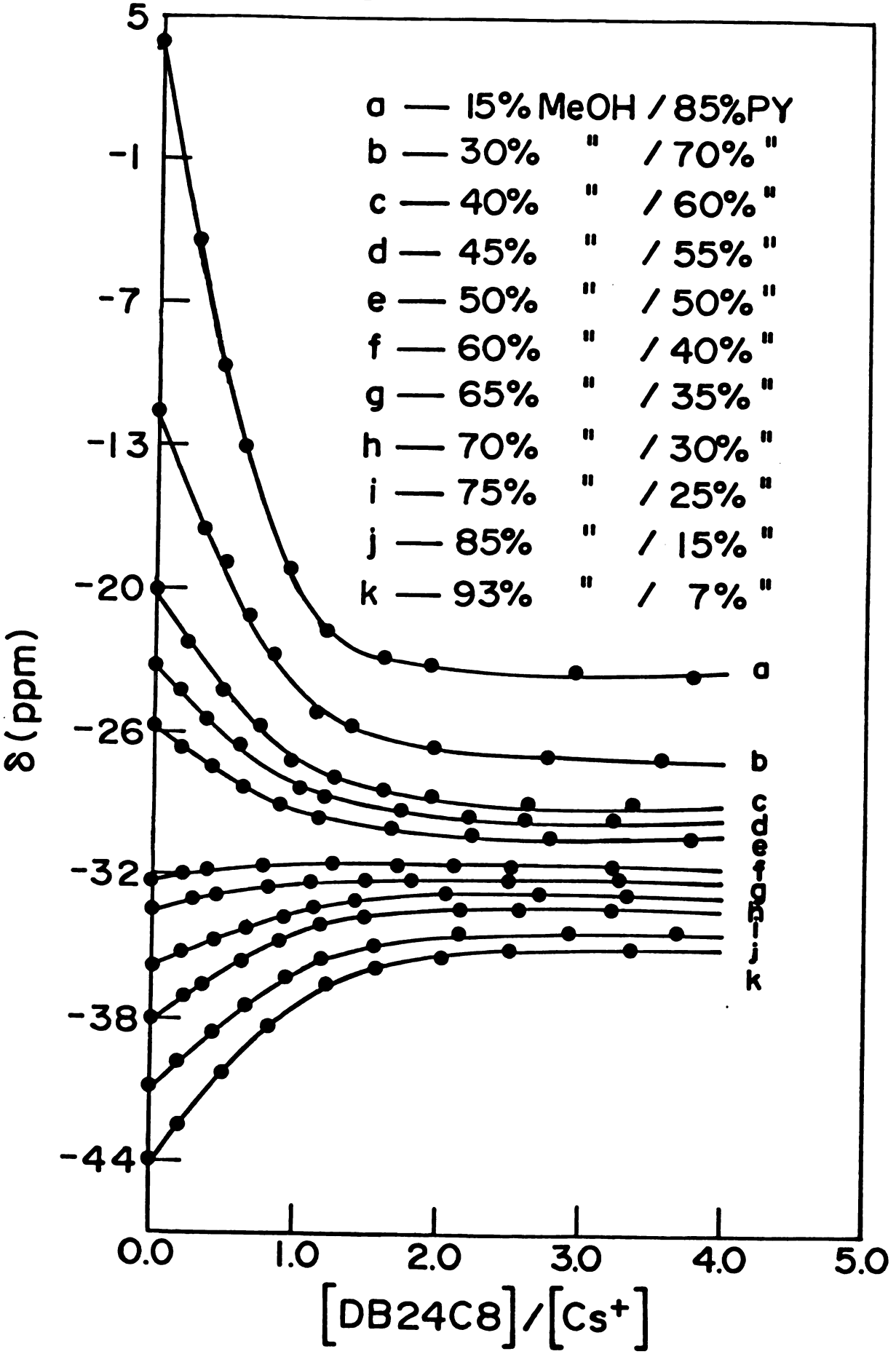
a — 15% MeOH / 85% PY
b — 30% " / 70% "
c — 40% " / 60% "
d — 45% " / 55% "
e — 50% " / 50% "
f — 60% " / 40% "
g — 65% " / 35% "
h — 70% " / 30% "
i — 75% " / 25% "
j — 85% " / 15% "
k — 93% " / 7% "
δ (ppm)
5
-1
-7
-13
-20
-26
-32
-38
-44
0.0
1.0
2.0
3.0
4.0
5.0
[DB24C8]/[Cs+]

Table 44. Formation Constants of $(DB24C8 \cdot Cs)^+$ Complex in DMSO-AC Mixed Systems (at 32 ± 1°C)

Solvent	Log K_f
Pure AC	3.77 ± 0.06
85% AC + 15% DMSO	2.91 ± 0.02
70% AC + 30% DMSO	2.38 ± 0.02
50% AC + 50% DMSO	1.94 ± 0.01
30% AC + 70% DMSO	1.73 ± 0.03
15% AC + 85% DMSO	1.44 ± 0.07
Pure DMSO	1.44 ± 0.04

Table 45. Formation Constants of $(DB24C8 \cdot Cs)^+$ Complex in MeOH-PY Binary System (at 32 ± 1°C)

Solvent	Log K_f
Pure MeOH[a]	3.65 ± 0.05
93% MeOH + 7% PY	3.32 ± 0.08
85% MeOH + 15% PY	3.42 ± 0.11
75% MeOH + 25% PY	3.47 ± 0.10
70% MeOH + 30% PY	3.45 ± 0.10
65% MeOH + 35% PY	3.71 ± 0.24
50% MeOH + 50% PY	3.31 ± 0.12
45% MeOH + 55% PY	3.52 ± 0.09
40% MeOH + 60% PY	3.59 ± 0.11
30% MeOH + 70% PY	3.69 ± 0.07
15% MeOH + 85% PY	3.94 ± 0.06
Pure PY[a]	4.00 ± 08

[a]Reference 70.

propylene carbonate-dimethylsulfoxide, and propylene carbonate-dimethylformamide solutions are shown in Figures 43 and 44. Investigation of these figures shows that the complexation process in mixed nonaqueous solvents is quite sensitive to the solvent composition.

It is interesting to note that in DMSO/AC solutions the variation of the stability constants of the $(C222 \cdot Cs)^+$ complex versus the solvent composition is not significant at low acetone concentrations (between 0 to ~ 15 Vol. % of acetone), suggesting that the metal ion, and possibly the ligand, are solvated only by the dimethylsulfoxide molecules. At higher contents of the acetone (> ~ 15 Vol. % of acetone), however, there is a substantial increase in the formation constants of the complex. It seems reasonable to assume that the dimethylsulfoxide molecules in the first solvation shell of the metal ion (and probably of the ligand) are replaced gradually by the acetone molecules upon addition of more acetone to the system. Since acetone is a much weaker solvating solvent than dimethylsulfoxide, the stability of the complex in inhanced by diminished complexation of the solvent for the metal ion. Another important point which can be deduced from the comparison of the plots in Figures 43 and 44 is that the curvature of the plots of log K_f against the composition of the binary solutions is more pronounced in the cases of acetone-dimethylsulfoxide and acetonitrile-

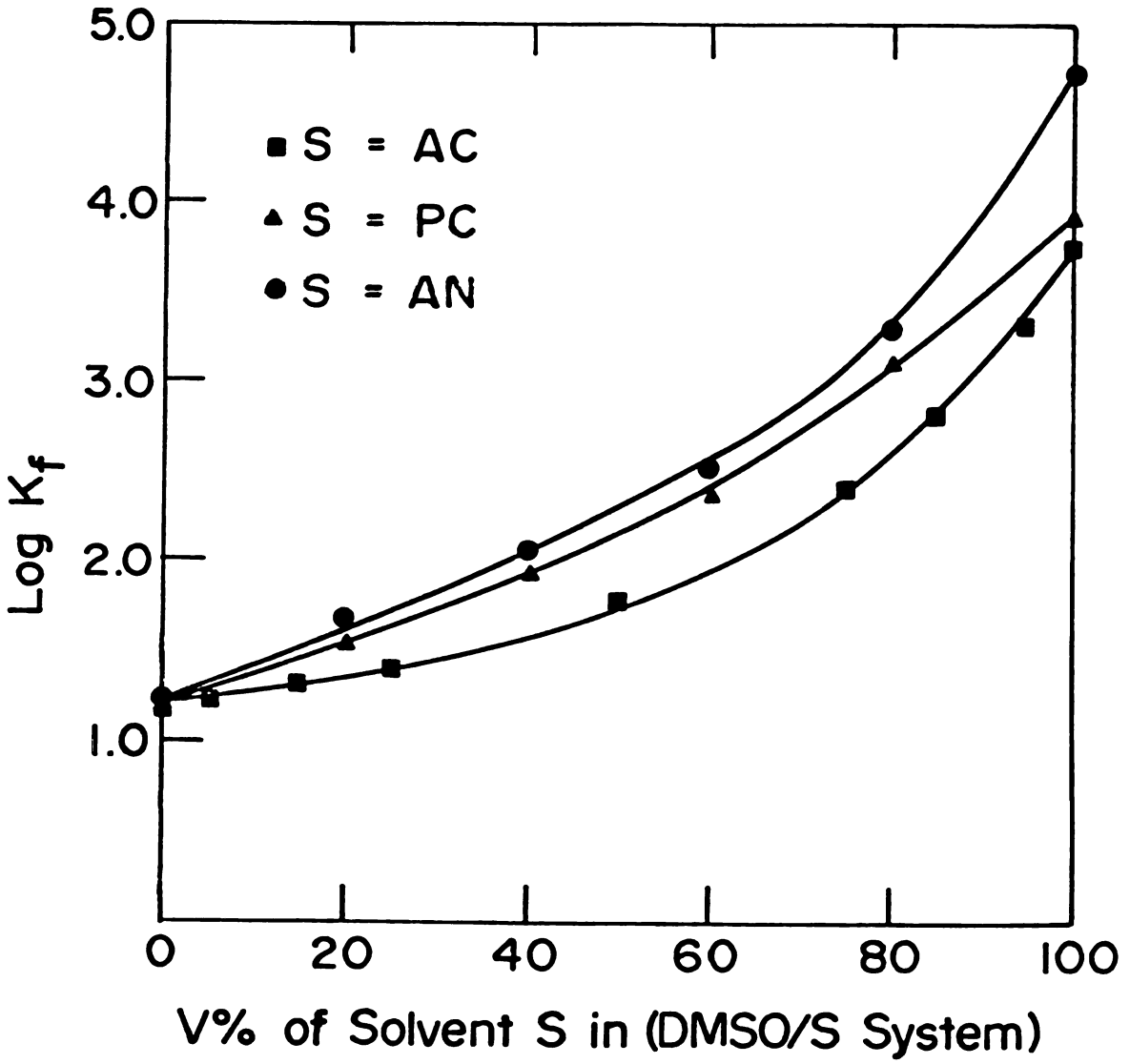

Figure 43. Variation of the stability constant of $(C222 \cdot Cs)^+$ complex with solvent composition in different binary solutions.

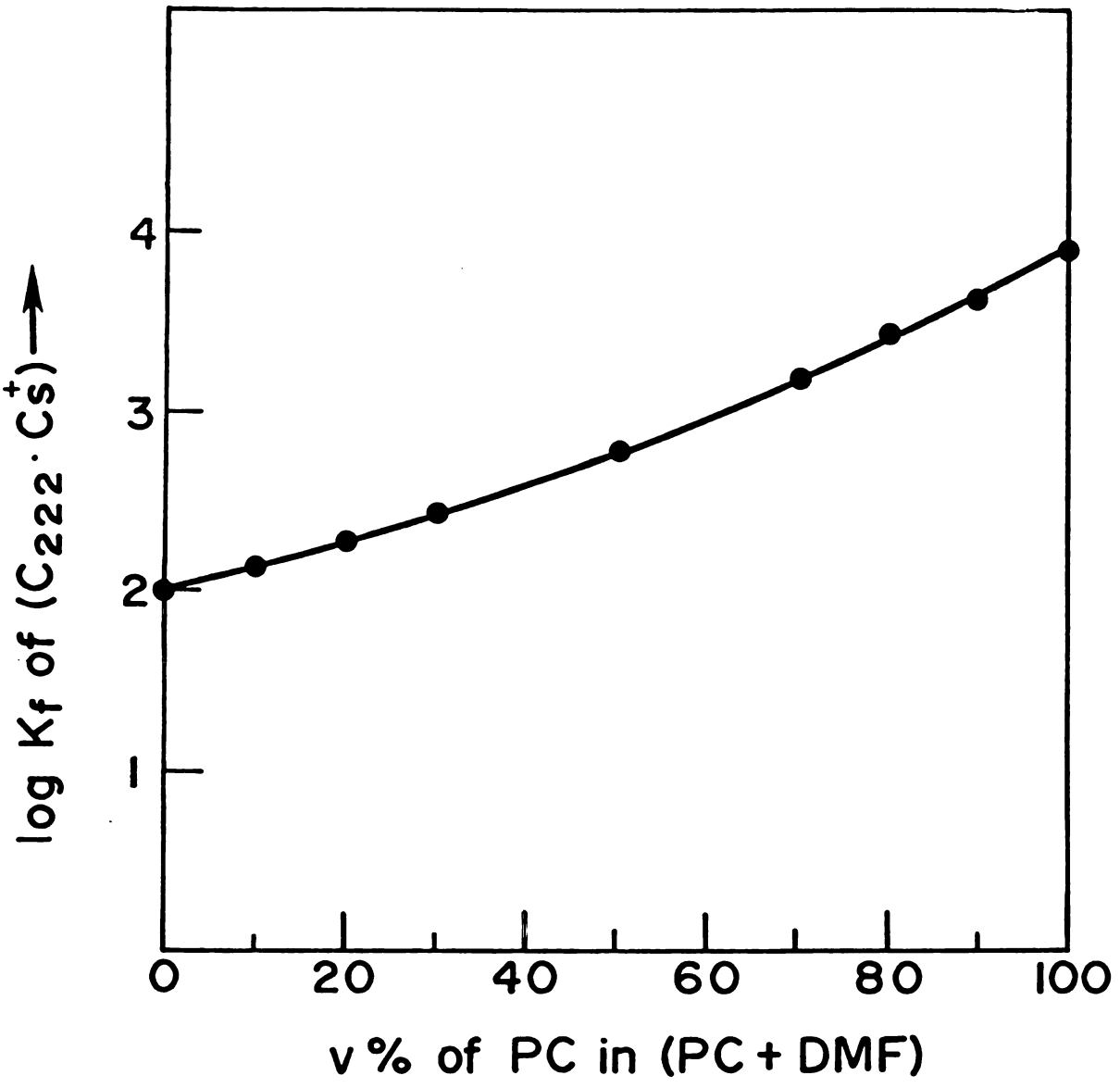

Figure 44. Variation of the formation constant of $(C222 \cdot Cs)^+$ complex with PC content in PC/DMF binary mixtures.

dimethylsulfoxide solutions than in the cases of propylene carbonate-dimethylsulfoxide and propylene carbonate-dimethylformamide systems. This is probably due to the differences in the cation and ligand solvation in these systems caused by changing of the medium dielectric constant, changing of the donor ability of the solvents, and variation of the solvents structure resulting from changing in composition of the mixed solutions.

Figure 45 shows the stability constants of the $(DB24C8 \cdot Cs)^+$ complex as a function of the pyridine and acetone concentrations in the pyridine-methanol and acetone-dimethylsulfoxide binary systems. A regular decrease in the formation constant of the complex in AC/DMSO mixtures is observed as the concentration of DMSO increases.

It is interesting to note that, while the stability constant of the $(DB24C8 \cdot Cs)^+$ complex varies monotonically with the solvent composition in AC/DMSO binary solutions, this trend is not followed in PY/MeOH systems. With increasing the concentration of the pyridine, the formation constant of the $(DB24C8 \cdot Cs)^+$ complex decreases initially to reach a minimum (at ~ 10-20 Vol. % of pyridine) then increases to a maximum (at ~ 25 Vol. % of pyridine) and decreases again to about 50 Vol. % of pyridine. This behavior may reflect changes occurring in the structure of the solvent mixture or in the solvation properties of the cyclic polyether and the cation at these solvent

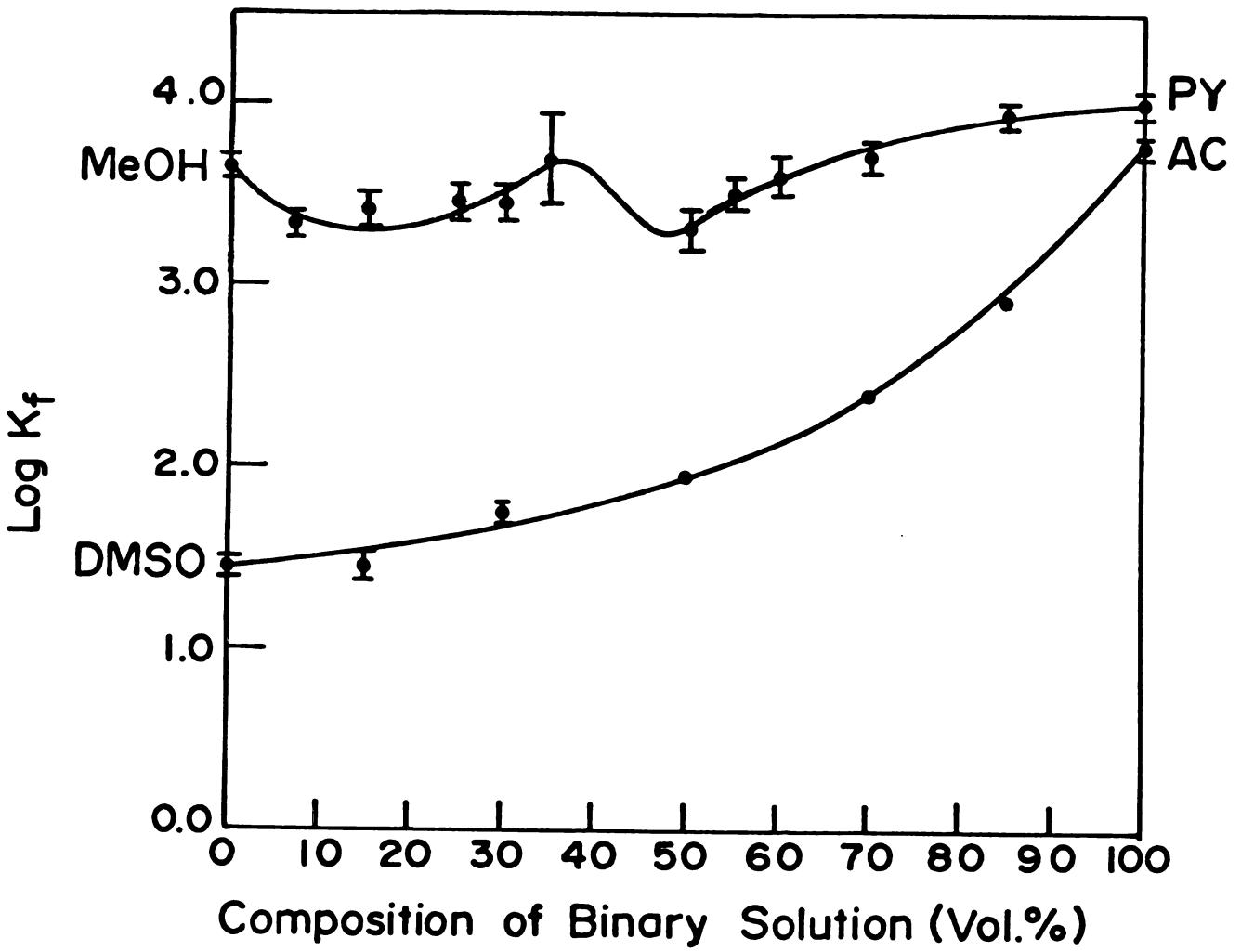

Figure 45. Variation of the stability constant of $(DB24C8 \cdot Cs)^+$ complex with the solvent composition in MeOH/PY and DMSO/AC binary solutions.

compositions. Some structural changes probably occur in the structure of the solvents when they mix with one another. These structural changes may result in changing the interaction of those solvents with the solutes compared to the pure solvents.

The estimated formation constants (derived from the plots in Figures 43 and 45 of the $(C222 \cdot Cs)^+$ and $(DB24C8 \cdot Cs)^+$ complexes and the inverse of the dielectric constants of the medium in various compositions of acetone-dimethylsulfoxide systems are listed in Table 46. Figure 46 shows the stability constants of these complexes as a function of the reciprocal of dielectric constant of the medium. As shown in this figure, the plots of log K_f against the inverse of the dielectric constant are slightly concave downward. Such a curvature could be explained in terms of specific solvent effects which may result from the chemical nature of the solvent in the mixed solutions.

The existence of a linear relation between the logarithm of the stability constants of the various complexes and the reciprocal of the dielectric constant of the solvents has been reported by several researchers (123-126). For example, Tur'yan et al (123, 127, 128) showed that for the complexes of lead chloride and thiocyanate there is a linear relation between pK and $\frac{1}{D}$ (D = dielectric const. of the medium) for aqueous alcoholic solutions. It should be noted that, this relation may

Table 46. Stimated Formation Constants of the $(C222 \cdot Cs)^+$ and $(DB24C8 \cdot Cs)^+$ Complexes in Various Compositions of AC/DMSO Binary Solutions

Solvent	D*	$\frac{1}{D}$	Log K_f	
			$(C222 \cdot Cs)^+$	$(DB24C8 \cdot Cs)^+$
Pure AC				
86.4% AC/13.6% DMSO	20.7	0.048	3.75	3.77
83.4% AC/16.6% DMSO	24.0	0.042	2.90	3.05
75% AC/25% DMSO	27.0	0.037	2.40	2.55
69.5% AC/20.5% DMSO	28.5	0.035	2.20	2.35
58.3% AC/41.7% DMSO	31.6	0.032	1.92	2.07
37.6% AC/62.4% DMSO	37.3	0.027	1.55	1.75
27.5% AC/72.5% DMSO	39.9	0.025	1.45	1.65
Pure DMSO	46.6	0.021	1.19	1.44

*D = Dielectric Constant (Reference 144).

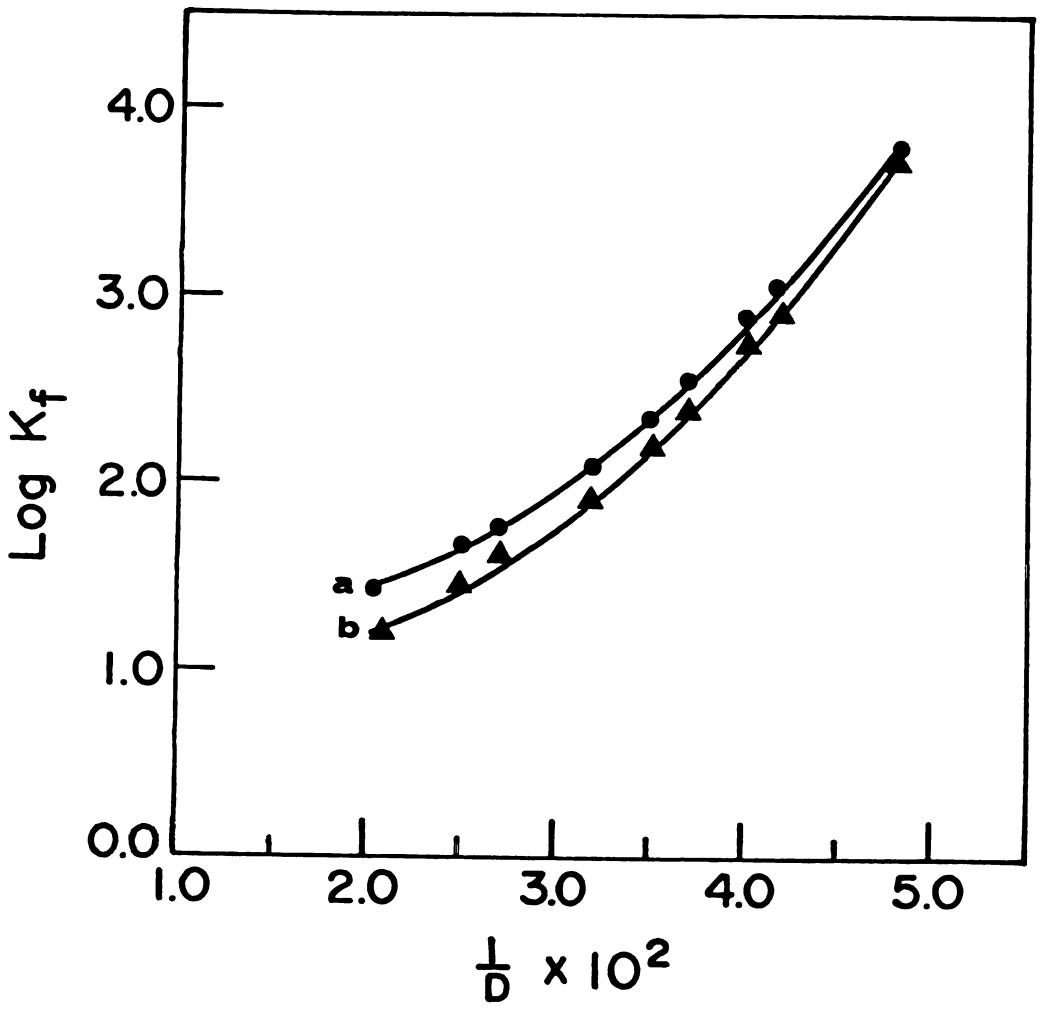

Figure 46. Variation of the stability constants of (a) $(DB24C8 \cdot Cs)^+$ and (b) $(C222 \cdot Cs)^+$ complexes with the reciprocal of the dielectric constant of the medium in AC/DMSO binary solutions.

only hold in the case of simple ion-ion reactions in chemically similar solvents, with no specific ion solvent interactions. However, this may not be true for the molecular-ion reactions.

Since the relation between log K and $\frac{1}{D}$ is not linear in the case of $(C222 \cdot Cs)^+$ and $(DB24C8 \cdot Cs)^+$ systems in AC/DMSO binary solutions, it can therefore be concluded that the stability of these complexes is a function of chemical nature of the solvent as well as of its dielectric constant.

Knowledge of the molecular state of the solvent and its nature in a binary mixed solvent is important in understanding the effect of the solvent on the complexation process.

D. Thermodynamic Parameters for Complexing of Cs^+ ion by DB27C9 and DB24C8 in DMF/AN Binary Solutions.

In the present investigation, the interactions between large macrocyclic crown ethers, dibenzo-27-crown-9 and dibenzo-24-crown-8 with cesium ion were studied in dimethylformamide/acetonitrile binary mixtures at various temperatures. At each temperature, the chemical shifts of the cesium-133 were monitored as a function of $DB27C9/Cs^+$ or $DB24C8/Cs^+$ mole ratios. In all cases, only one population averaged NMR signal was observed irrespective of the $Ligand/Cs^+$ mole ratio.

The cesium-133 chemical shifts measured at different temperatures for various systems are given in Tables 47-51 and the plots of the ^{133}Cs chemical shifts as a function of Ligand/Cs^+ mole ratios are represented in Figures 47-51. These plots show that the equilibrium between the Cs^+ ion and dibenzo-27-crown-9 and dibenzo-24-crown-8 in DMF/AN binary systems are temperature dependent. As the temperature decreases the plots show more pronounced curvature which is an evidence for the existence of exothermic reactions between the cesium ion and these ligands.

The formation constants of $(DB27C9 \cdot Cs)^+$ and $(DB24C8 \cdot Cs)^+$ complexes for the various compositions of DMF/AN system at different temperatures are listed in Tables 52 and 53. A monotonic increase in the stability constants of these complexes is observed as the temperature decreases. Plots of ln K_f versus $\frac{1}{T}$ for the data in Tables 52 and 53 are shown in Figure 52, and the corresponding thermodynamic parameters (ΔH_c°, ΔS_c° and ΔG° values) are given in Table 54. Thermodynamic data show that in all cases the complexes are enthalpy stabilized but entropy destabilized and the values of ΔH_c°, ΔS_c°, and ΔG_c° are dependent on the solvent compositions.

Discussion

An evaluation of the changes in H_c° and S_c° as a function of the change in the composition of the mixed solvent is interesting, because these values may be

Table 47. Mole Ratio - Chemical Shift Data for Complexation of DB27C9 with CsSCN (0.005M) in 10% AN + 90% DMF at Various Temperatures

L/Cs^+	Temperature					
	-10	0	10	20	30	40
0.00	7.33	5.38	3.98	2.13	0.50	- 1.05
0.22	1.74	0.34	- 0.04	- 1.05	- 1.98	- 2.76
0.38	- 1.90	- 2.29	- 2.52	- 2.99	- 3.53	- 4.00
0.68	- 7.64	- 7.25	- 6.79	- 6.40	- 6.32	- 6.25
1.08	-13.08	-12.06	-10.89	- 9.97	- 9.19	- 8.78
1.28	-15.01	-13.77	-12.44	-11.44	-10.43	- 9.64
1.74	-17.03	-15.87	-14.55	-13.37	-12.37	-11.21
2.32	-18.89	-17.96	-16.72	-15.63	-14.46	-13.45
3.02	-20.05	-19.27	-18.27	-17.26	-16.17	-15.17
4.30	-21.05	-20.59	-19.74	-18.81	-18.18	-17.26

Table 48. Mole Ratio - Chemical Shift Data for Complexation of DB27C9 with CsSCN (0.005M) in 30% AN + 70% DMF at Different Temperatures.

L/Cs^+	Temperature °C					
	-20	-10	0	10	20	30
0.00	12.13	10.18	8.63	7.08	5.21	3.59
0.18	5.69	4.60	3.60	2.74	1.49	0.56
0.36	0.80	0.18	- 0.21	- 0.45	- 1.21	- 1.53
0.60	- 6.18	- 5.79	- 5.48	- 5.17	- 4.86	- 9.70
1.02	-14.08	-12.54	-11.84	-10.60	- 9.82	- 8.89
1.30	-16.19	-15.17	-14.01	-12.85	-11.83	-10.84
1.54	-17.35	-16.49	-15.49	-14.47	-13.32	-12.07
2.42	-19.44	-18.82	-17.89	-17.26	-16.26	-15.25
3.24	-20.13	-19.59	-18.97	-18.43	-17.73	-16.88
4.32	-20.29	-20.13	-19.67	-19.29	-18.90	-18.13

Table 49. Mole Ratio - Chemical Shift Data for DB27C9 Complexes with 0.005M CsSCN in 70% AN + 30% DMF at Various Temperatures

L/Cs^+	Temperature °C					
	0	10	20	30	40	50
0.00	18.77	17.22	15.59	14.28	12.65	11.41
0.28	8.64	7.52	6.83	6.29	5.59	5.19
0.52	- 1.01	- 1.16	- 0.92	- 0.77	- 0.54	- 0.39
0.72	- 5.34	- 4.96	- 4.42	- 3.94	- 3.25	- 2.87
0.92	-10.15	- 9.30	- 8.26	- 7.44	- 6.51	- 5.89
1.16	-13.17	-12.48	-11.24	-10.39	- 9.07	- 8.60
1.56	-15.19	-14.89	-13.95	-13.10	-12.02	-11.39
2.18	-16.36	-16.28	-15.89	-15.27	-14.50	-13.80
3.16	-17.13	-17.13	-17.05	-16.59	-16.28	-15.89
3.98	-17.44	-17.44	-17.29	-16.97	-16.78	-16.59

Table 50. Mole Ratio - Chemical Shift Data for Complexation of DB24C8 with CsSCN (0.005M) in 30% AN + 70% DMF at Various Temperatures.

L/Cs^+	Temperature °C					
	-10	0	10	20	30	40
0.00	9.80	8.63	6.92	5.38	3.67	2.58
0.27	3.28	2.79	2.04	0.88	0.26	- 0.05
0.49	- 1.06	- 1.22	- 1.49	- 1.14	- 2.12	- 2.15
0.73	- 5.87	- 5.71	- 5.06	- 4.55	- 9.70	- 4.24
1.02	-10.84	- 9.90	- 8.66	- 7.82	- 7.73	- 6.65
1.20	-13.24	-11.99	-10.83	- 9.52	- 9.13	- 8.11
1.49	-15.64	-14.32	-13.38	-11.76	-11.06	-10.13
2.04	-17.74	-16.72	-15.33	-13.98	-13.39	-12.15
3.02	-19.24	-18.51	-17.59	-16.58	-15.95	-14.63
3.96	-19.83	-19.14	-18.49	-17.82	-17.26	-16.26

Table 51. Mole Ratio - Chemical Shift Data of DB24C8 Complex with CsSCN (0.005M) in 70% AN + 30% DMF at Different Temperatures

L/Cs^+	Temperature °C					
	0	10	20	30	40	50
0.00	19.15	17.53	15.82	14.20	12.64	10.32
0.20	13.50	12.18	10.86	9.62	8.77	6.98
0.44	5.74	5.20	4.58	3.73	3.49	2.50
0.72	- 2.10	- 1.78	- 1.70	- 1.85	- 1.34	- 1.47
0.96	- 8.68	- 8.06	- 7.28	- 6.74	- 5.81	- 5.04
1.16	-11.24	-10.46	- 9.37	- 8.91	- 7.75	- 6.74
1.64	-14.50	-14.11	-13.34	-12.64	-11.71	-10.39
2.14	-15.74	-15.35	-14.88	-14.57	-13.80	-12.71
2.76	-16.20	-16.20	-15.97	-15.73	-15.11	-14.57
3.10	-16.59	-16.36	-16.20	-16.04	-15.66	-14.89
4.32	-16.74	-17.07	-16.90	-16.97	-16.82	-16.44

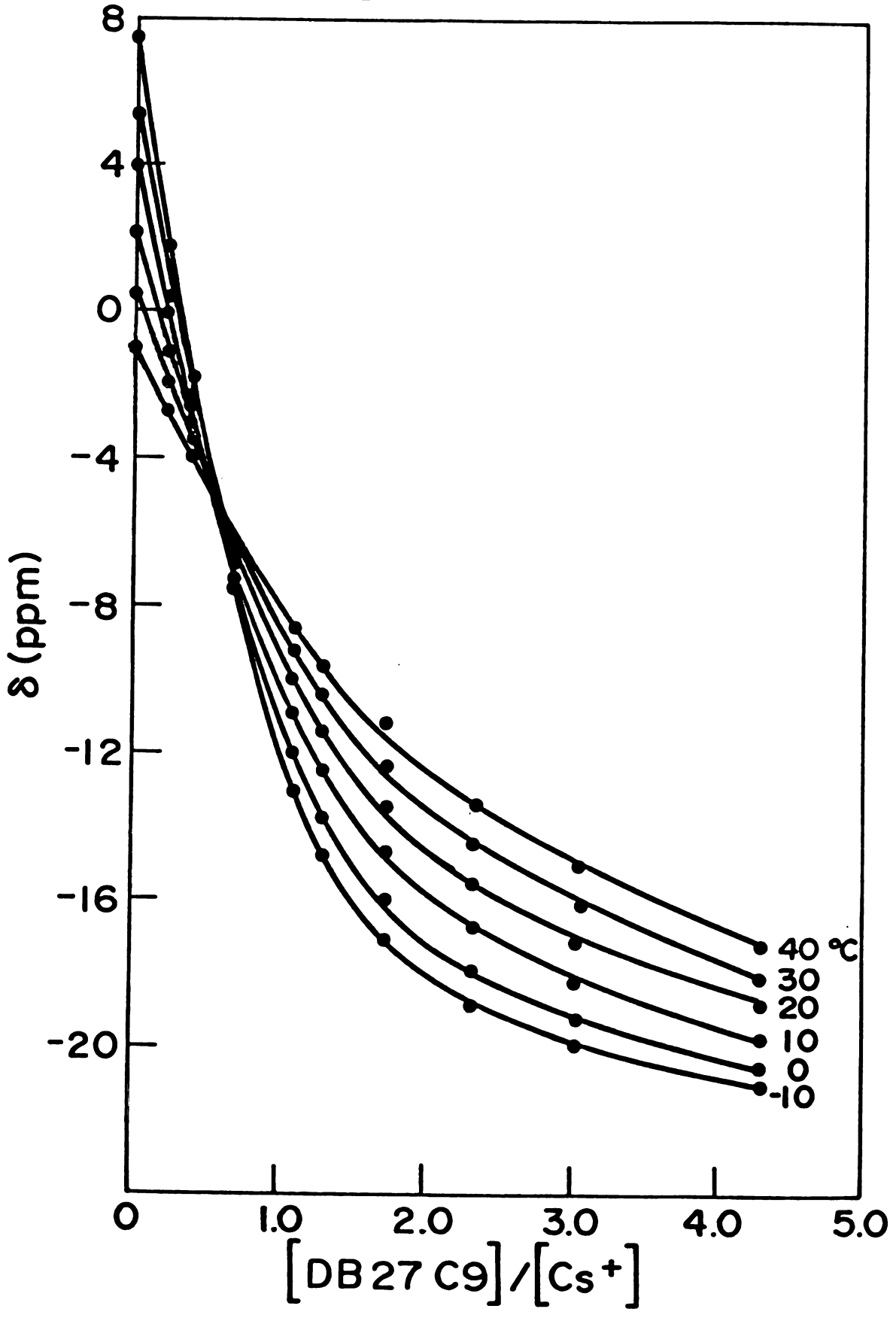

Figure 47. Cesium-133 chemical shifts vs. (DB27C9)/(Cs^+) mole ratio in 10% AN/90% DMF at various temperatures.

Figure 48. Cesium-133 chemical shifts as a function of (DB27C9)/(Cs^+) mole ratio in 30% AN/ 70% DMF at various temperatures.

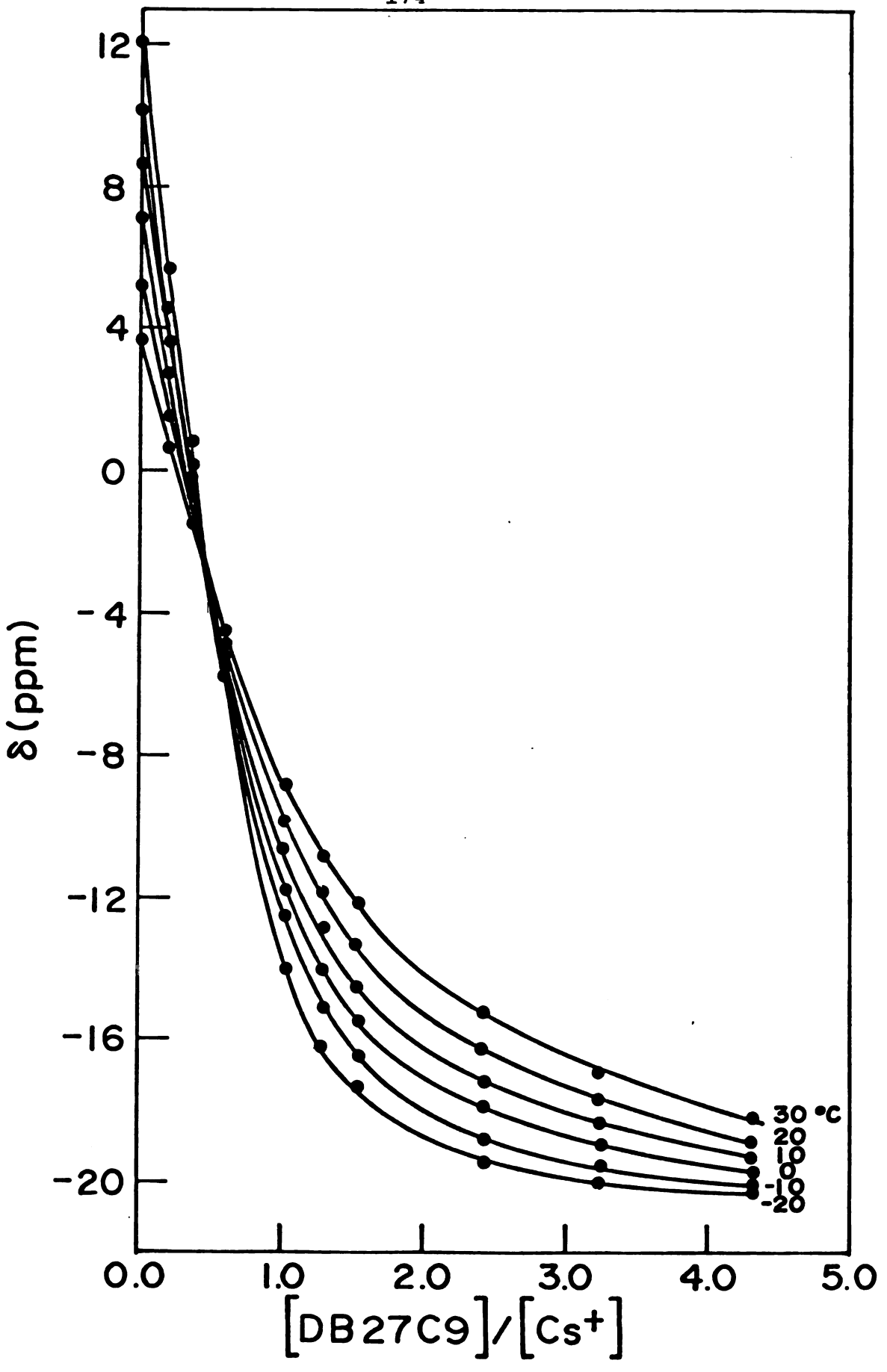
12
8
4
0
-4
-8
-12
-16
-20
δ(ppm)
0.0
1.0
2.0
3.0
4.0
5.0
[DB27C9]/[Cs+]
30 °C
20
10
0
-10
-20

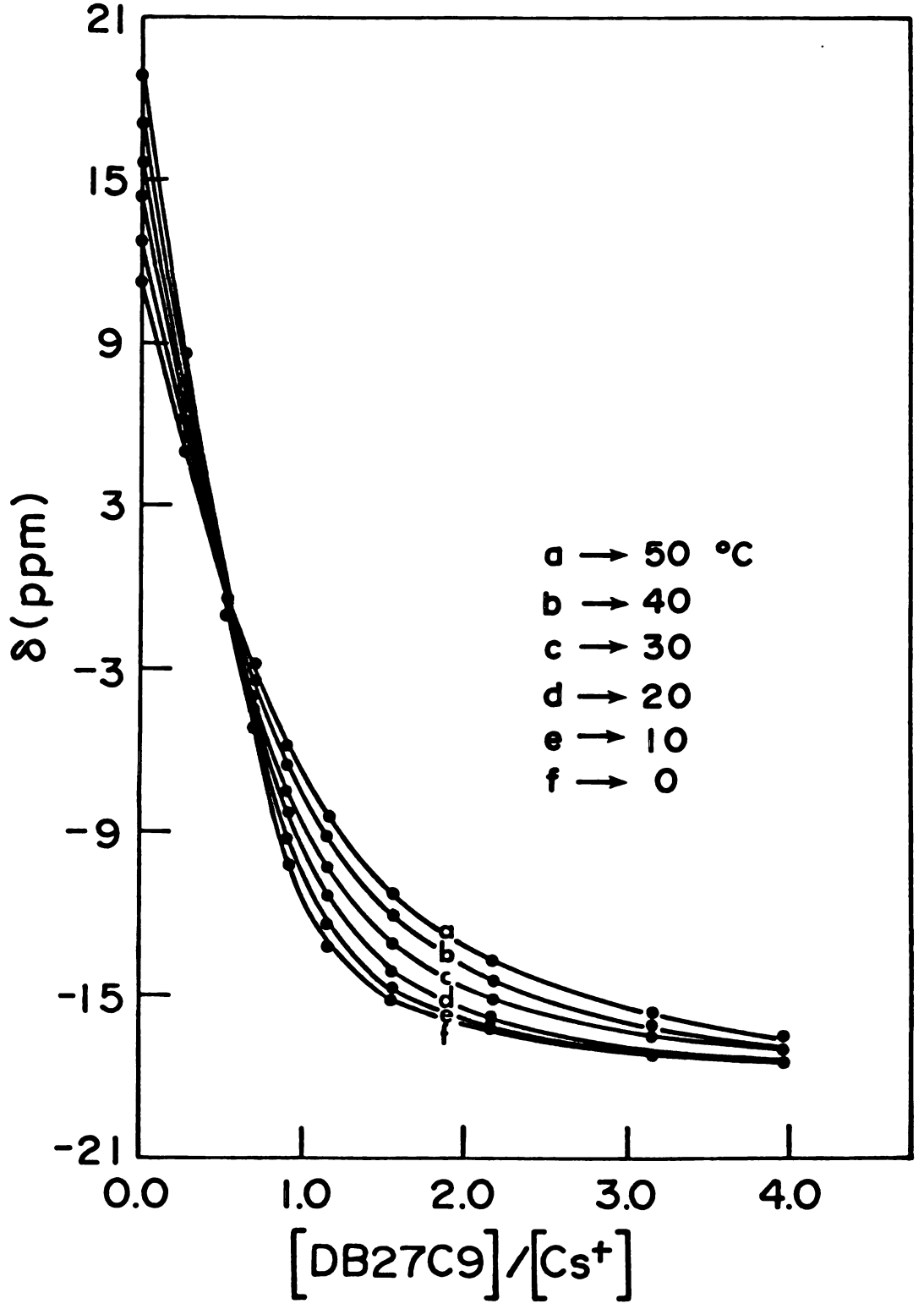

Figure 49. Cesium-133 chemical shifts vs. (DB27C9)/(Cs^+) mole ratio in 70% AN/30% DMF at various temperatures.

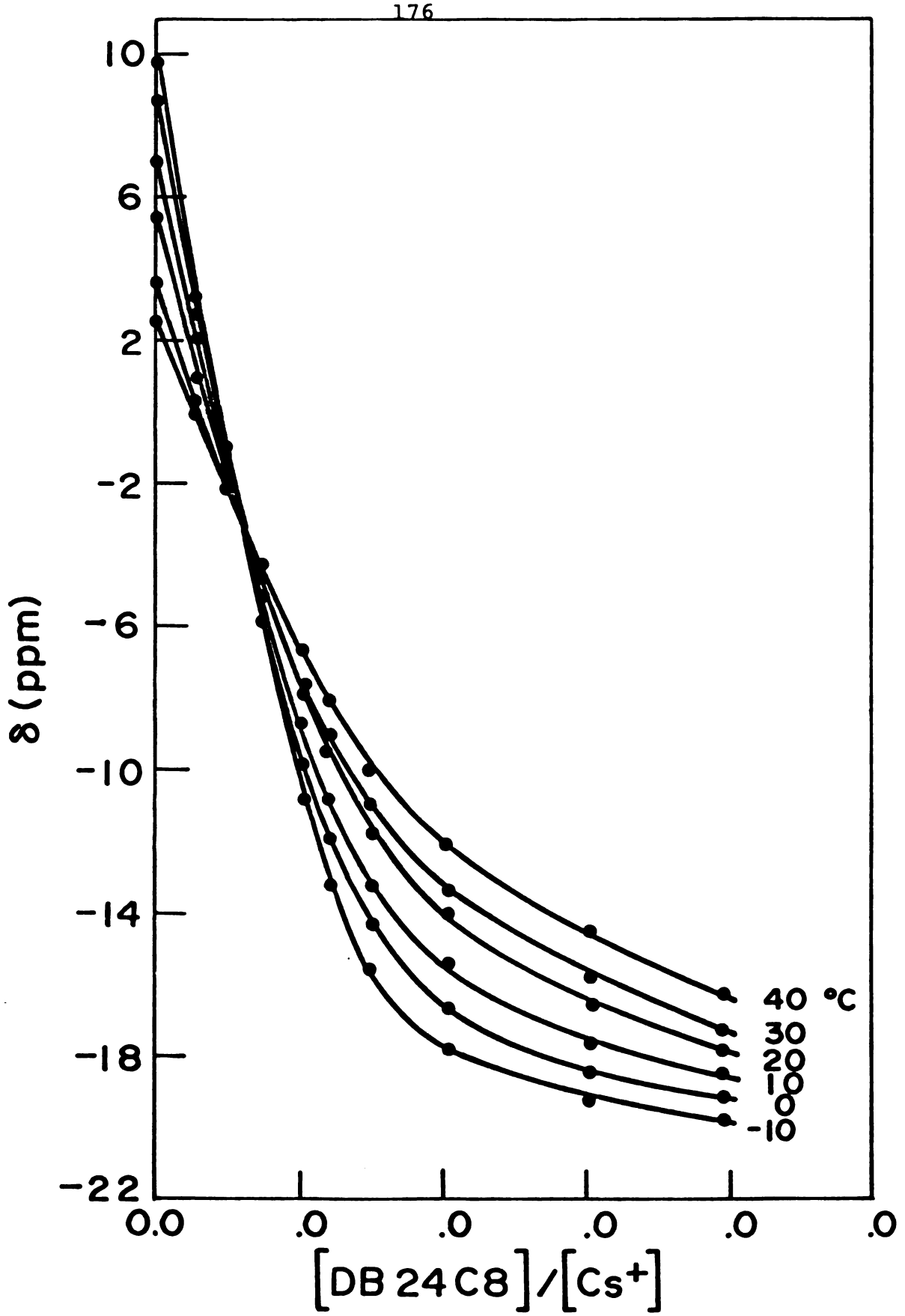

Figure 50. Cesium-133 chemical shifts vs. (DB24C8)/(Cs^+) mole ratio in 30% AN/70% DMF at various temperatures.

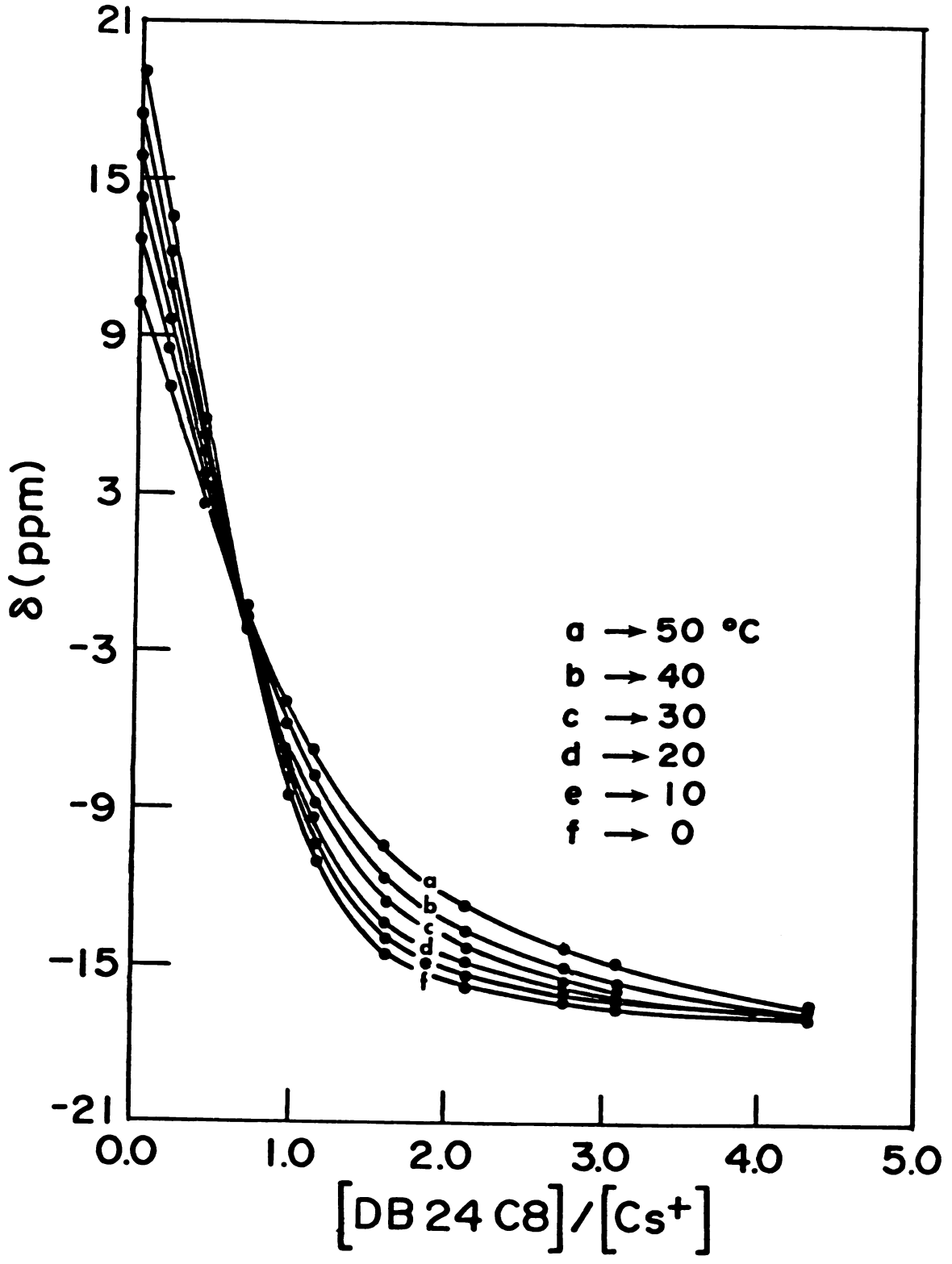

Figure 51. Cesium-133 chemical shifts vs. (DB24C8)/(Cs^+) mole ratio in 70% AN/30% DMF at various temperatures.

Table 52. Formation Constants of $(DB27C9.Cs)^+$ Complex in AN/DMF Binary Solvents at Various Temperatures.

Solvent	Temperature (°C)	Log Kf
10% AN + 90% DMF	-10	2.96 ± 0.01
	0	2.79 ± 0.01
	10	2.64 ± 0.02
	20	2.50 ± 0.01
	30	2.28 ± 0.01
	40	2.17 ± 0.05
30% AN + 70% DMF	-20	3.50 ± 0.04
	-10	3.20 ± 0.01
	0	3.03 ± 0.02
	10	2.89 ± 0.01
	20	2.69 ± 0.01
	30	2.55 ± 0.01
70% AN + 30% DMF	0	3.51 ± 0.03
	10	3.45 ± 0.02
	20	3.34 ± 0.03
	30	3.20 ± 0.02
	40	3.01 ± 0.02
	50	2.87 ± 0.02

Table 53. Formation Constants of $(DB24C8.Cs)^+$ Complex in AN/DMF Binary Solvents at Different Temperatures.

Solvent	Temperature (°C)	Log Kf
30% SN + 70% DMF	-10	3.11 ± 0.02
	0	2.98 ± 0.02
	10	2.78 ± 0.02
	20	2.54 ± 0.02
	30	2.44 ± 0.03
	40	2.29 ± 0.03
70% AN + 30% DMF	0	3.59 ± 0.05
	10	3.35 ± 0.02
	20	3.18 ± 0.01
	30	3.03 ± 0.01
	40	2.85 ± 0.02
	50	2.68 ± 0.02

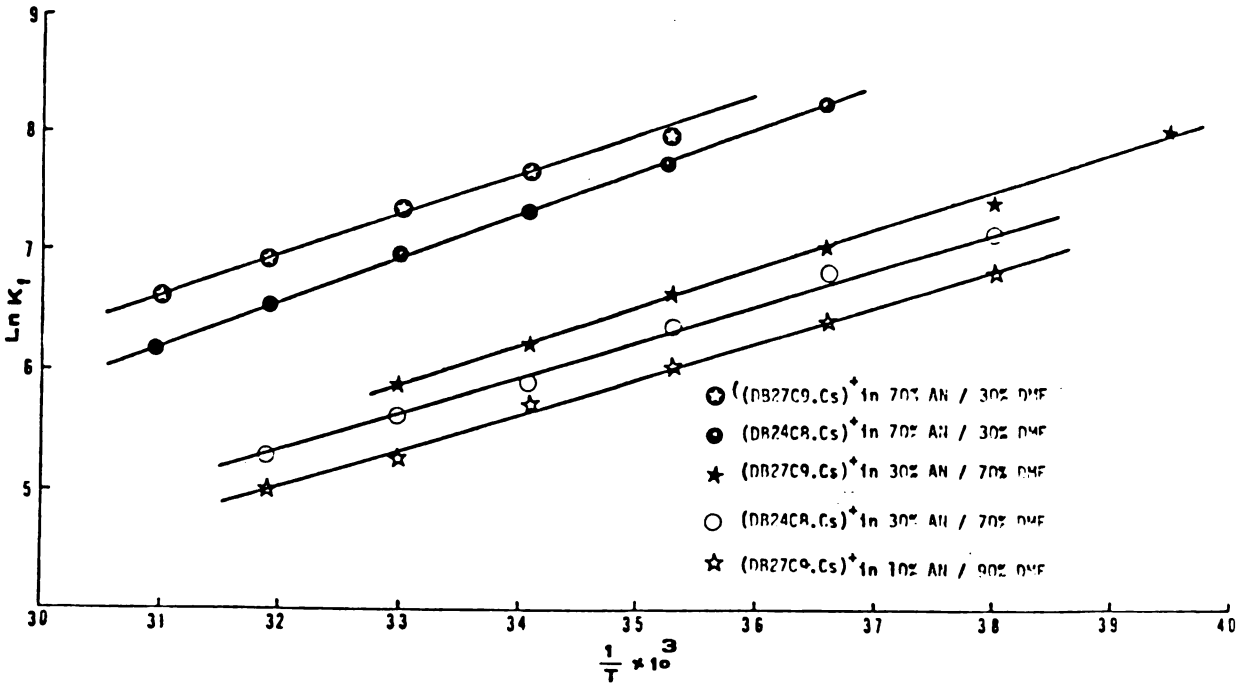

Figure 52. Van't Hoff plots for complexation of the Cs^+ ion by DB27C9 and DB24C8 in acetonitrile-dimethylformamide binary solutions.

Table 54. Thermodynamic Parameters for $(DB27C9 \cdot Cs)^+$ and $(DB24C8 \cdot Cs)^+$ Complexes in DMF and AN and Their Binary Mixtures.

Solvent	Log K_f (30°C)	$\Delta G°$ (30°C) (K·Cal/Mole)	$\Delta H°$ (K·Cal/Mole)	$\Delta S°$ (Cal/Mole K°)
$(DB27C9 \cdot Cs)^+$:				
Pure DMF	2.20 ± 0.01	-3.05 ± 0.01	-7.20 ± 0.37	-13.71 ± 1.19
10% AN + 90% DMF	2.28 ± 0.01	-3.16 ± 0.01	-6.08 ± 0.25	- 9.48 ± 0.87
30% AN + 70% DMF	2.55 ± 0.01	-3.54 ± 0.01	-6.51 ± 0.29	- 9.88 ± 1.05
70% AN + 30% DMF	3.20 ± 0.02	-4.44 ± 0.03	-6.30 ± 0.43	- 6.32 ± 1.41
Pure AN	3.89 + 0.03	-5.39 ± 0.04	-7.93 ± 0.42	- 7.95 ± 1.40
$(DB24C8 \cdot Cs)^+$:				
Pure DMF	2.15 ± 0.03	-2.98 ± 0.04	-6.12 ± 0.12	-10.29 ± 0.42
30% AN + 70% DMF	2.44 ± 0.03	-3.38 ± 0.04	-6.40 ± 0.31	- 9.97 ± 1.09
70% AN + 30% DMF	3.03 ± 0.01	-4.20 ± 0.01	-7.19 ± 0.21	- 9.94 ± 0.72
Pure AN[a]	3.94 ± 0.07	-5.47 ± 0.10	-8.12 ± 0.16	- 8.66 ± 0.48

[a] Reference (70).

related to the change in the structure of the solution and the solvent. Hardly any information about the thermodynamics of complexation is available in mixed solvents. The only available literature data appear to be those for methanol/water mixtures (47, 122). It was of interest to us, therefore, to perform some thermodynamic measurements in mixed nonaqueous solvents in order to see how the thermodynamics of complexation is affected by the solvent composition.

The free energy of the complexation (ΔG_c°), is related to the change in the enthalpy (ΔH_c°) and the change in the entropy (ΔS_c°) according to the following expression:

$$\Delta G_c^\circ = \Delta H_c^\circ - T\Delta S_c^\circ \ .$$

For formation of a stable complex ($\Delta G_c^\circ < 0$) there are five possible combinations: (a) $\Delta H_c^\circ < 0$ and dominant, $T\Delta S_c^\circ > 0$, (b) $\Delta H_c^\circ < 0$ and dominant, $T\Delta S_c^\circ < 0$, (c) $\Delta H_c^\circ < 0$, $T\Delta S_c^\circ > 0$ and dominant, (d) $\Delta H_c^\circ > 0$, and $T\Delta S_c^\circ > 0$ and dominant, (e) $\Delta H_c^\circ < 0$, $T\Delta S_c^\circ > 0$, and ΔH_c° and $T\Delta S_c^\circ$ are the same.

Experimental values of ΔH_c° and ΔS_c° for $(DB27C9\cdot Cs)^+$ and $(DB24C8\cdot Cs)^+$ systems (Table 54) show that in all cases the complexes are enthalpy stabilized but entropy destabilized (i.e. $\Delta H_c^\circ < 0$ and dominant, $T\Delta S_c^\circ < 0$). On the other hand, the thermodynamic parameters, (ΔG_c° and ΔS_c° values) vary with the composition of solvents.

It seems reasonable to assume that the decrease in entropy upon complexation is related to a change in the conformational entropy of the ligand. It is known that large macrocyclic ligands such as dibenzo-27-crown-9 and dibenzo-24-crown-8 are rather flexible in the free states, therefore, the negative entropy changes may be attributed to the increased ligand rigidity upon coordination. It should be stressed, however, that the conformational change of the ligand is not the only factor governing the change in entropy of complexation. Complexation reaction involves not only a change in the solvation of the cation, but also of the ligand. The relative enthalpy and entropy changes can be understood if ligand solvation is taken into consideration. The importance of ligand solvation on the macrocyclic effect has been pointed out by Hinze and Margerum (129) but, at the present time, the information on the interaction of macrocyclic ligands with the solvent molecules is exceedingly sparse.

The data collected in Table 54 show that in dimethylformamide-acetonitrile mixtures in the case of $(DB24C8 \cdot Cs)^+$ complex, lowering the concentration of dimethylformamide results in decrease in the ΔG_c° and ΔH_c° vlaues but an increase in the ΔS_c° values. In a strong solvating solvent such as dimethylformamide, the solvation of the metal ion (and probably of the ligand) will be stronger than in a solvent of lower solvating ability such

as acetonitrile. Therefore, less energy is necessary for desolvation step of the cation (and probably of the ligand) in the case of acetonitrile than dimethylformamide solutions. It would be expected, therefore, that the ΔH_c° values for the complexation reaction will be more negative as the acetonitrile composition of AN/DMF mixture increases, and the ΔS_c° value will increase due to the additional solvent molecules which may release in the reaction.

As it is seen from Table 54, while the thermodynamic parameters of $(DB24C8 \cdot Cs)^+$ are influenced by the solvent and vary regularly with the solvent composition, however, this order is not followed by $(DB27C9 \cdot Cs)^+$ complex, in which the thermodynamic quantities do depend somewhat on the solvent composition but not in a regular manner. This observation may be explained by the consideration of the anomaly thermodynamic behaviour of DB30C10 (70) and DB27C9 (page 126) in complexation with the cesium ion in acetonitrile solutions. It is reasonable to assume that acetonitrile may form a complex in solution with DB27C9, such as that reported with 18-crown-6 (107).

CHAPTER VI

MISCELLANEOUS

A. Ionic Solvation of Cs^+ Ion in Mixed Solvents

a. Results

Competitive solvation studies for Cs^+ ion were performed in H_2O-AN, H_2O-MeOH, H_2O-DMSO binary systems using the cesium-133 NMR signal. For this purpose, the ^{133}Cs chemical shifts were measured as a function of solvent composition in these mixtures. The data re presented in Table 55 and the plots of cesium-133 chemical shifts versus solvent composition are shown in Figures 53-55.

b. Discussion

Study of ion-solvent interaction and preferential solvation of an ion involves the determination of the effect of the solvent on the resonance frequency of the corresponding ion in solution. Some investigations of competitive solvation have been made by several researchers, using ^{59}Co (130, 131), ^{27}Al (132), ^{7}Li (133), ^{205}Tl (81, 84, 85, 102), and ^{23}Na (12, 134-138) NMR techniques.

When a solute is dissolved in a binary solvent, the solvation shell of the solute need not maintain the same composition as the bulk solvent, but it may be preferentially solvated by one of component. Frankel et al. (139) have suggested that a convenient measure of the

Table 55. Cesium-133 Chemical Shifts of Cesium Salt Solutions in Mixed Solvents

AN - H_2O (0.02M CsSCN)		MeOH - H_2O (0.02M CsI)		DMSO - H_2O (0.02M CsI)	
MF of AN	(ppm)	MF of MeOH	(ppm)	MF of DMSO	(ppm)
0.00	-0.01	0.00	0.28	0.00	0.28
0.06	3.39	0.06	-2.35	0.03	1.99
0.13	5.09	0.14	-5.45	0.09	5.56
0.22	6.80	0.23	-8.64	0.14	8.97
0.31	7.89	0.34	-12.60	0.23	15.56
0.45	10.13	0.47	-17.78	0.34	25.72
0.62	14.47	0.55	-20.65	0.41	31.38
0.76	19.26	0.74	-28.71	0.62	46.81
0.93	27.81	1.00	-39.81	0.89	62.55
1.00	33.71			1.00	67.29

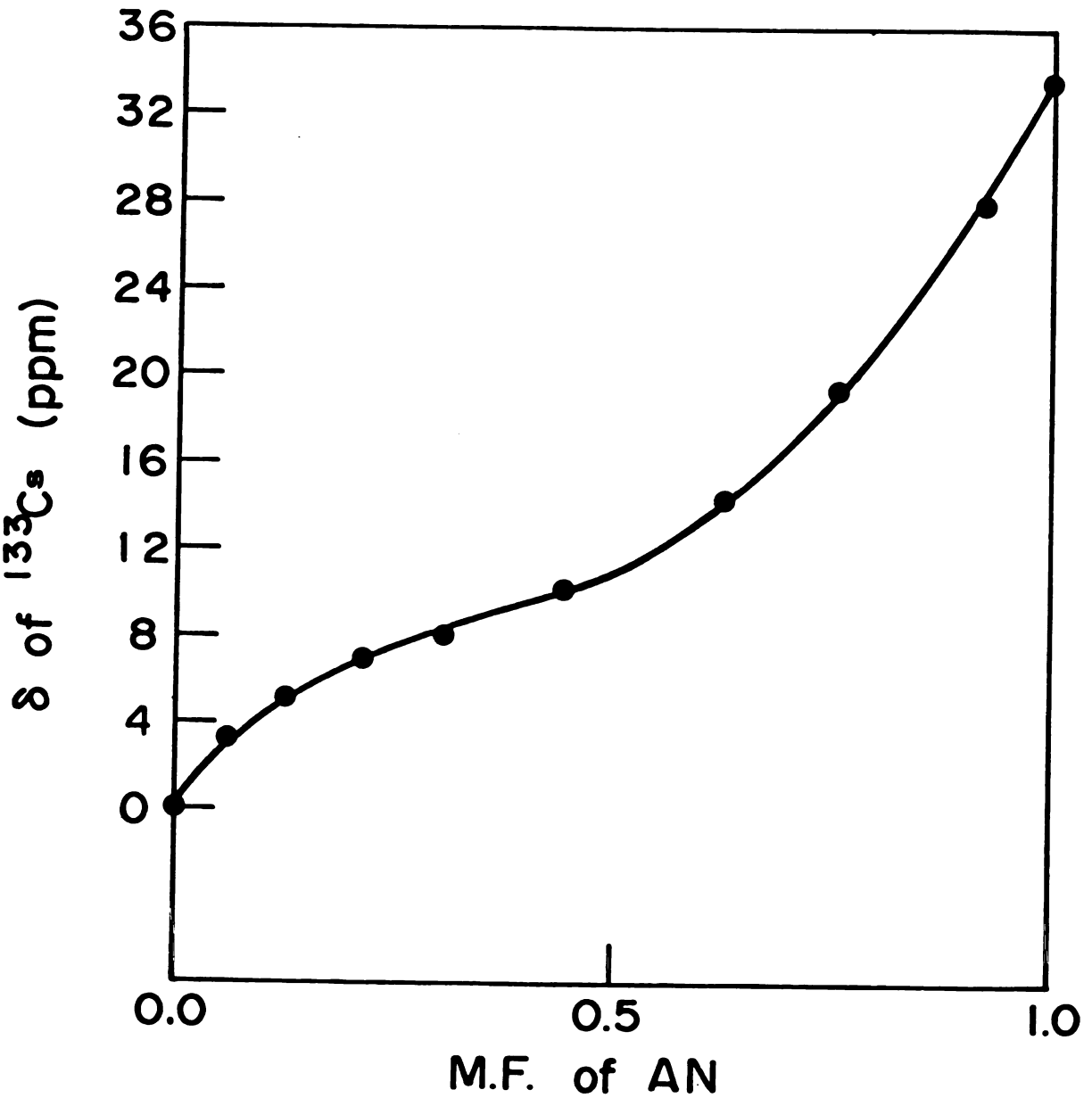

Figure 53. Cesium-133 chemical shifts vs. composition of AN in H_2O-AN binary mixtures.

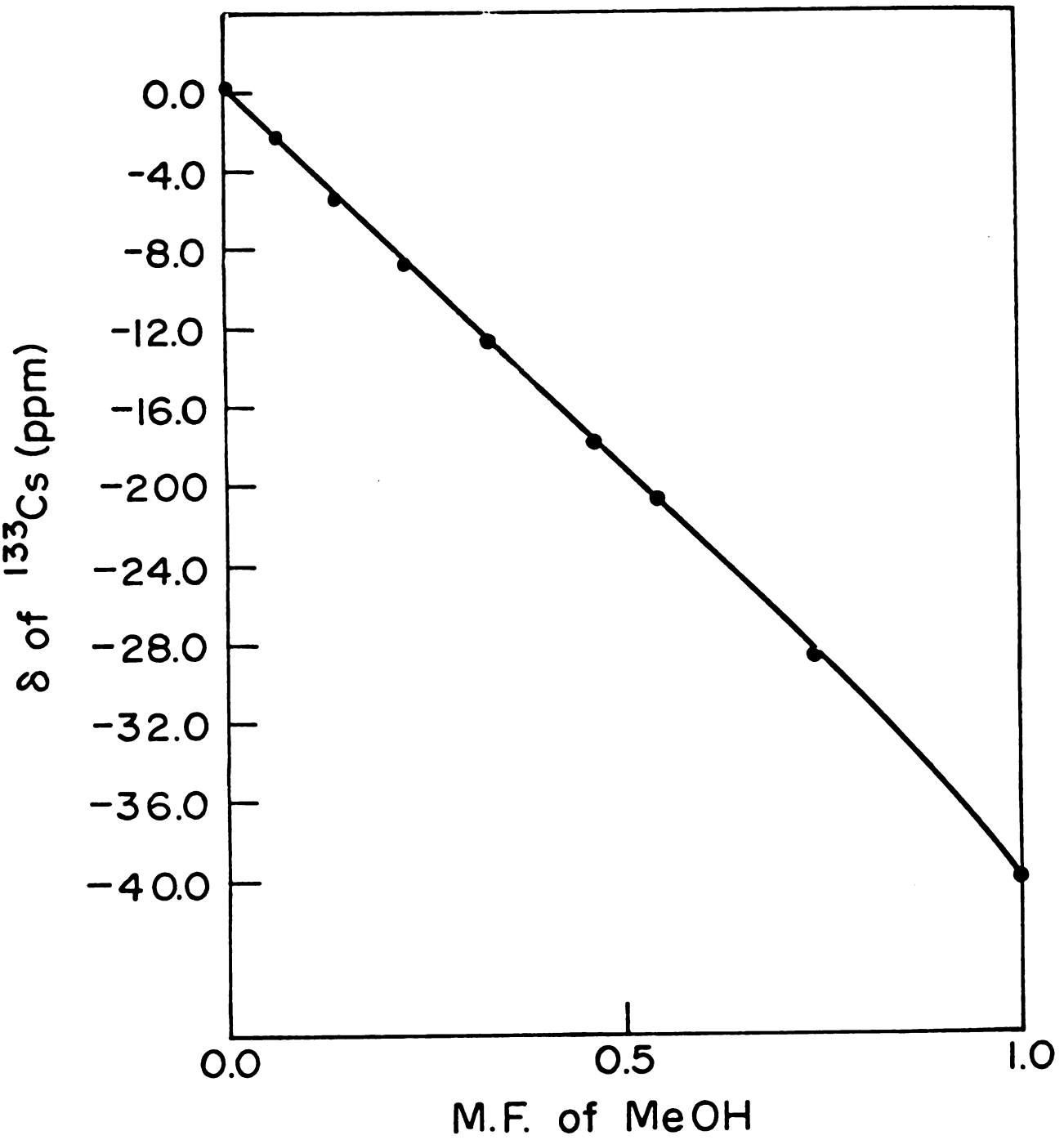

Figure 54. Cesium-133 chemical shifts vs. composition of MeOH in H_2O-MeOH binary solutions.

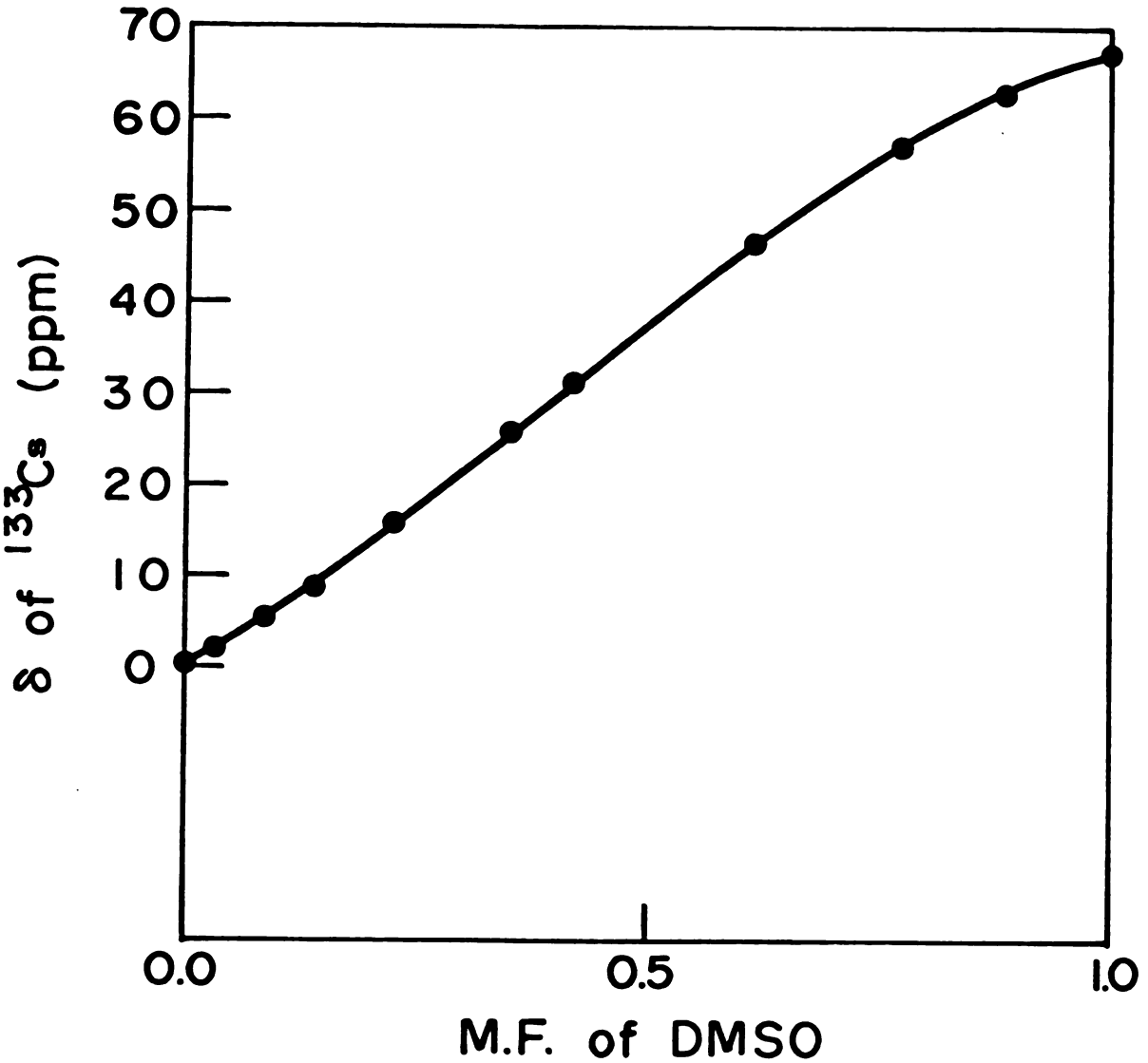

Figure 55. Cesium-133 chemical shift as a function of DMSO content in H_2O-DMSO binary solutions.

degree of preferential solvation in a binary solvent, is the bulk solvent composition at which both solvents participate equally in the contact solvation shell of the solute. It has been suggested that this is the composition in the chemical shift-solvent composition at which the chemical shift of the appropriate nucleus lies midway between the values for the pure solvents (Isosolvation point, I.S.P.). It should be noted that there does not seem to be the firm theoretical basis for this assumption.

The isosolvation points for H_2O-AN, H_2O-MeOH, and H_2O-DMSO systems found in this study, are 0.30, 0.48 and 0.55 mole fractions of water respectively. These data suggest that the order of the solvating ability of these solvents towards the Cs^+ ion is dimethylsulfoxide > water ~ methanol > acetonitrile. It is interesting to note that, despite the high donor ability of water (D·N = 33, obtained from ^{23}Na NMR measurements, 133), the cesium ion is more strongly solvated in dimethylsulfoxide (D·N = 29.8) than in water. It seems reasonable to assume that the enhancement of solvating ability of DMSO in H_2O-DMSO mixture, may result from breaking up the polymeric structure of this solvent by addition of water (see page 38). The position of the isosolvation points in H_2O-MeOH and H_2O-AN systems indicates that the solvating abilities of water and methanol are approximately equal, but water is a better solvating solvent than acetonitrile. This is not unexpected,

Table 56. I.S.P data, $K^{1/n}$, and $\Delta G°/n$ for Cs^+ ion in the binary mixed solvents

Mixture	I.S.P	$K^{1/n}$	$\Delta G°/n$ K.J/Mole
H_2O-AN	0.30	3.09 ± 0.09	-2.83
H_2O-MeOH	0.48	1.12 ± 0.01	-0.29
H_2O-DMSO	0.55	0.48 ± 0.04	1.85

because the donor ability of acetonitrile (DN = 14.1) is much lower than that of water.

Convington et al (140-142) have proposed an expression for the equilibrium constant for a solvent-exchange process. The equilibrium constants and the free energy of competitive solvation for the above mentioned systems were calculated using Convington's equation:

$$\frac{1}{\delta} = \frac{1}{\delta_p}\left(1 + \frac{1}{K^{1/n}\,\frac{X_B}{X_A}}\right) \qquad (1)$$

where δ = observed chemical shift relative to the resonance of Cs^+ in pure solvent A.

δ_p = total range of the chemical shift between two pure solvents.

$K^{1/n}$ = the geometric equilibrium constant

n = the solvation number of Cs^+ ion

X_A and X_B = the mole fraction of the two solvents

The geometric equilibrium constant, $K^{1/n}$, and $\frac{1}{\delta_p}$ are obtained from the slope and intercept of the plot of $1/\delta$ versus X_B/X_A respectively. The free energy of competitive solvation $\Delta G°/n$ is calculated by the following expression

$$\Delta G°/n = -RT \ln K^{1/n} .$$

The values of isosolvation point, $K^{1/n}$ (obtained by linear least square, KINFIT program), and $\Delta G°/n$ for each system are given in Table 56. We feel that the high sensitivity

of the resonance frequency of ^{133}Cs to the solvent environment makes it a useful system for the study of preferential solvation.

B. Complexation of the Tl^+ Ion by C222

Complexing of the Tl^+ ion by cryptand-222 was studied in acetone, acetonitrile, and dimethylsulfoxide solutions using thallium-205 NMR technique. The ^{205}Tl chemical shifts as a function of the C222/Tl^+ mole ratios are summarized in Table 57. Since the exchange between the free and complexed thallium ion is slow compared to the NMR time scale, two ^{205}Tl signals (corresponding to the free and the bond Tl^+ ion) are observed, as long as the mole ratio of C222/Tl^+ is between zero and unity (Figure 56). In general, if the exchange rate between the two cationic sites is larger than $\sqrt{2}/\pi\Delta\nu$ ($\Delta\nu$ is the difference between the resonance frequency in Hz of the free and complexed cation), only one population averaged signal isobserved, but when the exchange rate is smaller than $\sqrt{2}/\pi\Delta\nu$, then two NMR signals, corresponding to the free and bonded cation will be observed.

Thallium ion forms a very stable complex. The strength of the interaction between the Tl^+ ion and C222 is shown by the fact that no free ^{205}Tl resonance is observed at 1:1 or higher mole ratio of C222/Tl^+ even in strongly solvating solvent such as dimenthysulfoxide.

Table 57. Thallium NMR Study of $TlClO_4$ with C222 in Different Solvents

Solvent	Conc. Tl^+ (M)	C222/Tl^+ Ratio	^{205}Tl Resonance (ppm)
AN	0.005	0.00	-215.69
		0.60	-214.23 and 40.54
		1.00	40.18
		1.88	42.28
AC	0.01	0.01	-183.10
		0.50	-176.73 and 40.96
		1.00	38.00
		1.65	40.52
		4.66	39.82
DMSO	0.02	0.00	319.36
		0.48	316.61 and 67.89
		0.55	316.28 and 69.75
		0.69	314.16 and 69.04
		0.84	313.10 and 68.15
		0.92	314.20 and 68.52
		1.39	67.88
		2.21	68.84
		3.29	68.69

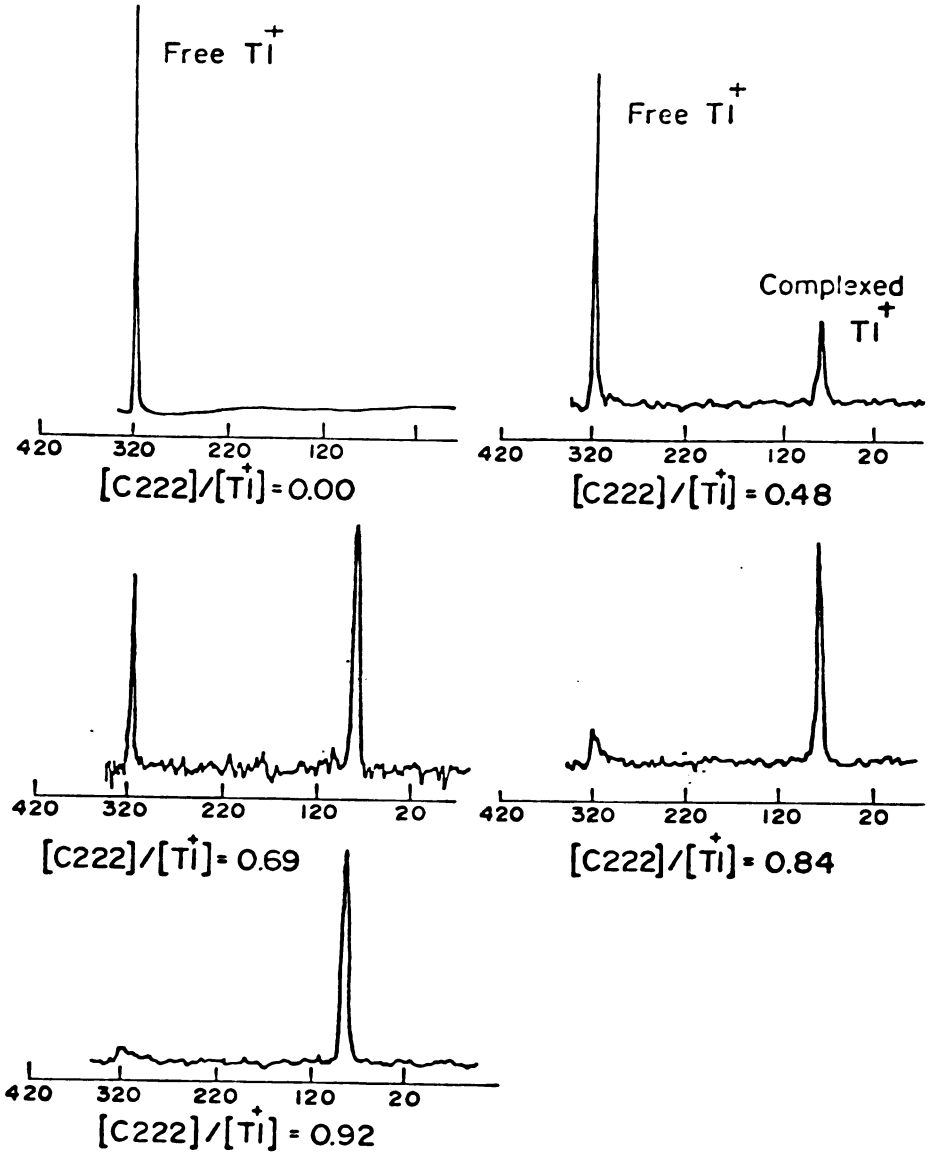

Figure 56. Thallium-205 NMR spectra of $(C222 \cdot Tl)^+$ complex at various $C222/Tl^+$ mole ratios in dimethylsulfoxide solutions.

Figure 57 provides a graphical representation of the ^{205}Tl chemical shifts of both free and complexed thallium ion as a function of C222/Tl^+ mole ratios in AN, AC, and DMSO solutions. It is interesting to note, that the metal ion-complexed resonance frequencies are not identical in these solvents, but the differences are small compared to those for the free solvated ion. This seems reasonable because in $(C222 \cdot Tl)^+$ where the ionophore (C222) occupies the coordination sites of the thallous ion, the solvent effect would be expected to be much smaller than free thallous ion.

C. Complexation Study of the Na^+, and Cs^+ Ions with Cyclo-(tetraethylene-glycol-2,6-Pyridine decarboxylate) in Various Solvents

a. Sodium ion

Complexation of the sodium ion with macrocyclic ligand cyclo-(tetraethylene-glycol-2,6-pyridine dicarboxylate) was studied in acetone, acetonitrile, and propylene carbonate solutions. The data obtained from these studies are given in Table 58, and the plots of ^{23}Na chemical shift as a function of the Ligand/Na^+ mole ratio are shown in Figure 58. In all three cases the log K_f value was found to be larger than 5, which indicates the formation of a very stable complex.

As shown in Figure (I) this macrocycle differs from the simple crown ethers because of the presence of

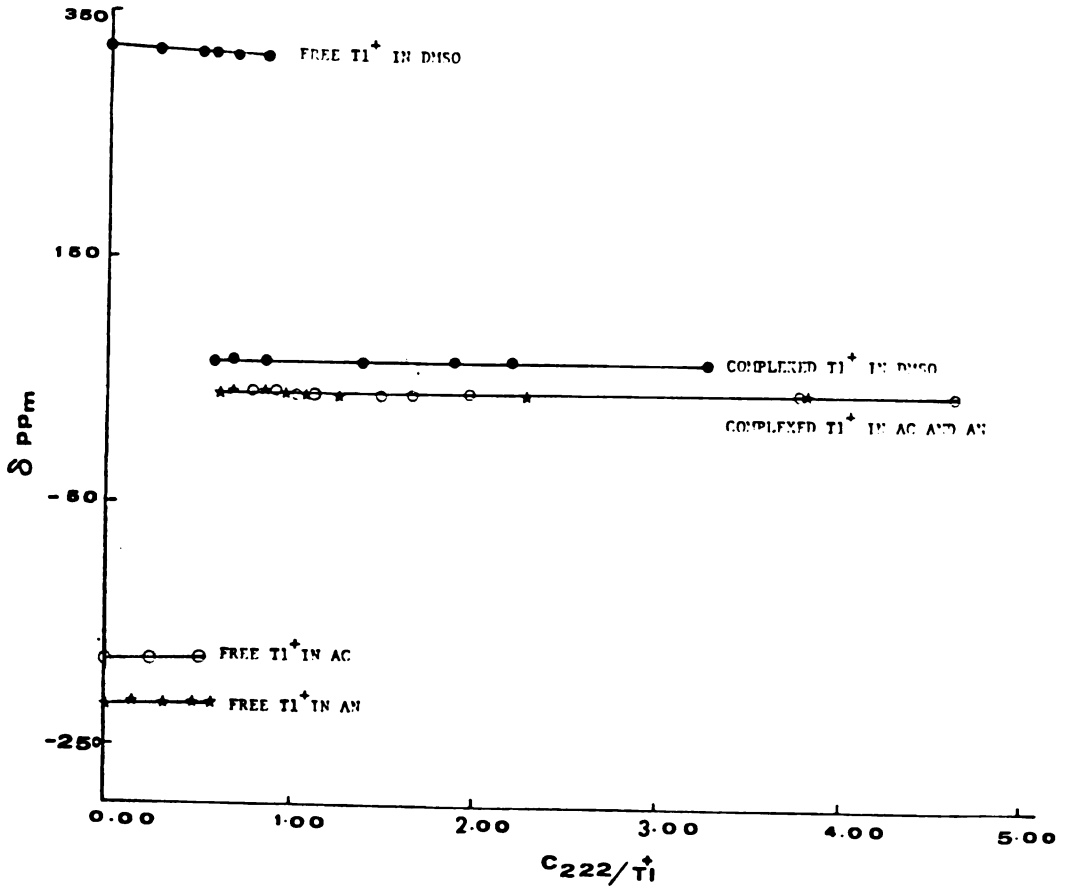

Figure 57. Thallium-205 chemical shifts of both free and complexed Tl^+ ion as a function of C222/Tl^+ mole ratio in various solvents.

Table 58. Mole Ratio Study of Sodium Tetraphenylborate (0.02M) in the Presence of Cyclo (tetraethylene-glycol-2,6-pyridine-dicorboxylate) in Various Solvents at 32 ± 1°C.

AC		AN		PC	
L/Na^+	δ (ppm)	L/Na^+	δ (ppm)	L/Na^+	δ (ppm)
0.00	- 7.95	0.00	- 7.30	0.00	- 8.97
0.27	- 9.34	0.30	- 8.92	0.28	- 9.98
0.60	-11.11	0.64	-11.23	0.65	-12.56
0.76	-12.19	0.77	-12.16	0.79	-13.63
0.89	-12.81	0.92	-12.92	0.90	-14.60
0.99	-13.69	1.02	-13.54	1.01	-14.98
1.15	-14.23	1.16	-13.69	1.15	-15.04
1.38	-14.30	1.92	-13.46	1.39	-14.90
1.90	-14.38	2.48	-13.54	1.94	-15.25
2.36	-14.19	3.02	-13.54	2.48	-14.85
3.02	-14.26	4.00	-13.54	3.03	-14.70
3.88	-14.30			3.94	-14.91

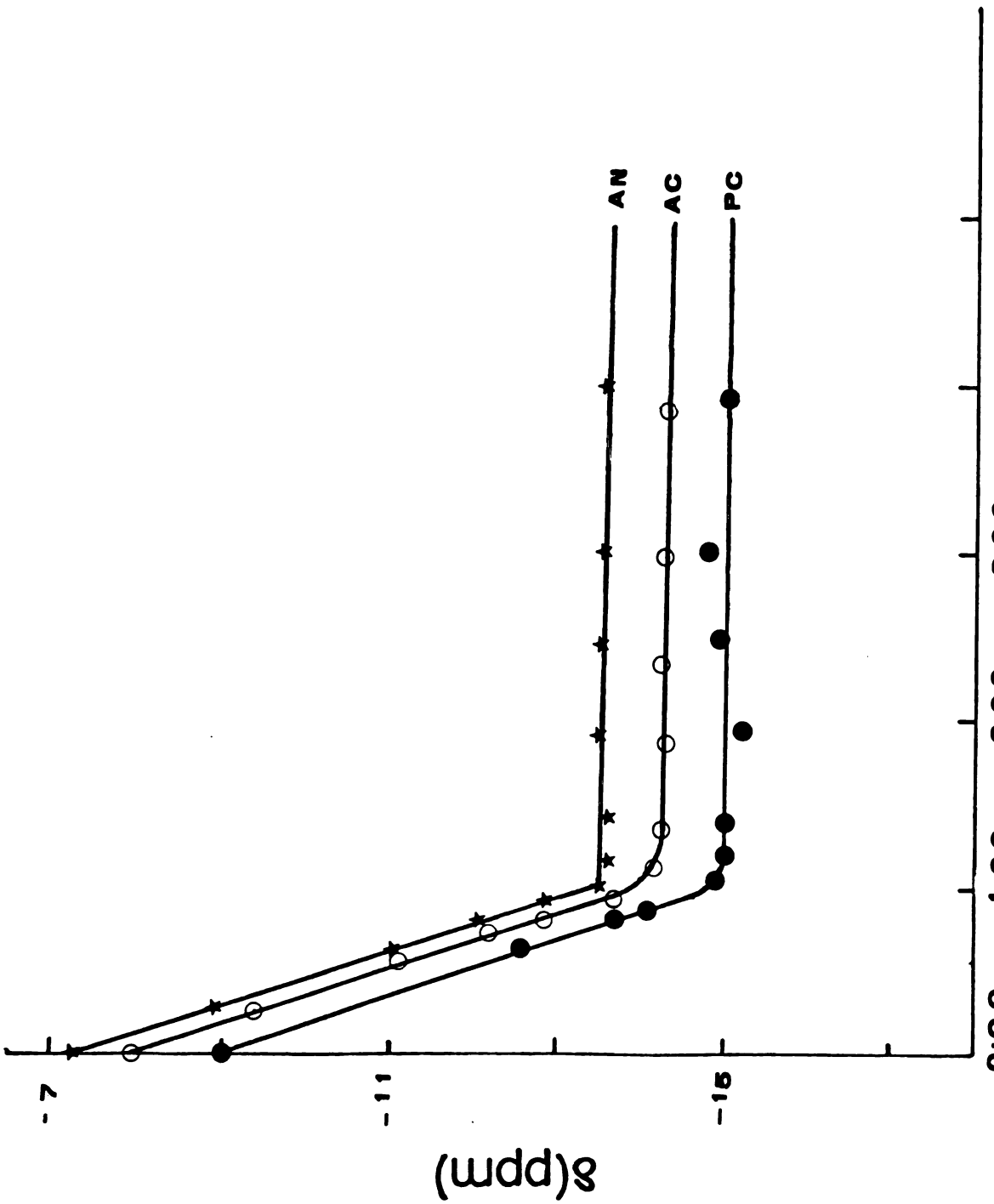

Figure 58. Sodium-23 chemical shifts vs. cyclo-(tetraethylene-glycol-2,6-pyridine dicarboxylate)/Na^+ mole ratio in various solvents.

pyridine ring and the ester groups in its strucutre. Substitution of a nitrogen atom for the oxygen in 18C6 causes a considerable drop in stability constants for alkali metal ions (6).

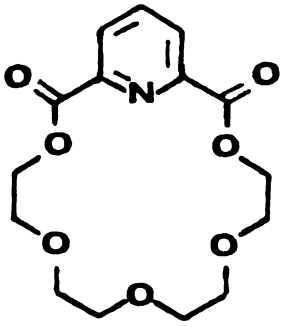

(I)

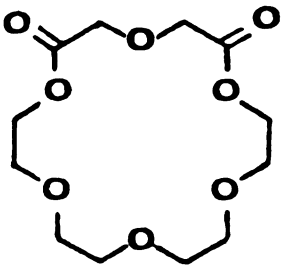

(II)

It has also been noted that addition of two carbonyl groups to 18C6 to form compound (II) causes a considerable drop in the stability and cation selectivity (143). Therefore, it is not the presence of the nitrogen or the carbonyl groups which are responsible for increasing the formation constant, but the aromatic ring may change the effect of carbonyl groups on the complexation.

b. Cesium ion

The data obtained from cesium-133 NMR studies for complexation of the Cs^+ ion with the cyclo (tetraethylene-glycol-2,6-pyridine dicarboxylate) in nitromethane, acetonitrile, propylene carbonate, and dimethylformamide solutions are given in Table 59. The plots of ^{133}Cs chemical shifts versus Ligand/Cs^+ moel ratios are shown in Figure 59. The values obtained for the stability constants

Table 59. Mole Ratio Study of Cyclo (tetraethylen-glycol-236-pyridine dicarboncylate) Complex with Cs^+ Ion in Various Solvents

PC*		DMF*		NM*		AN*	
L/Cs^+	δ (ppm)	L/Cs^+	δ (ppm)	L/Cs^+	δ (ppm)	L/Cs^+	δ (ppm)
0.00	-33.35	0.00	-0.02	0.00	-53.24	0.00	35.10
0.17	-29.55	0.13	0.98	0.26	-47.49	0.27	32.39
0.29	-26.83	0.26	2.14	0.46	-40.12	0.54	30.53
0.36	-25.05	0.35	2.76	0.61	-36.40	0.64	30.07
0.41	-24.35	0.46	3.54	0.76	-33.14	0.78	28.09
0.50	-21.10	0.49	3.54	0.88	-29.26	0.84	28.21
0.54	-20.71	0.58	4.47	0.93	-27.71	0.92	27.35
0.60	-19.54	0.65	4.93	1.03	-25.16	1.01	26.50
0.83	-14.51	0.80	5.71	1.09	-24.93	1.11	25.02
0.91	-12.57	0.89	6.17	1.24	-21.74	1.20	24.09
1.10	- 9.54	1.12	6.79	1.51	-18.80	1.54	21.38
1.25	- 8.15	1.30	7.34	1.84	-16.83	1.88	18.05
1.77	- 7.29	1.87	7.19	2.46	-16.17	2.37	13.71
2.43	- 8.69	2.48	5.71	3.14	-15.70	3.17	8.20
3.23	-10.08	2.34	3.69	4.30	-15.86	4.20	3.16
4.22	-11.87	4.26	1.83				

*Conc. of CsSCN = 0.02M.

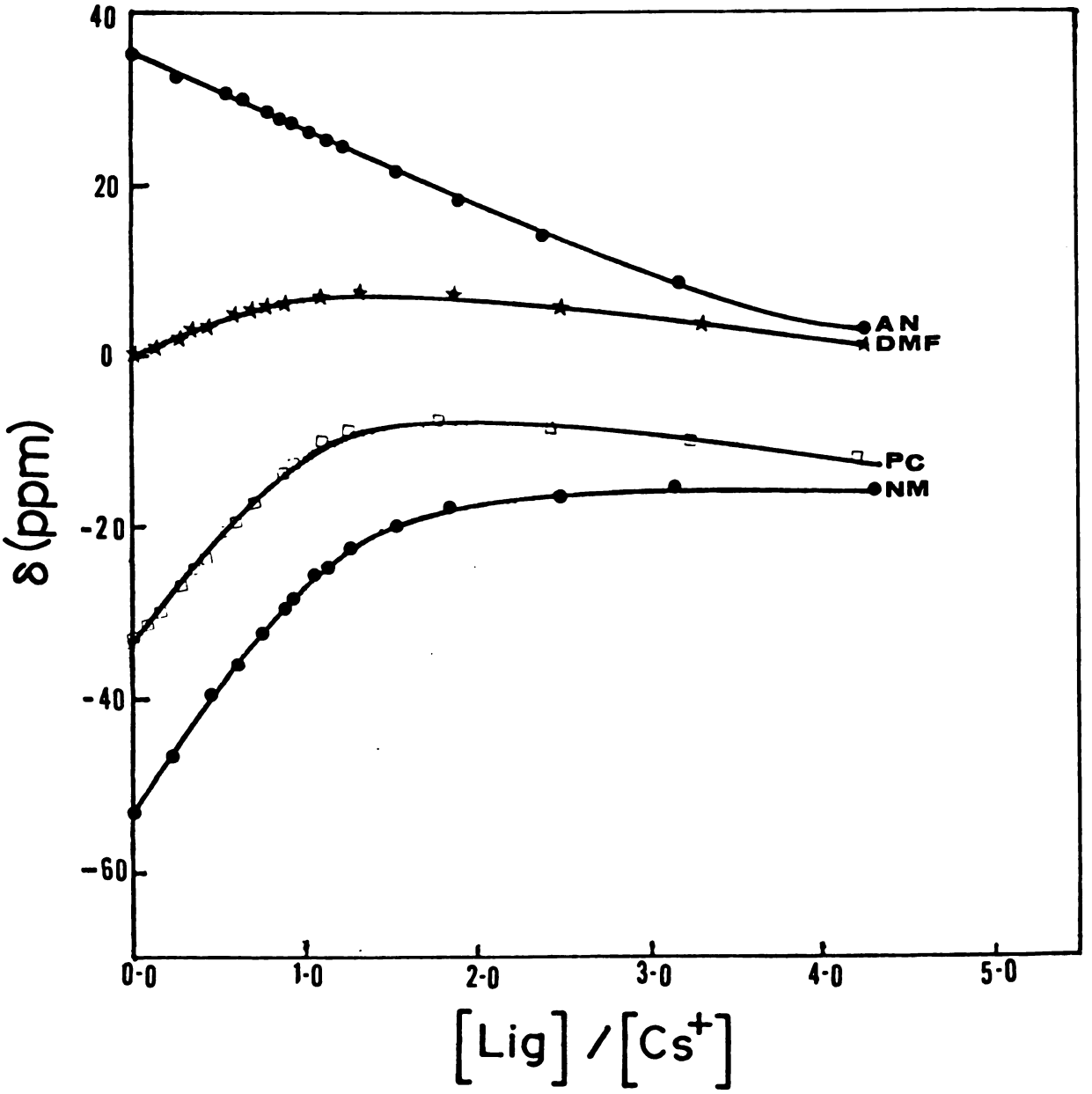

Figure 59. Cesium-133 chemical shifts vs. cyclo-(tetraethylene-glycol-2,6-pyridine dicarboxylate)/ Cs^+ mole ratio in various solvents.

of the complex in NM and AN solutions (assuming that only 1:1 complex is formed) are log K_f = 3.29 ± 0.19 and 1.93 ± 0.10 respectively. These results are not unexpected, since acetonitrile (DN = 14.1) has a stronger solvating ability than nitromethane (DM = 2.7).

It is interesting to note that in dimethylformamide and propylene carbonate solutions, the addition of the ligand to Cs^+ ion solutions results in a downfield shift as the Ligand/Cs^+ mole ratio increases from 0 to 1.5, then further addition of the ligand gives an upfield shift. The slight upward displacement of the ^{133}Cs chemical shift beyond the mole ratio of 1.5 is an evidence for a two-step complexation reaction, however, the small change in the ^{133}Cs chemical shifts in these solutions makes quantitative analysis of the data impossible.

D. Complexation of the Tl^+ Ion by B15C5

Complexation of the Tl^+ ion by monobenzo-15-Crown-5 was studied in acetone, dimethylsulfoxide, pyridine, and dimethylformamide solutions. The resulting data are given in Table 60 and the mole ratio plots are shown in Figure 60. In dimethylformamide and pyridine solutions the plots show little curvature without any break at any mole ratio, which is an evidence for the formation of a very weak complex between Tl^+ ion and B15C5 in these solvents. Computer analysis of the data for the $(B15C5 \cdot Tl)^+$ system in DMF and PY solutions gave the log of formation

Table 60. Chemical Shift-Mole Ratio Data for Complexation of Tl^+ Ion by B15C5 in Various Solvents

AC[a]		DMSO[b]		PY[a]		DMF[b]	
L/Tl^+	δ(ppm)	L/Tl^+	δ(ppm)	L/Tl^+	δ(ppm)	L/Tl^+	δ(ppm)
0.00	-180.39	0.00	329.33	0.00	- 5.65	0.00	132.15
0.22	-165.19	0.17	330.12	0.21	7.49	0.16	125.80
0.60	-146.40	0.44	331.27	0.37	19.30	0.55	112.85
0.94	-127.01	0.73	332.68	0.67	32.35	0.90	100.50
1.20	-122.61	0.88	334.09	0.96	54.42	1.19	33.18
1.26	-123.40	1.12	335.14	1.15	63.74	1.33	88.68
1.76	-136.08	1.28	336.02	1.40	83.32	1.54	82.51
2.12	-142.19	1.50	337.44	1.54	83.31	2.10	67.53
2.62	-156.44	2.09	340.52	1.98	115.32	2.58	54.39
3.32	-176.29	2.66	343.88	2.81	160.91	3.00	44.87
4.26	-195.16	3.10	346.17	3.27	184.10	3.70	29.70
4.78	-202.75	3.79	348.99	3.85	216.19	4.46	15.51
				5.56	296.60	5.58	- 4.25
				5.88	306.75		
				6.67	341.40		

[a]Conc. of $TlClO_4$ = 0.005M. [b]Conc. of $TlClO_4$ = 0.01M.

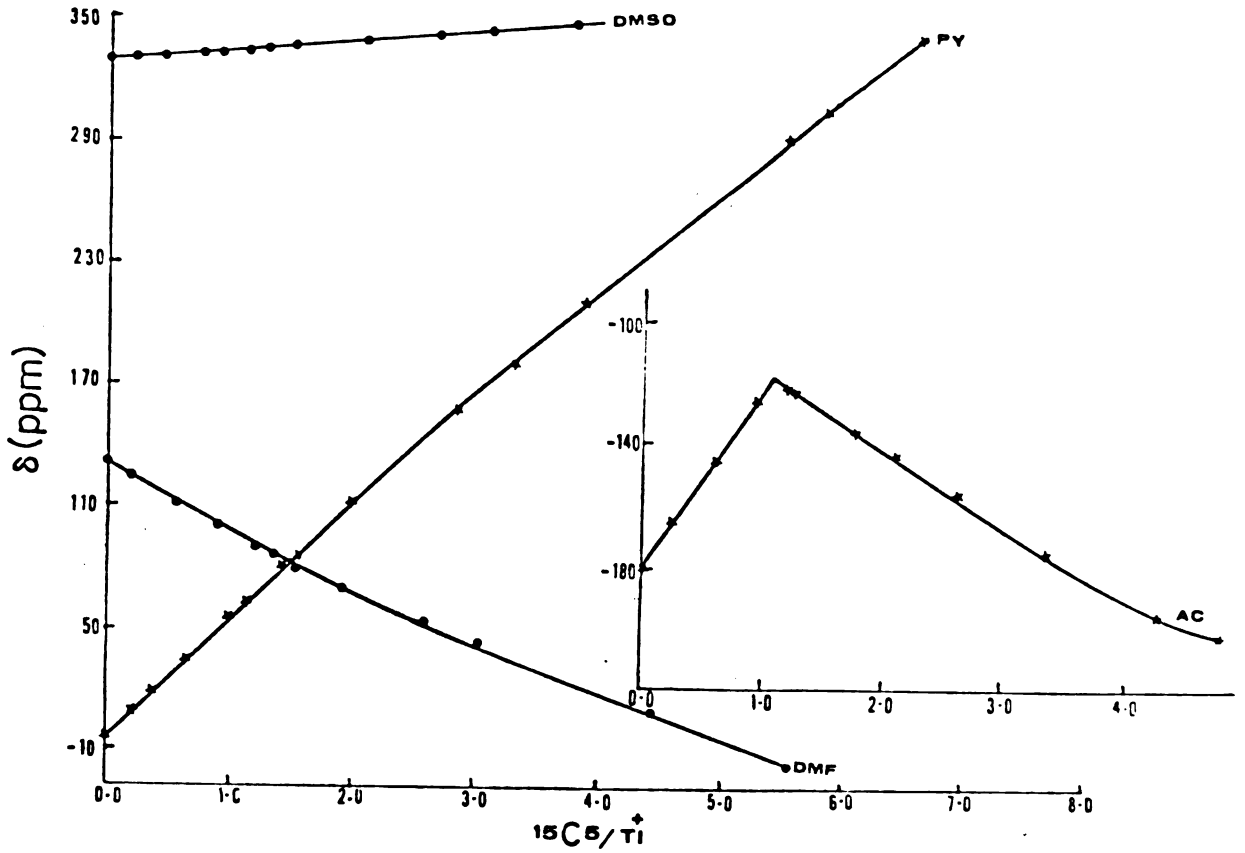

Figure 60. Thallium-205 chemical shifts vs. (15C5)/$(Tl)^{+}$ mole ratio in various solvents.

constant 1.01 ± 0.01 and 0.92 ± 0.03 respectively. These solvents (nitrogen donor, soft base) have a strong solvating ability towards Tl^+ ion (soft acid) and can compete quite successfully with the ligand in the complexation process.

As indicated in Figure 60, no significant variation in the ^{205}Tl chemical shift is observed upon addition of the ligand to the thallium salt in dimethylsulfoxide solutions. In this case the solvation of the Tl^+ ion must be strong enough to prevent complexation reaction.

The addition of B15C5 to a solution of Tl^+ ion in acetone (a solvent with a medium donicity; DN = 17.0) results in a downfield shift followed by a break at the 1:1 Ligand/Cation mole ratio; beyond the mole ratio of 1, an upfield shift is observed as the concentration of the ligand is increased. This behaviour shows that at least two complexes with the respective stiochiometry of 1:1 and 2:1 (sandwich) are formed in acetone solutions. It is obvious that the thallium ion is too large (ionic diameter = 2.8 A°) to fit into the ligand cavity, but it may lie above the ligand ring. Support for this observation is the stepwise formation of $(B15C5 \cdot Tl)^+$ and $(B15C5)_2 \cdot Tl^+$ complexes in this solvent.

As we expect, comparison of our results obtained from ^{205}Tl NMR studies on complexation of the Tl^+ ion with 18C6 (page 74) and B15C5 in nonaqueous solvents demonstrates

the weaker complexing ability of B15C5 than 18C6 for the Tl^+ ion. A possible reason for the lower stability of the complex formed between B15C5 and the Tl^+ ion is that this cation is too large to match the ligand cavity since the cavity diameter of the macrocycle (~ 2A°) is smaller than the cation diameter (2.8 A°), but the cavity of 18C6 (cavity diameter ~ 3A°) accommodates well Tl^+ ion. Another factor which may influence the decreasing of the complexation strength of B15C5 compared to 18C6 is the number of donor atoms which in the case of B15C5 is less than 18C6.

E. Thermodynamic Study of Complexation of DB21C7 with the Cs^+ Ion in DMF and PC

In order to determine the thermodynamic quantities for the complexation of the Cs^+ ion by DB21C7 in dimethylformamide and propylene carbonate solutions, the variations of the cesium-133 chemical shifts were determined as a function of temperature. All the ^{133}Cs chemical shifts measured at different temperatures are listed in Tables 61 and 62. The plots of ^{133}Cs chemical shifts as a function of DB21C7/Cs^+ mole ratio are shown in Figures 61 and 62. The formation constants of the $(DB21C7 \cdot Cs)^+$ complex at various temperatures are given in Table 63. As shown in this table, the stability of the complex varies significantly with the temperature, suggesting that the equilibrium between the Cs^+ ion and the ligand is temperature dependent.

Table 61. Mole Ratio Study of DB21C7 Complex with 0.005M CsSCN in DMF at Different Temperatures.

L/Cs^+	Temperature °C				
	30	40	50	60	70
0.00	-0.85	-2.28	-3.98	-5.92	-7.67
0.22	-0.49	-2.04	-3.60	-5.53	-7.40
0.49	-0.26	-1.73	-3.52	-5.29	-7.16
0.75	-0.01	-1.42	-3.10	-5.06	-6.46
1.06	0.25	-1.11	-2.67	-4.60	-6.23
1.41	0.48	-0.80	-2.20	-4.29	-5.99
1.76	0.59	-0.72	-2.13	-4.13	-5.76
2.39	0.75	-0.49	-1.90	-3.82	-5.22
3.25	0.79	-0.34	-1.74	-3.44	-9.75
3.82	0.87	-0.26	-1.58	-3.21	-4.62

Table 62. Mole Ratio Study of DB21C7 Complex with 0.005M CsSCN in PC at Different Temperatures.

L/Cs^+	Temperature °C				
	20	30	40	50	60
0.00	-33.81	-34.74	-36.22	-37.62	-38.23
0.18	-29.70	-30.71	-32.11	-33.42	-34.98
0.37	-25.82	-26.83	-28.31	-29.78	-31.64
0.55	-21.41	-22.64	-24.04	-25.74	-28.07
0.84	-15.51	-16.75	-18.76	-20.86	-22.88
1.10	-13.19	-14.11	-16.29	-18.38	-20.56
1.51	-11.64	-12.56	-14.35	-16.21	-17.92
1.88	-11.09	-12.18	-13.65	-15.20	-16.67
2.35	-11.09	-12.02	-13.11	-14.43	-15.90
3.04	-11.17	-11.87	-12.87	-14.12	-15.43
3.78	-10.94	-11.64	-12.56	-13.57	-14.97

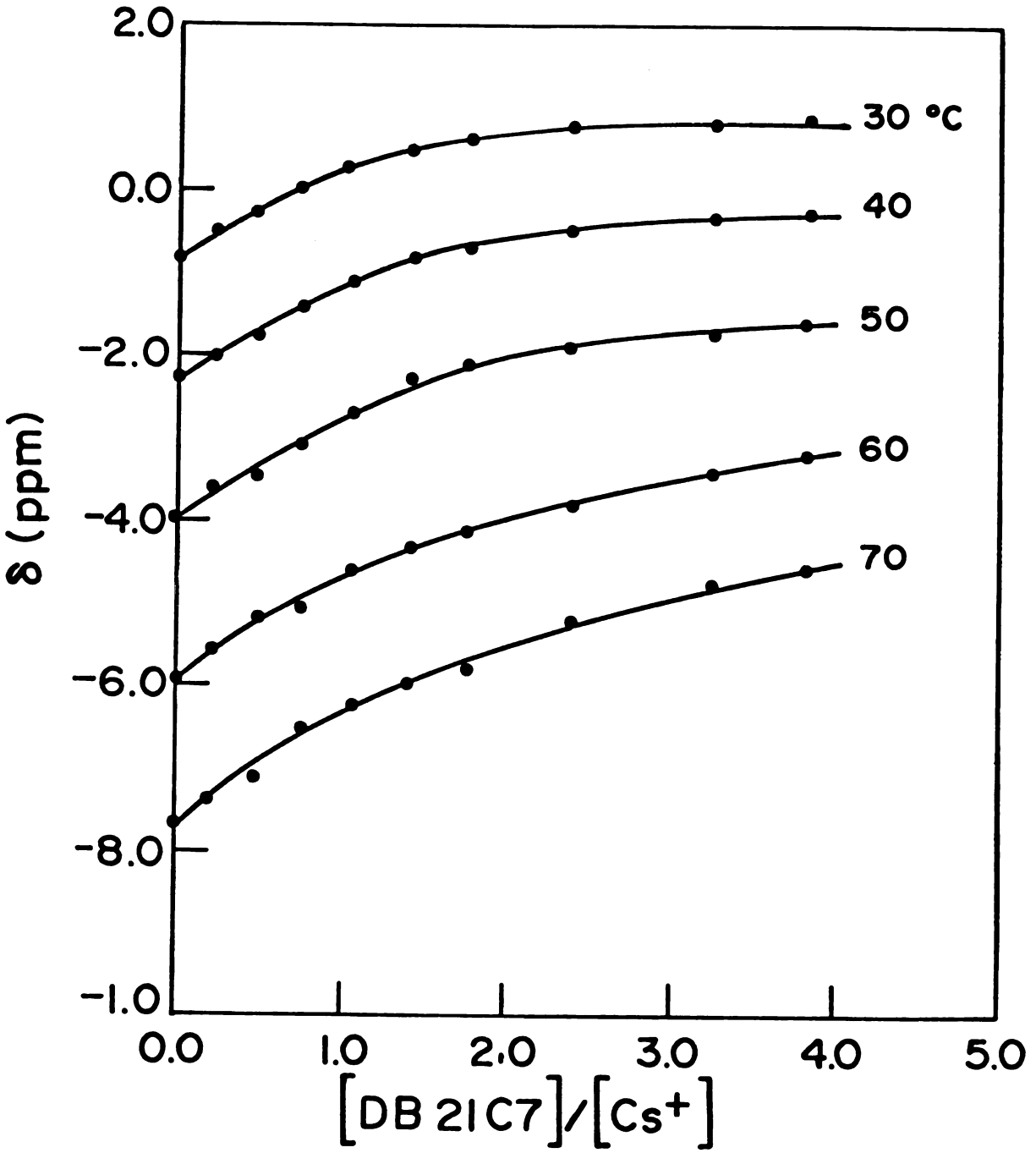

Figure 61. Cesium-133 chemical shifts vs. (DB21C7)/(Cs^+) mole ratio in DMF at various temperatures.

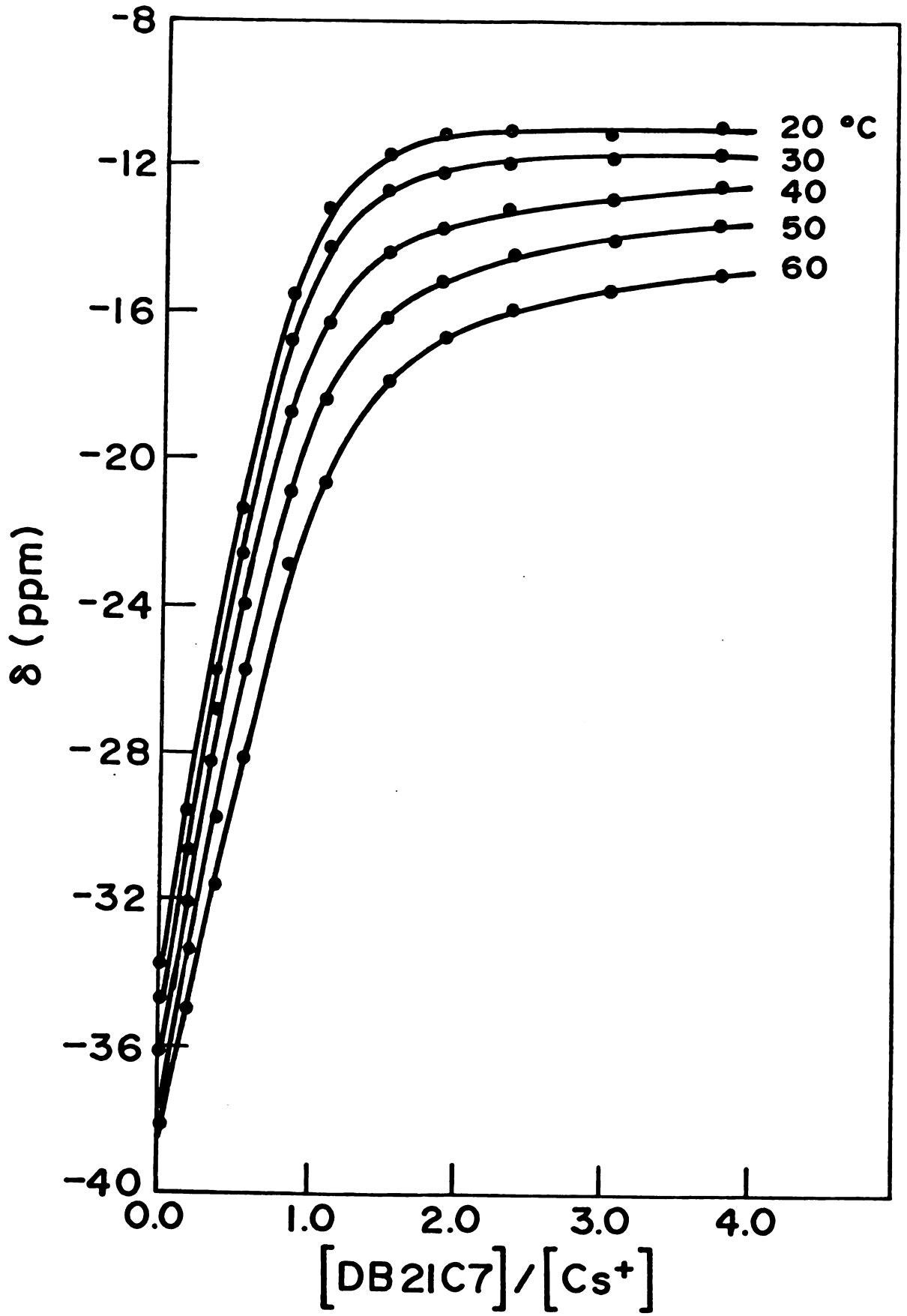

Figure 62. Cesium-133 chemical shift vs. (DB21C7)/(Cs^+) mole ratio in PC at various temperatures.

Table 63. Stability Constants of $(DB21C7\ Cs)^+$ Complex in DMF and PC at Various Temperatures.

Solvent	Temperature (°C)	Log K_f
Dimethylformamide	70	1.93 ± 0.12
	60	2.06 ± 0.06
	50	2.43 ± 0.09
	40	2.51 ± 0.05
	30	2.78 ± 0.05
Propylene Carbonate	60	3.16 ± 0.02
	50	3.25 ± 0.05
	40	3.47 ± 0.03
	30	3.80 ± 0.05
	20	4.12 ± 0.13

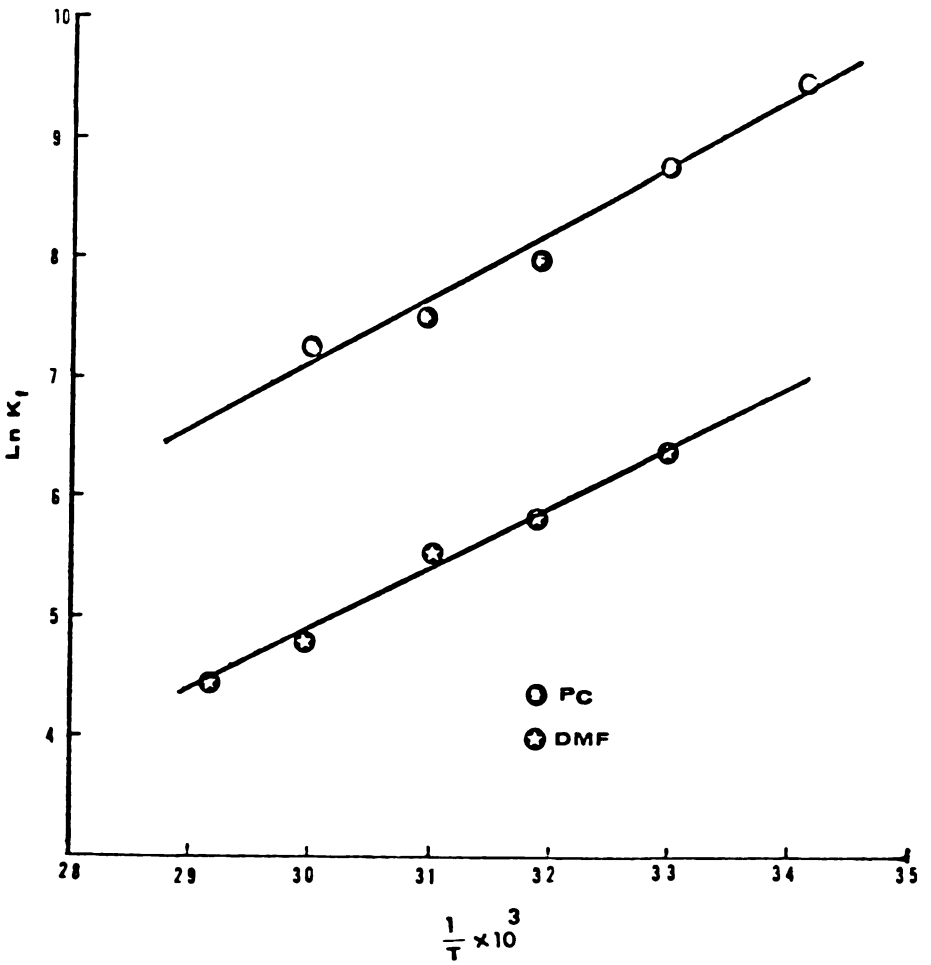

Figure 63. Van't Hoff plots of ln K_f vs. $\frac{1}{T}$ for $(DB21C7 \cdot Cs)^+$ system in PC and DMF.

Table 64. Thermodynamic Parameters for $(DB21C7 \cdot Cs)^+$ Complex in DMF and PC

Solvent	Log K_f (30°C)	ΔG° (K Cal/Mole)	ΔH° (K Cal/Mole)	ΔS° (Cal/Mole K°)
Dimethylformamide	2.78 ± 0.05	-3.85 ± 0.07	-10.28 ± 0.92	-21.16 ± 2.84
Propylene Carbonate	3.80 ± 0.05	-5.27 ± 0.07	-11.14 ± 1.14	-19.35 ± 3.65

Van't Hoff plots of ln K_f versus 1/T are shown in Figure 63. The enthalpies and entropies of the complexation were obtained by the usual manner from the slopes and intercepts of these plots. Table 64 summarizes the thermodynamic quantities of the $(DB21C7 \cdot Cs)^+$ complex in propylene carbonate and dimethylformamide solutions. Investigation of these data indicates that in both cases the complex is enthalpy stabilized but entropy destabilized. It seems reasonable to assume that the negative entropy upon complexation arises from a change in the conformational entropy of the ligand. Since dibenzo-21-Crown-7 is a flexible ligand (because of its large size), it will lose a large degree of freedom in the complexation process.

APPENDIX

APPENDIX

DETERMINATION OF COMPLEX FORMATION CONSTANTS BY THE NMR TECHNIQUE; DESCRIPTION OF COMPUTER PROGRAM KINFIT AND SUBROUTINE EQUATION

The equilibrium for a 1:1 (metal ion:ligand) complexation reaction can be written as:

$$M + L \rightleftharpoons ML \qquad (1)$$

and the concentration equilibrium constant is given by the following expression:

$$K = \frac{C_{ML}}{C_M \cdot C_L} \qquad (2)$$

where C refers to the molar equilibrium concentrations. Since in this case, the complexation reaction does not result in a separation or combination of charges and the concentrations of the reactants are very low (~ 0.01), we only consider the concentration formation constant. Under these conditions, the values of concentration constant will closely approximate the thermodynamic value.

Assuming that only cation-ligand interaction are important and the rate of exchange of the metal ion between the two sites (free cation in the bulk solution and complexed cation) is fast on the NMR time scale, the observed chemical shift of M (δ_{obs}) is a weighted average of the characteristic chemical shift of free cation and complexed cation:

$$\delta_{obs} = \delta_M X_M + \delta_{ML} X_{ML} \qquad (3)$$

where δ_M and δ_{ML} are the chemical shift of the free an complexed M respectively, X_M and X_{ML} are the fractions of the cation in the free and complex states. Therefore

$$\delta_{obs} = \delta_M X_M + \delta_{ML}(1 - X_M) = X_M(\delta_M - \delta_M L) + \delta_{ML} \quad (4)$$

The analytical concentration of M is:

$$C_M^T = C_M + C_{ML} \quad (5)$$

and the analytical concentration of ligand is:

$$C_L^T = C_{ML} + C_L \quad (6)$$

Therefore

$$C_{ML} = C_M^T - C_M \quad (7)$$

and

$$C_L = C_L^T - (C_M^T - C_M) \quad (8)$$

Then

$$K = \frac{(C_M^T - C_M)}{(C_M)(C_L^T - C_M^T + C_M)} \quad (9)$$

C_M is solved in (9)

$$C_M(C_L^T - C_M^T + C_M)K = C_M^T - C_M$$

$$KC_M^2 + (KC_L^T - KC_M^T + 1)C_M - C_M^T = 0$$

$$C_M = \frac{1}{2K}\{-(KC_L^T - KC_M^T + 1) \pm \sqrt{(KC_L^T - KC_M^T + 1)^2 + 4KC_M^T}\} \quad (10)$$

Since C_M cannot be negative, therefore the positive root is chosen:

$$C_M = \frac{(KC_M^T - KC_L^T - 1) + \sqrt{K^2C_L^{T^2} + K^2C_M^{T^2} - 2K^2C_L^TC_M^T + 2KC_L^T + 2KC_M^T + 1}}{2K} \qquad (11)$$

By substitution of C_M from (11) in equation (4) we can derive the following expression:

$$\delta_{obs} = [(KC_M^T - KC_L^T - 1) + (K^2C_L^{T^2} + K^2C_M^{T^2} - 2K^2C_M^T - C_L^T + 2KC_L^T + 2KC_N^T + 1)^{1/2}](\frac{\delta_M - \delta_{ML}}{2KC_M^T}) + \delta_{ML} \qquad (12)$$

In order to fit this equation, two constants and two parameters are used in the FORTRAN CODE:

$$U(1) = \delta_{ML} \qquad U(2) = K$$
$$CONST(1) = C_M^T \qquad CONST(2) = \delta_M$$

The input variables are the analytical concentration of the ligand (XX(1)) and the observed chemical shift (XX(2)).

The data input includes the control cards and the NMR data. The first card contains the number of data points (columns 1-5 (F.15)), the maximum number of iterations to be performed (columns 10-15 (F.15)), the number of constants (columns 36-40 (F.15)), and the maximum value of (Δ parameter/parameter) for convergence to be assumed (0.0001 works well) in columns 41-50 (F10.6). The subsequent cards include:

(1) a title card

(2) a card containing the values of CONST(1) columns 1-10 (F10.6) and CONST(2) columns 11-20 (F10.6)

(3) a card containing the initial estimates of the unknowns U(1) and U(2), in columns 1-10 and 11-20 (F10.6), respectively

(4) The fifth through N cards contain XX(1) in columns 1-10 (F10.6) variances on XX(1) in columns 11-20, XX(2) in columns 31-40 (F10.6) followed by the same parameters for the next data point.

The subroutine EQN for calculations of K (formation constant) and δ_{ML} (chemical shift of the complex) is listed below:

SUBROUTINE EQN

```
      COMMON KOUNT,ITAPE,JTAPE,IWT,LAP,XINCR,NOPT,NOVAR,NOUNK,X,U,ITMAX, EQN
     1WTX,TEST,I,AV,RESID,IAR,EPS,ITYP,XX,RXTYP,DXII,FOP,FO,FU,P,ZL,IO,E EQN
     2IGVAL,XST,Y,DT,L,M,JJ,Y,DY,VECT,NCST,CONST,NDAT,JDAT,MOPT,LOPT,    EQN
     3YYY,CONSTS
      COMMON/FREQT/IMETH
      COMMON/POINT/KOPT,JOPT,XXX
      DIMENSION X(4,300),U(20),WTX(4,300),XX(4),FOP(300),FO(300),FU(300) EQ
     1,P(20,21),VECT(20,21),ZL(300),IO(20),EIGVAL(20),XST(300),Y(10),
     2DY(10),CONSTS(50,16),NCST(50),ISW(N(50),RXTYP(50),DXII(50),IRX(50)
     3,MOPT(50),LOPT(50),YYY(50),CONST(16),XXX(15)
      GO TO (2,3,4,5,1,7,8,9,10,11,12) ITYP
    1 CONTINUE
      ITAPE=10
      JTAPE=11
      NOUNK=2
      NOVAR=2
      RETURN
    7 CONTINUE
      RETURN
    8 CONTINUE
      RETURN
    9 CONTINUE
      IF(IMETH.NE.-1) GO TO 35
      RETURN
   35 CONTINUE
      A=(U(2)**2)*(XX(1)**2)
      B=(U(2)**2)*(CONST(1)**2)
      C=-2.0*(U(2)**2)*(XX(1))*CONST(1)
      D=2.0*(U(2))*(XX(1))
      E=2.0*(U(2))*(CONST(1))
      AA=(U(2))*(CONST(1))
      BB=-(U(2))*XX(1)
      CC=(CONST(2)-U(1))/(2.0*(CONST(1))*(U(2)))
      S=((AA*BB-1.)*SQRT(ABS(A-B+C-D+E+1.)))*CC)*U(1)
      RESID=S-XX(2)
      RETURN
    3 CONTINUE
      RETURN
    4 CONTINUE
      RETURN
    5 CONTINUE
      IF(IMETH.NE.-1) GO TO 20
      RETURN
   20 CONTINUE
      RETURN
    6 CONTINUE
      RETURN
   10 CONTINUE
      RETURN
   11 CONTINUE
      RETURN
   12 CONTINUE
      RETURN
      END
```

REFERENCES

REFERENCES

1. C.J. Pedersen, J. Amer. Chem. Soc., 89, 7017 (1967).

2. J.M. Lehn and J.P. Sauvage, Chem. Comm., 1971, 440.

3. R.M. Izatt and D.P. Nelson, Science, 164, 443 (1969).

4. A.I. Popov and J.M. Lehn, "Physicochemical Studies of Crown and Cryptate Complexes" in Coordination Chemistry of Macrocyclic Compounds, G.A. Melson, editor, Plenum, New York, N.Y. (1979).

5. C. Moore and B.C. Pressman, Biochem. Biophys. Res. Commun., 15, 562 (1964).

6. R.M. Izatt, D.J. Eatough, and J.C. Christensen, Struct. Bonding, 16, 161 (1973).

7. C.J. Pedersen, J. Amer. Chem. Soc., 92, 391 (1970).

8. C.J. Pedersen, J. Amer. Chem. Soc., 92, 386 (1970).

9. J.D. Lamb, R.M. Izatt, C.S. Swain, and J.J. Christensen, J. Amer. Chem. Soc., 102, 475 (1980).

10. H.K. Frensdorff, J. Amer. Chem. Soc., 93, 600 (1971).

11. E. Mei, Michigan State University, Ph.D. Thesis (1977).

12. R.H. Erlich, A.I. Popov, J. Amer. Chem. Soc., 92, 4989 (1970).

13. M.K. Wong, A.I. Popov, J. Phys. Chem., 75, 56 (1971).

14. Y.M. Cahen, J.L. Dye, A.I. Popov, J. Phys. Chem., 79, 1289 (1975).

15. Y.M. Cahen, A.I. Popov, J. of Sol. Chem., 4, 599 (1975).

16. A.I. Popov, Pure and Appl. Chem., 51, 101 (1979).

17. A.R. Hourdakis, Michigan State University, Ph.D. Thesis (1978).

18. E.M. Arnett, T.C. Moriarity, J. Amer. Chem. Soc., 93, 4908 (1971).

19. F. Vogtle and Weber, Angew. Chem., 89, 126 (1974).

20. D.J. Cram et al., Pure Appl. Chem., 43, 327 (1975).

21. J.M. Lehn and J.P. Sauvage, J. Amer. Chem. Soc., 97, 6700 (1975).

22. D. Bright and M.R. Truter, J. Chem. Soc., B, 1544 (1970).

23. M.A. Bush and M.R. Truter, Chem. Commun., 1439 (1970).

24. M. Dobler, J.D. Dunitz and P. Seiler, Acta Crystallogr., Sect. B, 30, 2741 (1974).

25. D. Moras, B. Metz, and R. Weiss, Acta Crystallogr., Sect. B, 29, 383 (1973).

26. B. Metz, D. Moras and R. Weiss, J. Amer. Chem. Soc., 93, 1806 (1971).

27. B. Metz, D. Moras and R. Weiss, Chem. Commun., 444 (1971).

28. J.D. Dunitz and P. Seiler, Acta Crystallogr., Sect. B, 30, 2739 (1974).

29. C.J. Pedersen and H.K. Frensdorff, Angew. Chem. Internal. Edit., 11, 16 (1972).

30. N.S. Poonia and M.R. Truter, J. Chem. Soc., Dalton Trans., 2062 (1972).

31. M.A. Bush and M.R. Truter, J. Chem. Soc. Perkin II, 345, (1972).

32. D. Live and S.I. Chan, J. Amer. Chem. Soc., 98, 3769 (1976).

33. D.E. Fenton, M. Mecer, N.S. Poonia, and M.R. Truter, Chem. Commun., 66 (1972).

34. D.L. Hughes, J. Chem. Soc. Dalton Trans., 2374 (1975).

35. M. Shamsipur and A.I. Popov, J. Amer. Chem. Soc., 101, 4051 (1979).

36. E. Mei, A.I. Popov, and J.L. Dye, J. Phys. Chem., 81, 1677 (1977).

37. J.S. Shih, Michigan State Univeristy, Ph.D. Thesis (1978).

38. J.J. Christensen, D.J. Eatough, R.M. Izatt, Chem. Rev., 74, 351 (1974).

39. J.D. Lamb, R.M. Izatt, J.J. Christensen, J.D. Eatough, in "Coordination Chemistry of Macrocyclic Compounds", G.E. Melson, Ed., Plenum Press: New York, 1979, pp. 145-217.

40. J.S. Bradshaw, in "Synthetic Multidentate Macrocyclic Compounds", R.M. Izatt, J.J. Christensen, Eds., Academic Press: New York, 1978, pp. 53-109.

41. C.J. Pedersen, J. Org. Chem., 36, 254 (1971).

42. J.S. Bradshaw, J.Y. Hui, B. L. Haymore, J.J. Christensen and R.M. Izatt, J. Hetero. Chem., 10, 1 (1973).

43. J.R. Dann, P.P. Chiesa, and J.W. Gates, J. Org. Chem., 26, 1991 (1961).

44. J.S. Bradshaw, J.Y.K. Hui, Y. Chan, B.L. Haymore, R.M. Izatt, and J.J. Christensen, J. Hetero. Chem., 11, 45 (1974).

45. J.S. Bradshaw, R.A. Reeder, M.D. Thompson, E.D. Flanders, R.L. Carruth, R.M. Izatt, and J.J. Christensen, J. Org. Chem., 41, 134 (1976).

46. N.K. Dalley, J.S. Smith, S.B. Larson, K.L. Matheson, J.J. Christensen and R.M. Izatt, J.C.S. Chem. Commun., 84 (1975).

47. J.D. Lamb, R.M. Izatt, J.J. Christensen and D.J. Eatough, "Thermodynamics and Kinetics of Cation-Macrocyclic Interaction" in Coordination Chemistry of Macrocyclic Compounds, G.A. Melson, editor, Plenum, New York, N.Y. (1979).

48. B. Metz, D. Moras, and R. Weiss, J. Inorg. Nucl. Chem., 36, 785 (1979).

49. B. Dietrich, J.M. Lehn, and J.P. Suavage, Tetrahedron Lett., 2885 (1969).

50. E. Graf and J.M. Lehn, J. Amer. Chem. Soc., 97, 5022 (1975).

51. B. Dietrich, J.M. Lehn, and J.P. Sauvage, J. Chem. Soc., Chem Commun., 16 (1973).

52. J.M. Lehn, Structure Bonding, 16, 1 (1973).

53. L.L. Hsu, Michigan State University, Master Thesis (1976).

54. E. Mei, A.I. Popov and J.L. Dye, J. Amer. Chem. Soc., 99, 6532 (1977).

55. Y.M. Cahen, J.L. Dye and A.I. Popov, J. Phys. Chem., 79, 1292 (1975).

56. E. Mei, L. Liu, J.L. Dye, and A.I. Popov, J. Solution Chem., 6, 771, (1977).

57. J.M. Lehn, J.P. Sauvage, and B. Dietrich, J. Amer. Chem. Soc., 92, 2916 (1970).

58. B. Dietrich, J.M. Lehn and J.P. Sauvage, Tetrahedron, 29, 1647 (1973).

59. H.E. Simmons and C.H. Park, J. Amer. Chem. Soc., 90, 2428 (1968).

60. B. Dietrich, J.M. Lehn, J.P. Sauvage, and J. Blanzat, Tetrahedron, 29, 1629 (1973).

61. J.M. Lehn, Pure and Appl. Chem., 49, 857 (1977).

62. B. Metz, D. Moras, and R. Weiss, Chem. Comm., 217 (1970).

63. D. Moras, B. Metz and R. Weiss, Acta Crystallogr., B29, 388 (1973).

64. D. Moras and R. Weiss, Acta Crystallogr., B29, 396 (1973).

65. D. Moras and R. Weiss, Acta Crystallogr., B29, 400 (1973).

66. J. Cheney, J.M. Lehn, J.P. Sauvage, and M.E. Stubbs, J.C.S. Chem. Commun., 1100 (1972).

67. J.M. Lehn, M.E. Stubbs, J. Amer. Chem. Soc., 96, 4011, (1974).

68. J.M. Lehn, and J. Simon, Helv. Chim. Acta, 60, 141 (1977).

69. R.M. Izatt, J.H. Rytting, D.P. Nelson, B.L. Haymore, and J.J. Christensen, J. Amer. Chem. Soc., 93, 1619 (1971).

70. M. Samsipur, Michigan State Univeristy, Ph.D. Thesis (1979).

71. E. Kauffmann, J.M. Lehn, and J.P. Sauvage, Helv. Chim. Acta, 59, 1099 (1976).

72. W.E. Morf, D. Ammann, R. Bissig, E. Pretsch, and W. Simon, "Cation Selectivity of Neutral Macrocyclic and Nonmacrocyclic Complexing Agents in Membranes" in Progress in Macrocyclic Chemistry, R.M. Izatt, editor, J. Wiley and Sons, New York (1979).

73. D.K. Cabbiness and D.W. Morgerum, J. Amer. Chem. Soc., 91, 6540 (1969).

74. M. Kodama, J. Chem. Soc. Chem. Commun., 891 (1975).

75. L. Fabrizzi, P. Pooletti, A.B.P. Lever, Inorg. Chem., 15, 1502 (1976).

76. T.E. Jones, L.L. Zimmer, L.L. Diadario, D.B. Rorabacher, L.A. Ochrymowvez, J. Am. Chem. Soc., 97, 7163 (1975).

77. A.I. Popov "The Use of Alkali Metal Nuclear Magnetic Resonance in the Study of Solvation and Complexation of Alkali Metal Ions" in Solute-Solvent Interactions, J.F. Coetzee and C.D. Richie, editors, M. Dekker, Inc., New York (1976).

78. R.G. Baum and A.I. Popov, J. Solution Chem., 4, 441 (1975).

79. Y.M. Cahen and A.I. Popov, J. Solution Chem., 4, 599 (1975).

80. M.K. Wong, W.J. McKinney, and A.I. Popov, J. Phys. Chem., 75, 56 (1971).

81. J.F. Hinton and R.W. Briggs, J. Magn. Reson., 19, 393 (1975).

82. J.J. Detchter and J.I. Zink, J. Amer. Chem. Soc., 97, 2937 (1975).

83. J.F. Hinton and R.W. Briggs, J. Magn. Reson., 25, 555 (1977).

84. R.W. Briggs and J.F. Hinton, J. Solution Chem., 6, 827 (1977).

85. R.W. Briggs, and J.F. Hinton, J. Solution Chem., 7, 1 (1978).

86. J.F. Hinton and E.S. Amis, Chem. Rev., 67, 367 (1967).

87. W.J. Dewitte, L. Liu, E. Mei, J.L. Dye, and A.I. Popov, J. Solution Chem., 6, 337 (1977).

88. N.F. Ramsey, Phys. Rev., 78, 699 (1950).

89. A. Saika and C.P. Slichter, J. Chem. Phys., 22, 26 (1954).

90. W.G. Schneider and A.D. Buckingham, Discuss. Faraday. Soc., 34, 147 (1962).

91. J. Kondo and J. Yamashita, J. Phys. Chem. Solids, 10, 245 (1959).

92. C. Deverell and R.E. Richards, Mol. Phys., 10, 551 (1966).

93. R.G. Barnes and W.V. Smith, Phys. Rev., 93, 95 (1954).

94. J.P. Manners, K.G. Morallee, and R.J.P. Williams, J. Chem. Soc. D., 965 (1970).

95. A.G. Lee, Coord. Chem. Rev., 8, 289 (1972).

96. R.W. Briggs and J.F. Hinton, J. Magn. Reson., 32, 155 (1978).

97. R. Freeman, R.P.H. Gasser, R.E. Richards, and D.H. Wheeler, Molecular Phys., 2, 75 (1959).

98. R. Freeman, R.P.H. Gasser, and R.E. Richards, Molecular Phys., 2, 301 (1959).

99. M. Bacon and L.W. Reeves, J. Amer. Chem. Soc., 95, 272 (1973).

100. S.O. Chan and L.W. Reeves, J. Amer. Chem. Soc., 96, 404 (1974).

101. J.J. Dechter and J.I. Zink, J. Amer. Chem. Soc., 97, 2937 (1975).

102. J.J. Dechter and J.I. Zink, Inorg. Chem., 15, 1690 (1976).

103. C. Schramm and J.I. Zink, J. Magn. Reson., 26, 513 (1977).

104. M.S. Greenberg and A.I. Popov, Spectrochimica Acta, 31A, 697 (1975).

105. R.W. Briggs and J.F. Hinton, J. Magn. Reson., 33, 363 (1979).

106. C. Srivanavit, J.I. Zink, and J.J. Dechter, J. Amer. Chem. Soc., 99, 5876 (1977).

107. G.W. Gokel, D.J. Cram, C.L. Liotta, H.P. Harris, and F.L. Cook, J. Org. Chem., 39, 2445 (1974).

108. D.D. Traficante, J.A. Simms, and M. Mulcay, J. Magn. Res., 15, 484 (1974).

109. J.W. Cooper, "An Introduction to Fourier Transform NMR and the Nicolet 1080 Data System", Nicolet Instrument Corp., Madison, WI, 1972.

110. E. Mie, J.L. Dye, and A.I. Popov, J. Amer. Chem. Soc., 99, 5308 (1977).

111. J.R. Zimmerman and M.R. Foster, J. Phys. Chem., 61, 282 (1957).

112. D.H. Live and S.I. Chan, Anal. Chem., 42, 791 (1970).

113. M.S. Greenberg, Michigan State Univeristy, Ph.D. Thesis (1974).

114. J.L. Dye and V.A. Nicely, J. Chem. Ed., 48, 443 (1971).

115. R.L. Bonder, M.S. Greenberg, and A.I. Popov, Spectrosc. Lett., 5, 489 (1972).

116. E.T. Roach, P.R. Handy, and A.I. Popov, Inorg. Nucl. Chem. Lett., 9, 359 (1973).

117. A.J. Smetana, Michigan State Univeristy, Ph.D. Thesis (1979).

118. V. Gutmann and E. Wychera, Inorg. Nucl. Chem. Lett., 2, 257 (1966).

119. L.A. Greenbauer, Michigan State University, MS Thesis (1978).

120. D. Lin and A.I. Popov, to be published.

121. R.G. Pearson, J. Amer. Chem. Soc., 85, 3535 (1963).

122. R.M. Izatt, R.E. Tery, D.P. Nelson, Y. Chan, D.J. Eataugh, J.S. Bradshaw, L.D. Hansen, and J.J. Christensen, J. Amer. Chem. Soc., 98, 7626 (1976).

123. Ya. I. Tur'yan and N.G. Chebotar, Russ. J. Inorg. Chem., No. 3, 273 (1959).

124. Ya. I. Tur'yan and B.P. Zhantalai, Russ. J. Inorg. Chem., No. 8, 848 (1960).

125. S.N. Andreev and A.I. Chaiko, Russ. J. Inorg. Chem., No. 7, 1045 (1971).

126. M. Molina, M. Angst., E.K. Garcia, and C.V. Melios, J. Inorg. Nuclear Chem., 34, 3215 (1972).

127. Ya. I. Tur'yan and R. Ya. Shtipel'man, Russ. J. Inorg. Chem., No. 4, 366 (1959).

128. Ya. I. Tur'yan, Russ. J. Inorg. Chem., No. 4, 369 (1959).

129. F.P. Hinz and D.W. Margerum, Inorg. Chem., 13, 2941 (1974).

130. L.S. Frankel, T.R. Stengle, and C.H. Langford, Chem. Commun., 393 (1965).

131. L.S. Frankel, C.H. Langford, and T.R. Stengle, J. Phys. Chem., 74, 1376 (1970).

132. D. Canet, J.J. Delpuech, M.R. Khaddar, and P. Rubini, J. Magn. Resonance, 9, 329 (1973).

133. A.K. Convington, R. Lamtzkea and J.M. Thain, J. Chem. Soc. Faraday, 70, 1869 (1974).

134. E.G. Bloor and R.G. Kidd, Can. J. Chem., 46, 3425 (1968).

135. R.H. Erlich and A.I. Popov, J. Amer. Chem. Soc., 93, 5620 (1971).

136. R.H. Erlich, M.S. Greenberg, and A.I. Popov, Spectrochim. Acta, 29A, 543 (1973).

137. M. Herlam and A.I. Popov, J. Amer. Chem. Soc., 94, 1431 (1972).

138. M.S. Greenberg, R.L. Bonder, and A.I. Popov, J. Phys. Chem., 77, 2449 (1973).

139. L.S. Frankel, C.H. Langford and T.R. Stengle, J. Phys. Chem., 74, 1376 (1970).

140. A.K. Convington, T.H. Lilley, K.E. Newman, and G.A. Porthouse, J. Chem. Soc. Faraday Trans., 1, 963 (1973).

141. A.K. Convington, K.E. Newman and T.H. Lilley, J. Chem. Soc. Farady Trans., 1, 973 (1973).

142. A.K. Convington and J.M. Thain, J. Chem. Soc. Faraday Trans., 1, 1879 (1974).

143. R.M. Izatt, J.D. Lamb, G.E. Maas, R.E. Asay, J.S. Bradshaw, and J.J. Christensen, J. Amer. Chem. Soc., 99, 365 (1977).

144. S. Schiavo, R.M. Fuoss, G. Marrosu, and G. Guida, J. of Solution Chem., 8, 557 (1979).